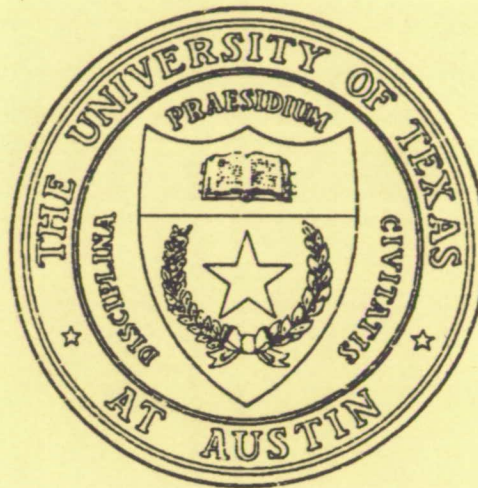NASW-4435

IN-37-CR
141650
P-163

Design of a Compliant Wheel for a Miniature Rover to be Used on Mars

Final Report

Submitted to:
Donald Bickler
Group Supervisor
JET PROPULSION LABORATORY
Pasadena, California

Prepared by:
Mark Carroll
Jess Johnson
Jimmy Yong (Team Leader)

Mechanical Engineering Design Projects Program
THE UNIVERSITY OF TEXAS AT AUSTIN
Austin, Texas

Fall 1991

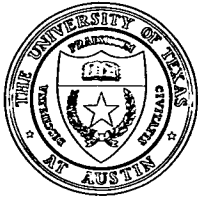# Design of a Compliant Wheel for a Miniature Rover to be Used on Mars

Final Report

Submitted to:
Donald Bickler
Group Supervisor
JET PROPULSION LABORATORY

Pasadena, CaliforniaPrepared by:
Mark Carroll
Jess Johnson
Jimmy Yong (Team Leader)

Mechanical Engineering Design Projects Program
THE UNIVERSITY OF TEXAS AT AUSTIN
Austin, Texas

Fall 1991

November 20, 1991

Don Bickler
Group Supervisor
Jet Propulsion Laboratory
Oak Grove
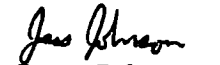Pasadena, California 91109

Dear Mr. Bickler :

    Enclosed is our report for the project titled "Design of a Compliant Wheel for a Miniature Rover to be Used on Mars." This report outlines the problem as interpreted by the design team, as well as describes the procedures followed to obtain an original wheel design. Squirm for this design was not eliminated, but axial and tangential deflections were reduced to 17% of the radial value.

    We wish to thank you for sponsoring our project and the help you have provided. The presentation of our report will be held on December 3, at 3:00 P. M. in room 4.110 of the Engineering Teaching Center II (ETC), located on the campus of The University of Texas at Austin. (At the intersection of 26th and Speedway). We realize that at this time your schedule will not allow you to attend, but if for some reason your plans change, please feel free to join us.

<div align="right">

Sincerely,

Mark Carroll

Jess Johnson

Jimmy Yong (Team Leader)

</div>

Enclosure : Project Report

Acknowledgements

Table of Contents

Table of Contents (continued):

Table of Contents (continued):

List of Tables

List of Figures

Notation

b   Width

c   Coefficient of cohesion

D,d   Wheel diameter

d   Deflection (WES Equations)

G   Soil penetration gradient

h   Section height

k_c Cohesive modulus of soil deformation

k_ϕ Frictional modulus soil of soil deformation

MC   Moisture content

n   Exponent of soil deformation

P   Pull

P_{opt} Optimum pull

p   Angle of soil friction

W   Wheel load

W_{opt} Optimum wheel load

z   Sinkage

Executive Summary

The Jet Propulsion Laboratory has identified the need for a compliant wheel for a miniature martian rover vehicle. This wheel must meet requirements of minimum mass, linear radial deflection, and reliability in cryogenic conditions over a five year lifespan. Additionally, axial and tangential deflections must be no more than 10% of the radial value.

The team designed a wheel by use of finite element and dimensionless parameter analysis. Due to the complex geometry of the wheel, a finite element model describing its behavior was constructed to investigate different wheel configurations. Axial and tangential deflections were greatly reduced but did not meet design criteria. A composite material was selected for its high strength, toughness, fatigue resistance, and damping characteristics. The team chose a Kevlar fiber filled thermoplastic composite.

This report is divided into four primary sections. First the Introduction section gives background information, defines the task, and discusses the scope and limitations of the project. Second, the Alternative Designs section introduces alternative design solutions, addresses advantages and disadvantages of each, and identifies the parameters used to determine the best design. Third, the Design Solution section introduces the methods used to evaluate the alternates, and gives a description of the design process used. Finally, the Conclusion and Recommendations section evaluates the wheel design, and offers recommendations pertaining to improvement of the design solution.

I. Introduction

The Jet Propulsion Laboratory (JPL) is currently studying an unmanned mission to Mars. There are many mission scenarios under consideration. Several of these programs require a small, six-wheeled all-terrain vehicle to explore the surface of the planet. The objective of this project was to design a 12.7 centimeter (cm) compliant wheel for this type of vehicle.

This report describes the process the team used to select and design the small rover wheel. Before discussing the design solution, the project background, design task, and design criteria are outlined. Design methodology and the scope and limitations of the project are also discussed. Also, alternative concepts are described and evaluated for adherence to design criteria. The embodiment of the design is then discussed and conclusions and recommendations are made.

1.1 Sponsor Background

JPL, located in Pasadena, California, is owned and operated by the California Institute of Technology. JPL was founded in 1936 as the Guggenheim Aeronautical Laboratory at the California Institute of Technology, and was later renamed JPL in 1944. Research was primarily devoted to ballistic missiles until 1958 when JPL joined NASA. Since that time, research has primarily focused on the exploration of space and JPL

has been responsible for missions to Venus, Jupiter, and other planets in the solar system [1].

1.2 Project Background

One of the major projects proposed by NASA for the early 21st century is a manned mission to Mars. Unmanned missions will precede the manned exploration of the planet in order to provide a better understanding of the surface and atmosphere of Mars.

A representative unmanned mission is the Mars Rover Sample Return Mission. It is designed to collect soil samples which will provide geological information about the surface of Mars. Several possible mission and system configurations have been proposed. One possible scheme is outlined graphically in Figure 1. In this mission, two vehicles are launched consecutively by Titan IV/Centaur-class rockets. One rocket carries a rover and an earth return vehicle (ERV), and the other rocket carries an ascent vehicle for lifting sample materials from the martian surface into orbit. Both rockets contain Mars orbiters and landers that deliver the payloads to the surface. Once Mars orbit has been achieved, a suitable landing site is chosen based on information gathered from orbital photographs. The two landers will then land in close proximity to each other on the martian surface. Directed from Earth, the rover collects samples and delivers them to the ascent vehicle. The rover may collect samples for weeks or months depending on the mission agenda. When the desired samples are collected, the ascent vehicle travels into martian orbit

where it docks with the ERV. The sample cannister assembly is transferred to the ERV which then returns to Earth [2].
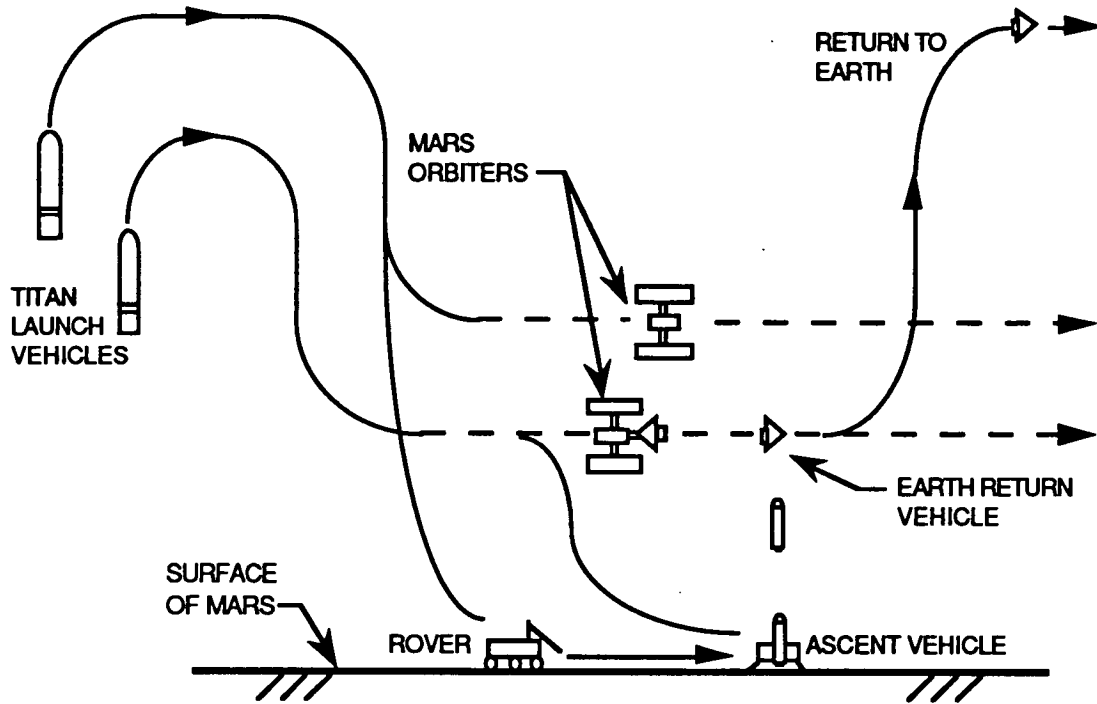
Figure 1 : Mars Rover Sample Return Mission

The six-wheeled vehicle shown in Figure 2a was developed by JPL for use on the moon and is being re-engineered for the Mars environment. The two major engineering challenges facing the martian rover are the terrain and the temperature. Data from the Viking missions shows the martian landscape to be plains covered with lava flows, fine sand (less than 100 micrometers), and rocks ranging from centimeter to meter size. This topography is considered typical of Mars. The temperatures measured by the probes were between 130 and 290K [3,4]. To meet these challenges the rover is being reduced in size and re-configured. Also,

metal alloys as well as new cryogenic composite materials are being considered for rover construction.

The segmented frame of the original six-wheel rover shown in Figure 2a has been replaced with a jointed frame to improve climbing ability (Figure 2b). The new chassis, designed by Mr. Don Bickler, incorporates a bogie, or truck, on each side of the vehicle which rigidly links the first and second wheels. The two bogies act independently, providing a pivoting suspension linkage which transmits the contact forces seen by one wheel into the wheel on the opposite end of the bogie. Thus, as one wheel is deflected, the grip of the other is increased. The bogies are pivoted off the main chassis which rigidly links the two rear wheels of the rover. These modifications allow the rover to climb uneven obstacles. A smoother ride is provided by transmitting input forces from one wheel to another, rather than into the main chassis.

There are several advantages to a smaller rover design. A scaled down rover reduces the overall mass and volume of the mission payload. Mobility will not be dramatically affected since the smaller rover will be able to go around most obstacles as well as over them. Furthermore, several compact rovers can be sent in the place of one large rover, allowing exploration of different areas simultaneously. A greater number of rovers also reduces the impact of a rover failure on the mission.
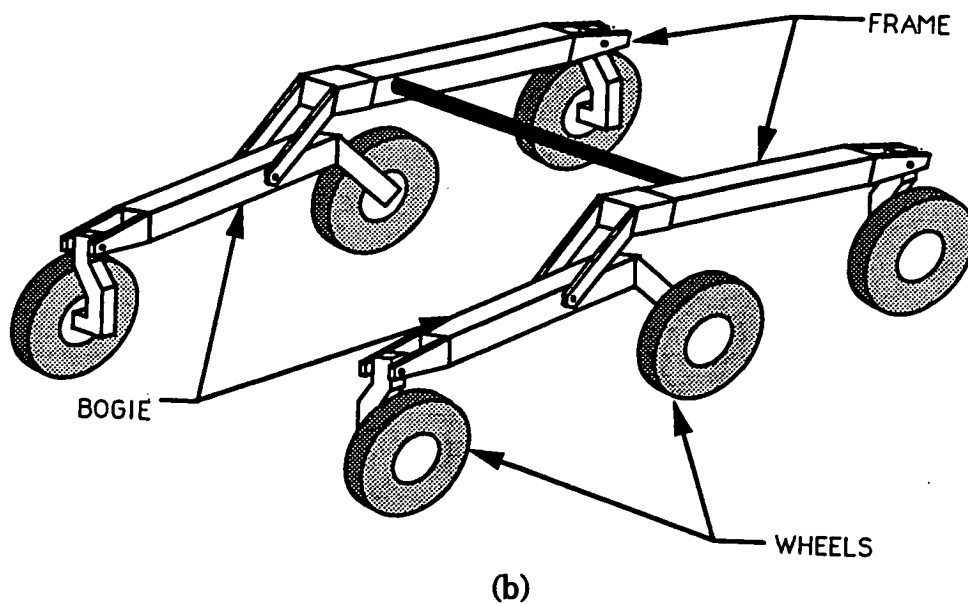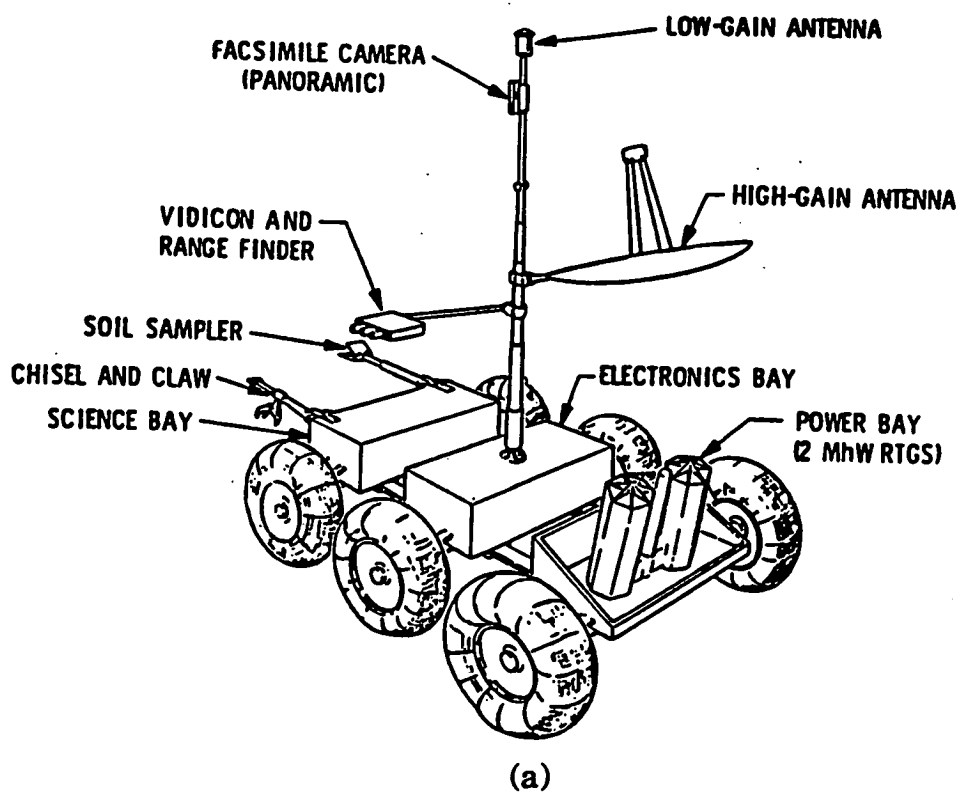
Figure 2: (a) Six-wheel JPL rover [From Ref. 3, p. 626.]
(b) Current rover design

Wheels are being used on the rover instead of tracked, elastic loop, or articulated leg systems. Wheels weigh less, are more reliable, and are more efficient than the other systems [5]. Also, track systems have limited mobility in sandy soils [6].

The wheel diameter of the remote controlled vehicle will be 12.7 cm. Current designs indicate the compact rover will be an all-wheel-drive vehicle with a mass of five kilograms, and a maximum speed of ten cm per second [6]. The low speeds are necessary to reduce vibrations caused by the rough terrain [7].

Equipped with a pair of video cameras, the rover will be able to return 3-D television pictures to its terrestrial operators. The great distance between the Earth and Mars will cause transmission delays as great as 40 minutes which will prevent the direct operation of the vehicle. This shortcoming is circumvented with the use of an inertial guidance system.

The inertial guidance system allows the operator to designate a path in the 3-D display using a computer-graphics overlay. This path includes references to landmarks and allows the rover to avoid obstacles and holes. The planned path is transmitted to the rover which then travels the designated path guided only by gyrocompass and wheel odometers. Accelerometers, tilt meters, and feature tracking allow on board processors to verify the path. At the end of the planned path, or whenever a hazardous condition is detected, the rover stops. It then transmits a stereo panorama and awaits a response [8].

1.3 Task

The objective of the design team was to design a wheel for the Mars Surface Rover (MSR). Due to the different environmental conditions of Mars and remote operation of the vehicle, the wheel design used by the Apollo program's Lunar Rover Vehicle (LRV) cannot be used. The lunar rover wheel was designed for smooth, sandy terrain and lunar daytime temperatures (384 K) [4]. In addition, the LRV wheel used a bias-ply construction. Bias-ply construction refers to the angle between the circumferential wheel centerline and the centerline of the carcass wires (Figure 3.). Small axial and tangential deflections, or squirm, occur as the opposing wires successively contact the surface. The zig-zag path resulting from the squirm of the wheel will cause error propagation within the inertial navigation system because the deflections are too small for the system to detect [6,9]. In addition, squirm consumes energy that would otherwise be applied to linear translation.
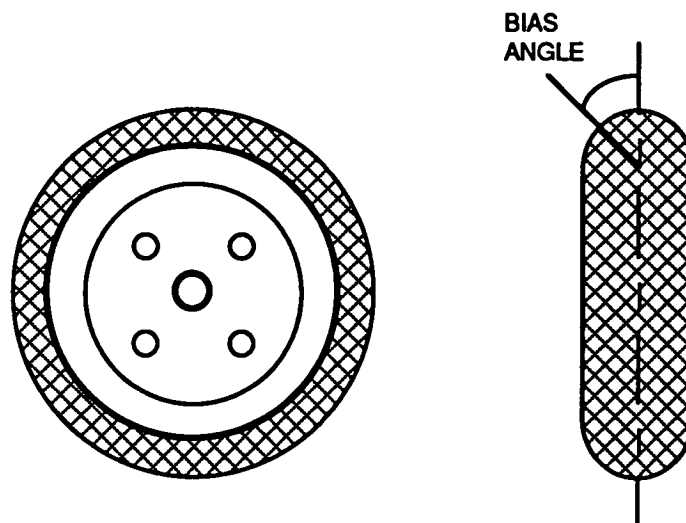
Figure 3 : Bias ply wheel construction

Several design constraints have been specified by JPL. As with all components of a space mission, a low mass design is essential. Low operating temperatures (130K) require a cryogenic material. The wheel must be able to traverse rocks, sand, and lava flows while withstanding solar radiation over a five year life span. The spring constant of the wheel must be as linear as possible in the radial direction. To minimize squirm, axial and tangential deflections can be no more than 10% of the radial deflection value (Figure 4). The maximum torque requirement for the wheel is 40% of the vehicle weight suspended at the wheel radius [6].

Force Applied

Force Applied

Force Applied

Axial Deflection　　　　Radial Deflection　　　　Tangential Deflection
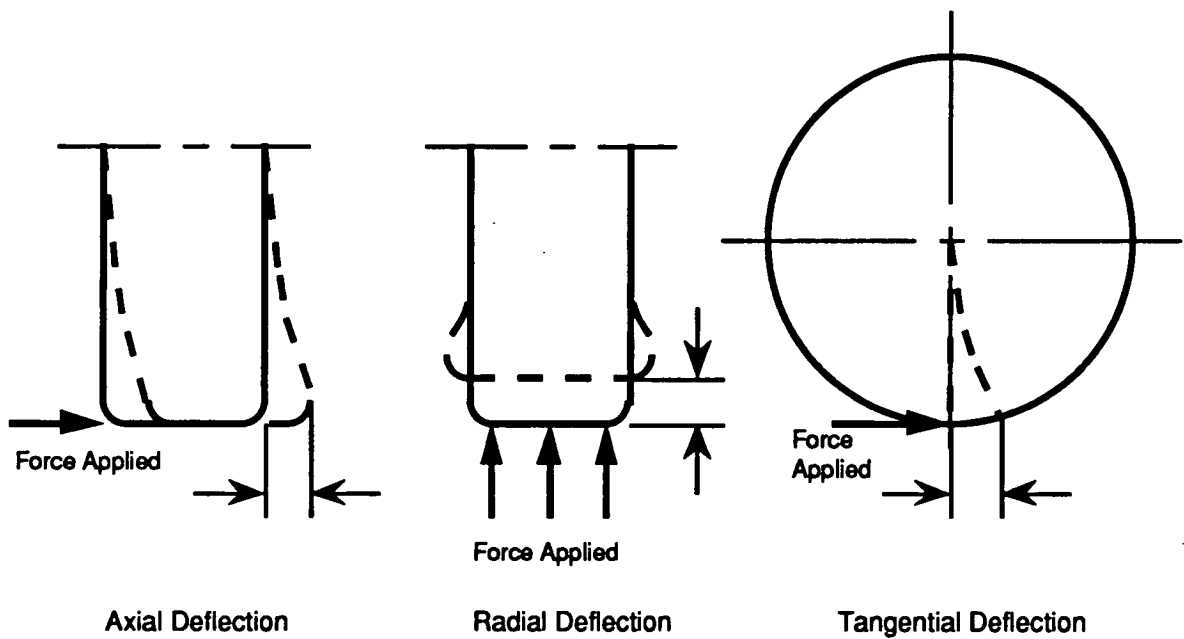
Figure 4 :　Axial, radial, and tangential deflection

8

1.5 Design Methodology

The team used the Pahl and Beitz method [10] to produce a design solution. An extensive literature search was performed in order to determine what materials could be used and what existing designs were applicable to the problem. This included a review of papers, periodicals, books, and a patent search. Appendix A contains a listing of relevant patents found by the team. To further outline the design criteria of the wheel, a specification list was made. A function structure based on these specifications decomposed the operation of the wheel into specific sub-function variants. These variants were then combined to form design alternatives. Appendix B contains the specification list and function structure.

The design team was able to produce seventeen wheel concepts from the function structure. A decision matrix was used to select a design solution. Analytical methods developed by the Waterways Experimental Station were used to evaluate wheel/soil interaction and finite element analysis was used to model wheel deflection and refine the design solution.

1.6 Scope and Limitations

The focus of this project was to produce an original wheel design that met the deflection criteria provided by JPL. Finite element analysis was used to model the wheel deflections. The design team specified a material but did not investigate the effects of cryogenic thermal cycling on the

design. Wear and fatigue properties of the material were considered during the selection process, but no testing was performed. The design was not experimentally evaluated or tested for adherence to design criteria and the effect of grousers or treads was not investigated.

II. Alternative Designs for Mars Rover Wheels

2.1 Introduction

The design team was able to generate many different concepts during the brainstorming phase of the project. Of the ideas generated, seventeen designs were selected for initial evaluation. A subjective evaluation of each designs' attributes led to the selection of the ten alternate design candidates listed in this section of the report. The eight ideas not evaluated are shown in Appendix C.

This section of the report describes the alternative designs and examines their mechanical behavior. To clarify evaluation of the designs, feasibility analysis and decision matrix criteria are explained. A description of each design is given and its feasibility is considered. Advantages and disadvantages are discussed and decision matrix criteria are applied to judge how well each alternative meets the design goals.

Alternative designs that resemble ideas already patented or in existence are referenced. Resemblance is coincidental and not intentional. The alternatives were conceived independently and prior to a patent search.

2.2 Feasibility Analysis

The ten designs described in this section were chosen from the original group of seventeen because they appeared to be viable and could be engineered to meet the design criteria. In all of these, a linear or near

linear compliance was expected. There were no obvious indications in any of the remaining alternatives that would suggest an excessive amount of squirm or energy consumption. Calculations were needed to further determine the feasibility of the remaining designs.

The preliminary analysis was intended to eliminate designs shown to be unworkable, or impractical. However, wheel geometry does not lend itself to accurate evaluation without the performance of in depth analysis. Due to time constraints, simplifying assumptions were made in order to predict the behavior of a given design.

To provide compliance, the alternative designs use spring elements. The radial deflection of these elements was evaluated by analyzing the behavior of a representative element in two dimensions. For example, the hoop element shown in Figure 5 can be broken up into segments and modeled as a series of leaf springs. Radial deflection can be approximated for a given load in this case. Further calculations may be used to approximate dimensions and predict performance of the spring elements, but the initial assumptions limit the accuracy of these results. For these reasons, preliminary analysis was used only to approximate the dimensions of the spring elements.

No analytical method was found by the design team that accurately described the behavior of a wheel under the complex loading encountered when climbing steep inclines or obstacles. For example, in the case discussed in the previous paragraph, no analysis was found for a leaf spring that is side loaded and simultaneously put in complex bending. Large deflection of the spring will change its mass moment of inertia appreciably, and thus change the torsion the spring may withstand. Due to

the number of simultaneous forces and moments acting on the wheel, simple beam analysis does not yield an accurate modeling of the true behavior of the wheel (Figure 6).
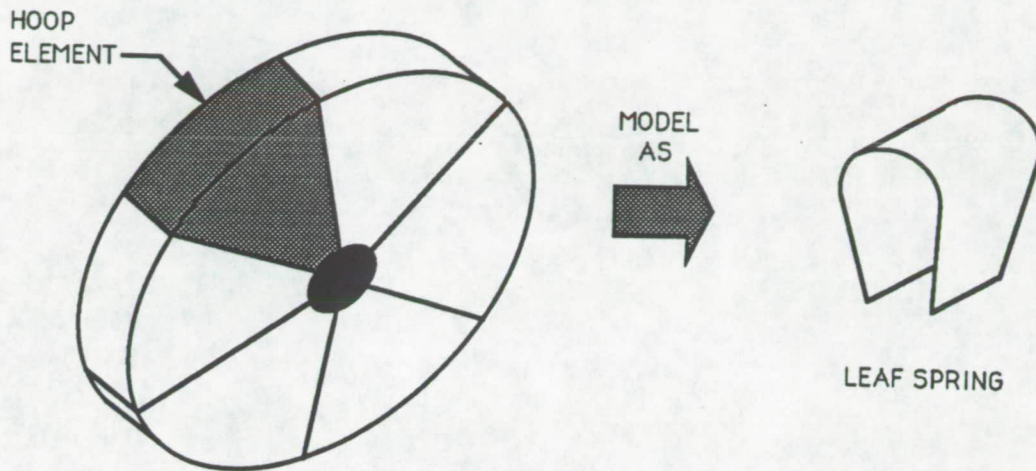
Figure 5 : Hoop element modeled as a leaf spring for analytical purposes

Feasibility calculations for all design alternatives are shown in Appendix D. In order to assure comparable results, the same material, load, and wheel width were used. The values used for calculations are shown in Table 1.

Calculations were performed to determine the necessary cross sectional thickness of the spring elements for each alternate. The smallest thickness commercially available for spring steel is 0.001 cm [11]. Cross-sectional thicknesses below this would indicate an unworkable design alternative.
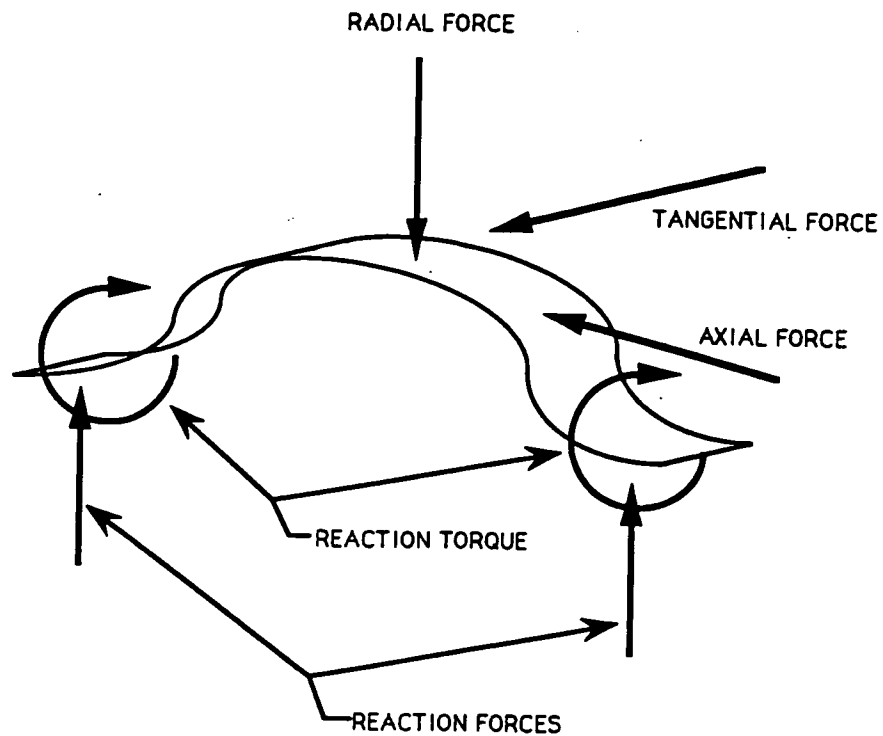
Figure 6 : Forces on a leaf spring during wheel operation

Table 1.

Values Used For Feasibility Analysis

Material	Steel
Young's Modulus	207 E9 Pascals
Gravitational Constant (Mars)	$3.7 \, m/s^2$
Load per Wheel	3.1 Newtons (N)
Spring Constant	3,100 N/m
Deflection	0.1 cm
Wheel Width	5 cm

2.3 Decision Matrix Criteria

The decision matrix was given four criteria - mass, radial deflection, energy efficiency, and reliability. These criteria were chosen because they could be applied to all design configurations.

The minimization of mass is very important in the design of the wheel. A low mass wheel design not only reduces the payload of the transport rocket, but also affects the design mass of the rest of the vehicle as well as its energy consumption. If the mass of the wheel is reduced, the forces generated at the supporting axle are reduced as well, allowing a smaller (lighter) axle. The axle itself then requires smaller bearings. In this manner, a low mass construction has a ripple effect throughout the entire vehicle design.

Radial deflection of the wheel serves two purposes. First, deflection of a compliant wheel reduces the impulse load placed on the axle by momentarily storing potential energy in the deflected wheel, and then dissipating the energy as the wheel regains its original shape. In doing so, the time period of the input force is increased, with a subsequent reduction in the peak load carried by the axle. Again, this allows a mass reduction of the supporting components. Secondly, radial deflection serves to increase the contact patch of the wheel, allowing a small radius compliant wheel to have the contact area of a larger wheel, without increasing its width, diameter, or mass (Figure 7) [12].
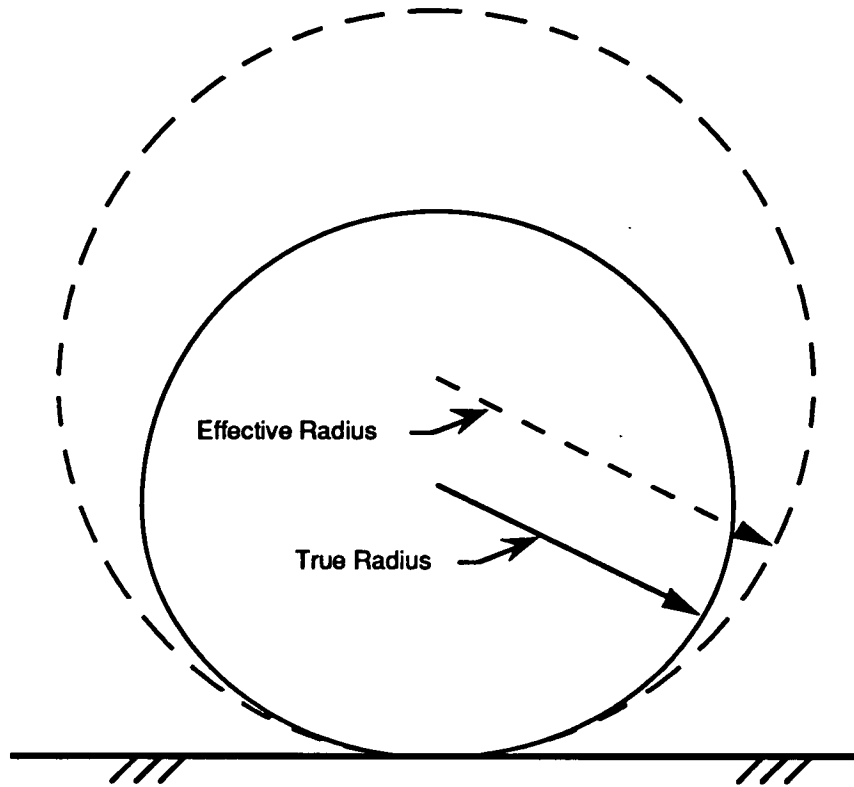
Figure 7 : Effective radius of a compliant wheel

In this report, energy efficiency refers to the energy consumption of the wheel design. Energy is consumed by deformation of both the wheel and soil. For the decision matrix, only axial and tangential deflections of the wheel were considered. As discussed above, these deflections contribute to squirm. An efficient wheel would be one that deflects a minimum amount in the axial and tangential directions.

Reliability refers to how well the design will perform over its service life. A design is considered reliable if it has a low number of components and can still perform after minor component loss.

2.4 Alternative One : Sigma Wheel

The Sigma Wheel is made compliant by segmenting its web and contact surface (Figure 8). This design relies on the deflection of both the contact surface and the connecting web (Figure 9). A varying cross-sectional thickness throughout the spring portion of the wheel ensures that the contact surface remains parallel to the axle when deflected. The change in cross-section will alter the mass moment of inertia, maintaining uniform radial deflection across the contact surface.

If the cross-section were constant, the wheel would not be able to maintain contact with the surface across its entire width when deflected. Axial deflection will be dependent upon the angle between the web and the axle, and will exist in some amount as a function of this angle. It should be noted however that the axial deflection of one wheel would cancel the deflection of the opposing wheel on even ground.

FLEXIBLE
SEGMENT

SHAFT
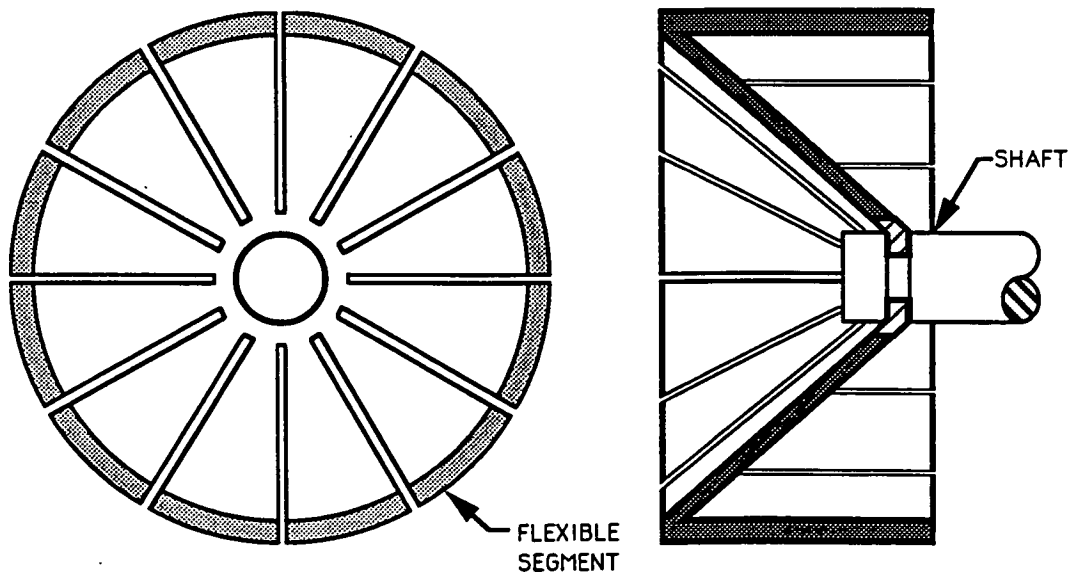
Figure 8 : The Sigma Wheel
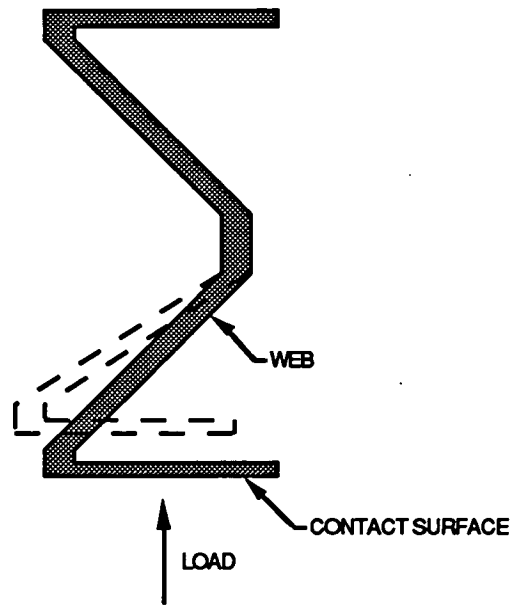
Figure 9 : A single element of the Sigma Wheel under load

Calculations indicate that small deflections are possible if the thickness of the web is below 0.03 cm. This calculation considers one segment of the Sigma Wheel under full load with constant cross section. Tracking for this design may be poor, because of the inherent axial deflection of the design. In addition, if the varying cross section of the web and contact surface areas are not fabricated to exact specifications, additional axial deflection will be introduced.

A thin wall construction will give the Sigma Wheel a low mass design. The wheel can also be designed to provide linear radial deflection and reduce energy consumption. As mentioned above, radial and axial deflection may be balanced to meet the design criteria. Tangential deflection may be reduced by decreasing the number of wheel segments. A smaller number of wider wheel segments will offer greater resistance to

18

torsional bending but will give a rougher ride. These criteria need to be balanced to yield the best combination. This design will provide a high degree of reliability due to its simple geometry. Reliability can be further enhanced by constructing the wheel from one piece of material. Stress concentrations caused by fasteners or weld imperfections would be reduced significantly.

An advantage that the Sigma Wheel has over some of the other alternatives is that the loss of one of the wheel segments will not completely disable the wheel. A disadvantage is that the inherent axial deflection for this design can be minimized, but not removed entirely. Due to the relationship between axial and radial deflection, radial deflection may have to be minimized to control axial deflection. This limitation may require unreasonably small spring travel to reduce axial deflection.

2.5 Alternative Two : V-Wheel

The V-Wheel consists of two opposed, thin conic sections arranged in a V-shape with the knee of the V circling the circumference of a rigid hub section (Figure 10). Compliance is provided by the deflection of the two conic sections.

For a deflection of 0.1 cm, the thickness of the sheet should be 0.02 cm. Calculations use an angle of 140 degrees for the V section. The design will track straight if the sheets each deflect the same amount under load.

The mass of the V-Wheel can be reduced by removing unneeded material from the hub and web areas of the wheel. The radial deflection of

the V-section will be near linear for small deflections. Energy efficiency for this design is higher than most of the design alternatives. Axial deflection is near zero for this design if both sides of the V simultaneously deflect the same amount. Also, tangential deflection will be near zero for the continuous sheet. Based upon the simplicity of this design, reliability for this design appears good.
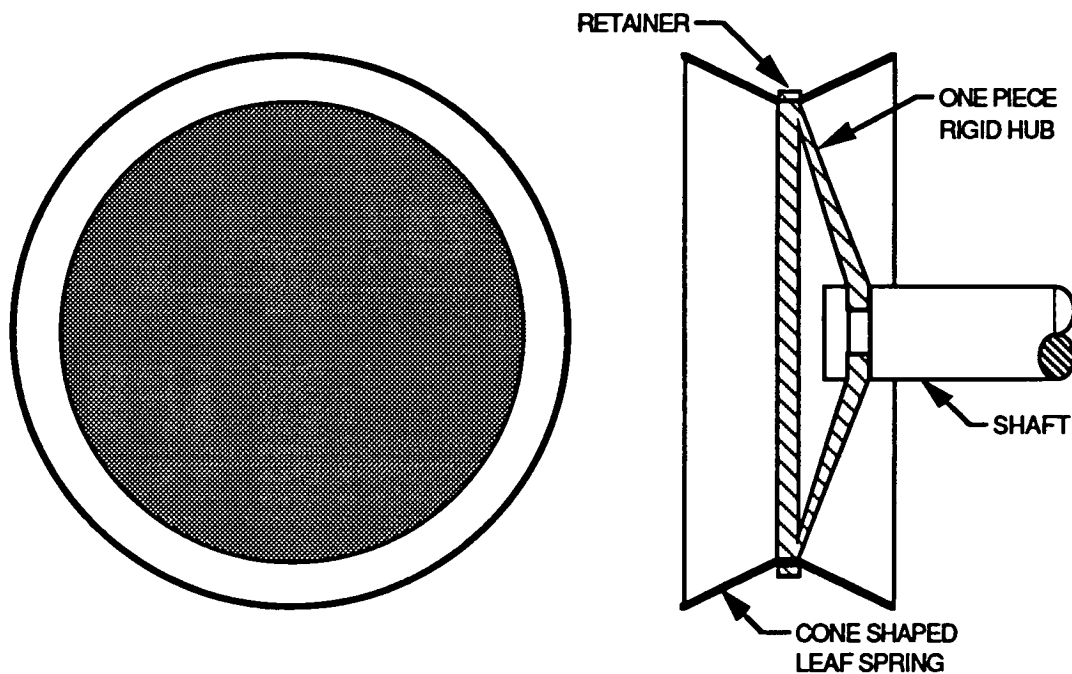
Figure 10 : The V-Wheel

This design has the advantages of simple construction, and a low number of parts. Also the small contact surface in the undeflected state will provide low rolling resistance on hard surfaces, with the contact area increasing proportionally with load.

The greatest disadvantage of the V-Wheel is that it is best suited to hard, smooth surfaces. The V-shaped cross section of this design may

cause the wheel to dig into the martian sand, rather than ride on top of it. Further, the thin edge of the spring section is also the contact surface, making it prone to abrasive wear and tearing on sharp or jagged surfaces. This problem is exaggerated by the small contact area the wheel provides in its undeflected state. Another disadvantage of this design is that as the V deflects radially, an axial component is introduced. Like the Sigma Wheel this axial component will consume energy, but should not contribute to tracking error.

2.6 Alternative Three : Corrugated Spring Wheel

The Corrugated Spring Wheel is a wheel with a rigid hub and web supporting a corrugated spring that circumscribes the rim of the wheel (Figure 11). Corrugations are oriented with the channels running along the axis of rotation. The corrugated spring is attached to the rim at the valleys of the corrugations. To provide a smoother ride and reduce tangential deflection, this corrugated spring is covered with a circumferential strip of material which is attached at the peaks of the corrugations.

In order to provide the desired spring constant, a single section of the corrugated spring will have a thickness of 0.005 cm. The tracking of this wheel will be good because of its low potential for axial deflection.

The mass of the large hub and web of the Corrugated Spring Wheel can be reduced by making them thin or hollow. Linear radial deflection for this design is limited to a fraction of the height of the corrugations. The nature of the design lends itself to efficiency. A wheel of this construction

with any appreciable width will have a very high axial stiffness. Tangential deflection is reduced by the addition of the outer element. With only three components, high reliability is anticipated for this design.

CONTINUOUS
CORRUGATED
SPRING

FLEXIBLE
COVER
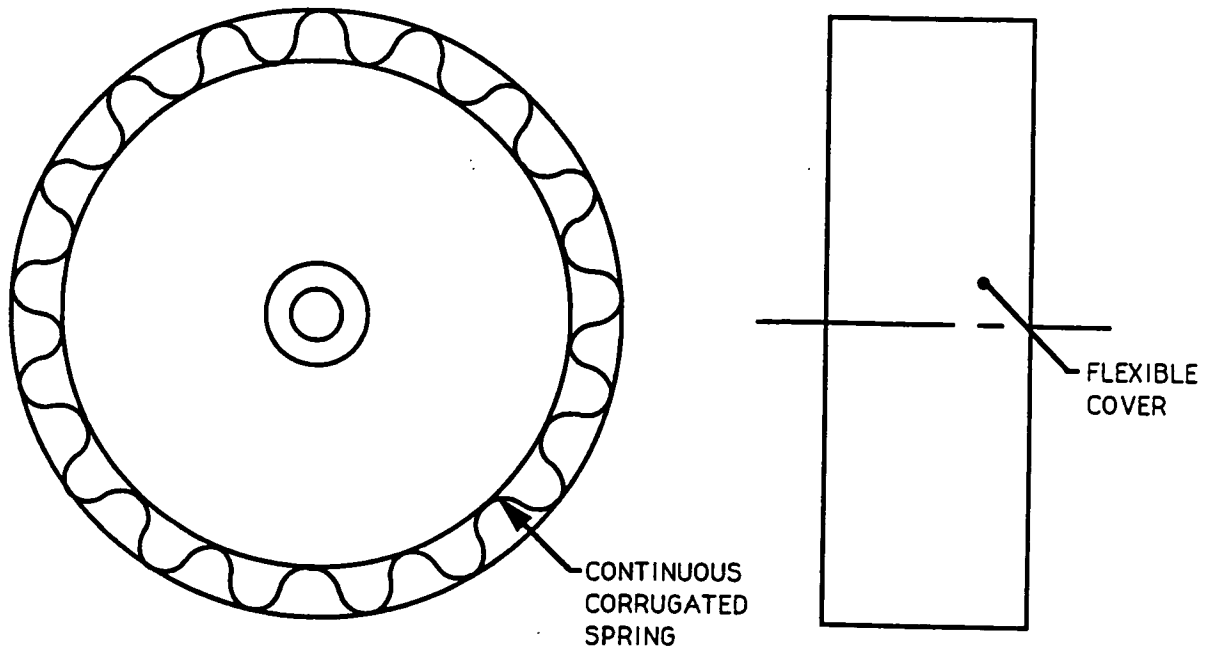
Figure 11 : The Corrugated Spring Wheel

An advantage of the Corrugated Spring Wheel is that the thin spring surface, which may be vulnerable to wear, is shielded by the circumferential belt of material. A disadvantage of this design is its limited amount of radial travel. In order to minimize tangential deflection, the height of the corrugations must be limited, which will reduce radial deflection and increase stiffness.

2.7 Alternative Four : Tab Wheel

The Tab Wheel uses a thin compliant sheet of material attached to a rigid hub. Equally-spaced tabs, bent through a constant radius, allow the sheet to serve as both sidewall and contact surface (Figure 12). The radius allows them to deflect, giving the design its radial compliance. During operation, only one or two of the tabs are loaded radially, while all of the tabs share axial and tangential loading.
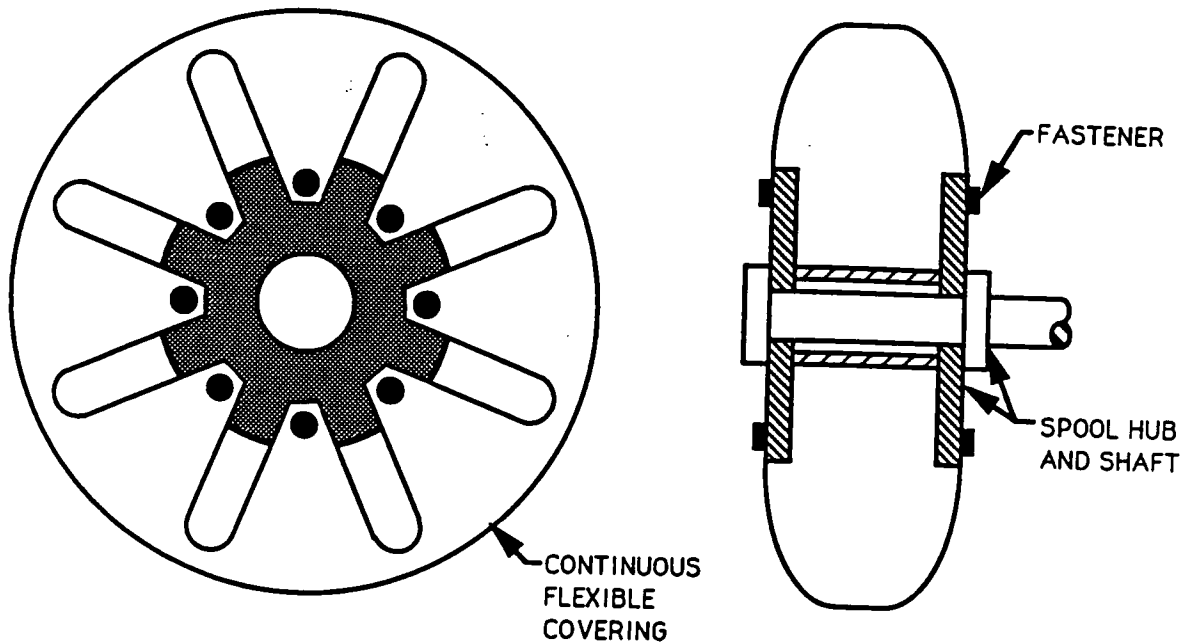
Figure 12 : The Tab Wheel

Damping for the Tab Wheel can be added by inserting a fabric bag between the spring material and the hub. The bag is attached to both the

hub and the inside of the sheet material. Deflection of the wheel will force the atmosphere inside the bag through an orifice, providing compression damping by dissipating some of the energy otherwise absorbed and stored by the wheel deflection. As the shape of the wheel is restored by the spring energy, atmosphere is drawn back through the orifice, providing rebound damping.

Deflection calculations for the Tab Wheel indicate that the thickness of the sheet will be 0.03 cm. The radial design provides low, rolling resistance and straight tracking.

A spool hub in conjunction with thin sheet material will provide a low mass design. Small deflections will give near linear radial compliance. The wheel will permit radial deflection much more readily than tangential or axial deflection, and can be designed for efficient operation. Reliability for this alternative should be high, since it has only two components that are simply connected.

One advantage of the Tab Wheel is that its mass may be reduced by making the sidewalls large in relation to the hub. In addition, making the sidewall portion of the tabs large will not require as great a bend radius for a given amount of radial deflection. A disadvantage of the design is that it exposes the thin spring material to surface wear. However, since the majority of the wheel compliance will result from deflection of the sidewalls, the center of the contact surface may be overlaid with another layer of material.

2.8 Alternative Five : Mesh Wheel

As mentioned in Section 1.4, a bias-ply metal mesh wheel was used on the LRV. The Mesh Wheel uses a radially woven metal mesh which surrounds a rigid hub (Figure 13). Flanges along the outside edge of the hub hold the mesh in place. The radial weave uses a 90 degree bias angle, with one set of fibers circling the perimeter of the wheel. Like the Tab Wheel, a damping bag may be added.

The Mesh Wheel resembles a resilient wheel patented in 1973 by Mr. Edward M. Hawes. A copy of the patent is shown in Appendix A.
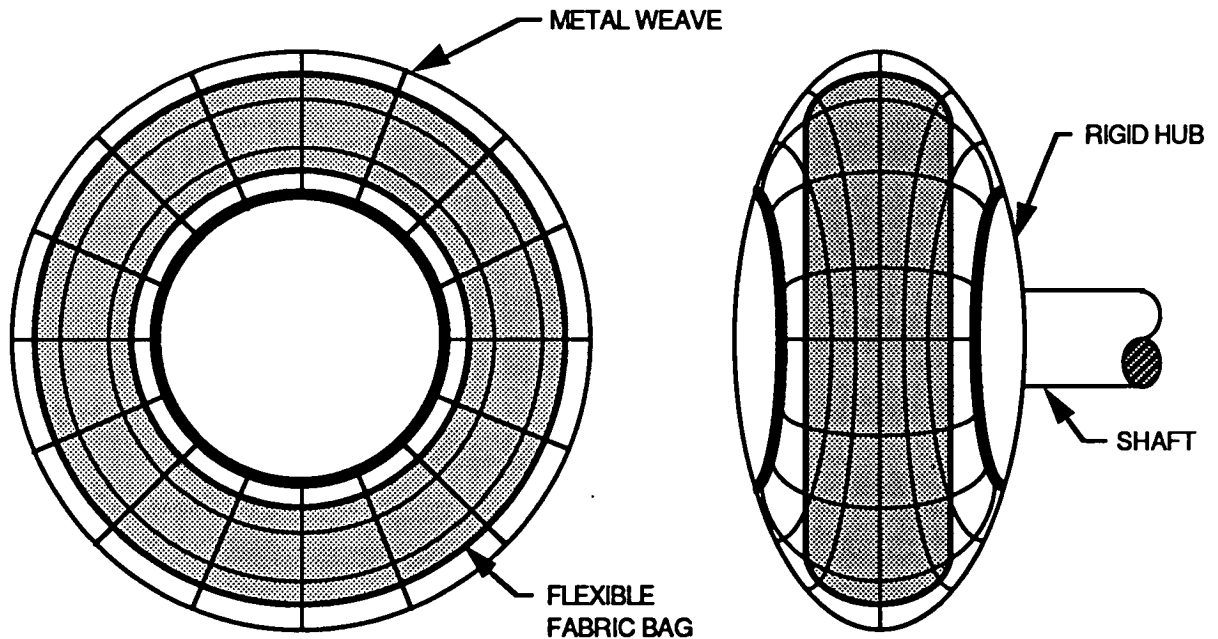
Figure 13 : The Mesh Wheel

The mesh system under load is too complex for simple feasibility calculations. Modeling a single radial strand of the weave yields a strand diameter of 0.02 cm.

The mass of this alternative is difficult to anticipate without knowing the thickness or density of the weave. Radial deflection for this wheel should be linear due to the radial design of the mesh wheel. Energy efficiency is also difficult to anticipate since axial and tangential deflection will be dependent upon weave characteristics. In this case, reliability is increased by the high number of fiber components. Failure of several fibers should not dramatically affect performance.

An advantage of the Mesh Wheel is that the team may draw on design techniques developed for radial pneumatic tire design. Radial construction can be used to eliminate wheel squirm and reduce tracking error and energy consumption. Also, research on metal elastic weave construction has been performed previously for the LRV wheel.

A disadvantage of the Mesh Wheel, based upon LRV wheel performance, is the amount of dust the weave will entrain while in operation. The entrainment of sand posed two serious problems for the operation of the LRV. First, picking up sand from the surface and accelerating it into the atmosphere consumed an appreciable amount of energy and limited performance of the vehicle. The entrained sand added mass to the wheel at its radius, dramatically affecting the torque requirements of the motor. As the sand was thrown off, the wheel lost the energy stored in the sand's inertia. Second, this dust tended to stay suspended much longer in the low-gravity environment, impairing visibility.

The Mars rover will operate at a much lower velocity and a higher gravitational constant compared to the LRV. Due to these differences the impairment of visibility may be minimal, but should be considered. However, the efficiency of the smaller Mars rover is much more critical, because of limited energy storage capacity.

2.9 Alternative Six : Hoop Spring Wheel

The Hoop Spring Wheel uses a rigid hub and rim, connected by cylindrical hoop springs radially distributed in the web area of the wheel (Figure 14). The axes of the cylinders are parallel to axis of wheel rotation, and are enclosed by an outer layer of thin sheet material which serves as the contact surface. This outer sheet of material is attached to the inner spring cylinders, increasing the effective torsional spring constant of the wheel. The overall radial spring constant will be lower than the tangential spring constant because more springs are in tangential shear than in radial compression.

Mr. James D. Wormley patented a similar design in 1977. A copy of his patent is listed in Appendix A. The Hoop Spring Wheel also resembles an LRV wheel proposed by the Bendix Corporation.

Calculations based on the radial deflection of a single hoop spring element indicate a thickness of 0.02 cm for the hoop springs. Tracking will be straight, since there is no appreciable axial deflection.

FLEXIBLE WHEEL COVER

SHAFT

RIGID HUB

FLEXIBLE SPRING TUBES
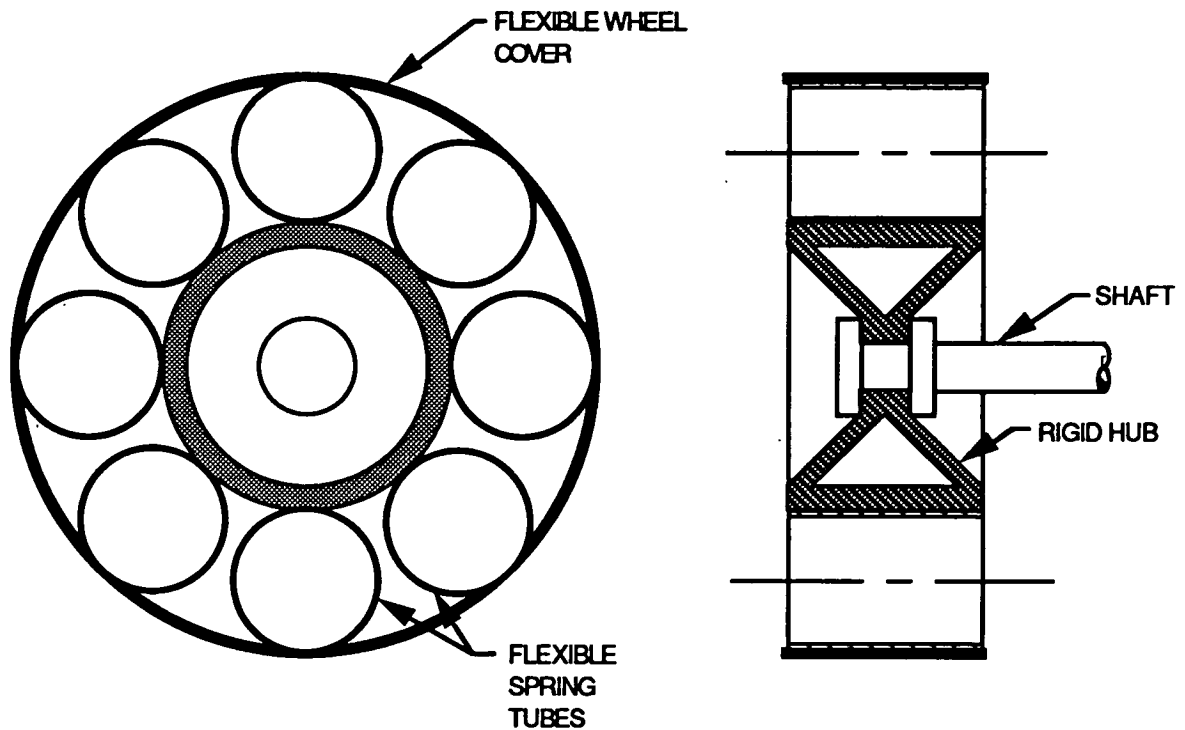
Figure 14 : The Hoop Spring Wheel

The mass of the Hoop Spring Wheel will be low due to the use of thin sheet material throughout the design, with the exception of the small hub. In response to an input force from the contact area, the top spring will be put in compression, the bottom spring in tension, and the side springs in shear. For all but very small deflections, the radial spring rate will be non-linear, because of the interaction of the springs. Energy efficiency should be good since axial deflection can be made near zero by making the springs wide in the axial direction. Also, as mentioned above, the spring constant is greater tangentially than it is radially. Reliability for this design will be low due to the complexity of the design.

The principle advantages and disadvantages of this design relate to its deflection characteristics. While the Hoop Spring Wheel has near zero axial deflection, non-linear radial deflection violates the design criteria. Also, radial compliance will be non-uniform as the wheel rolls, due to the sequential loading of the hoop springs.

2.10 Alternative Seven : Spoked Wheel

The Spoked Wheel uses a spoked wheel design, with compliance provided at the rim of the wheel by evenly spaced leaf springs transversely mounted around the circumference of the wheel (Figure 15). The springs are pinned at their attachment points on each side of the rim.

A 0.03 cm spring thickness gives the desired spring constant. The spoke wheel will give straight tracking provided the wheel remains true.

The mass of this wheel will be low, due to the use of a small spool type hub and thin spokes. The leaf springs will give near linear compliance, provided the travel of the springs is small. In the axial and tangential directions, this configuration should provide a very stiff design so energy consumption will be low. Overall reliability of the design will be low due to the complexity of the wheel, and the placement of the spring material at the contact surface.

While spoked wheels have proven themselves in other applications to be both light and reliable, they have a tendency to go out of true after repeated cyclic loading. This multi-component design is more susceptible to fatigue failure than less complex designs. For example, the high

number of fasteners or welds required will add stress concentrations to the wheel, which is critical at low temperatures. In addition, the spring members on the perimeter of the wheel will cause uneven compliance due to their discrete spacing.
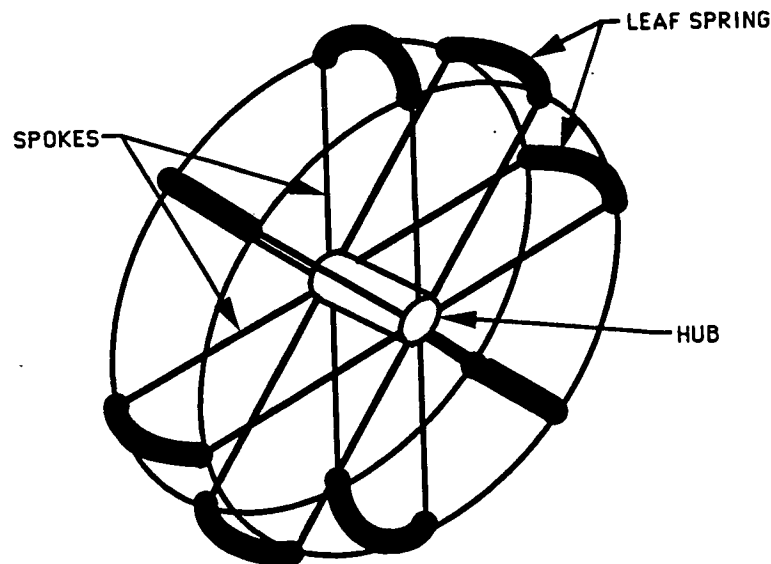
Figure 15 : The Spoked Wheel

2.11 Alternative Eight : Leaf Wheel

The Leaf Wheel uses transversely mounted leaf springs radially distributed about the circumference of a rigid hub (Figure 16). Unlike the Spoked Wheel, the springs are not pinned to the hub, but are held passively by retainers at their ends. The retainers permit the springs to slide a small amount in the axial direction before contacting the retainer walls. When

the spring is loaded, it will deflect linearly until its ends contact the walls. Upon contact, the spring rate will continue to be linear, but at a higher rate. The purpose of this is to provide two linear spring rates for the wheel, while using only one set of springs.
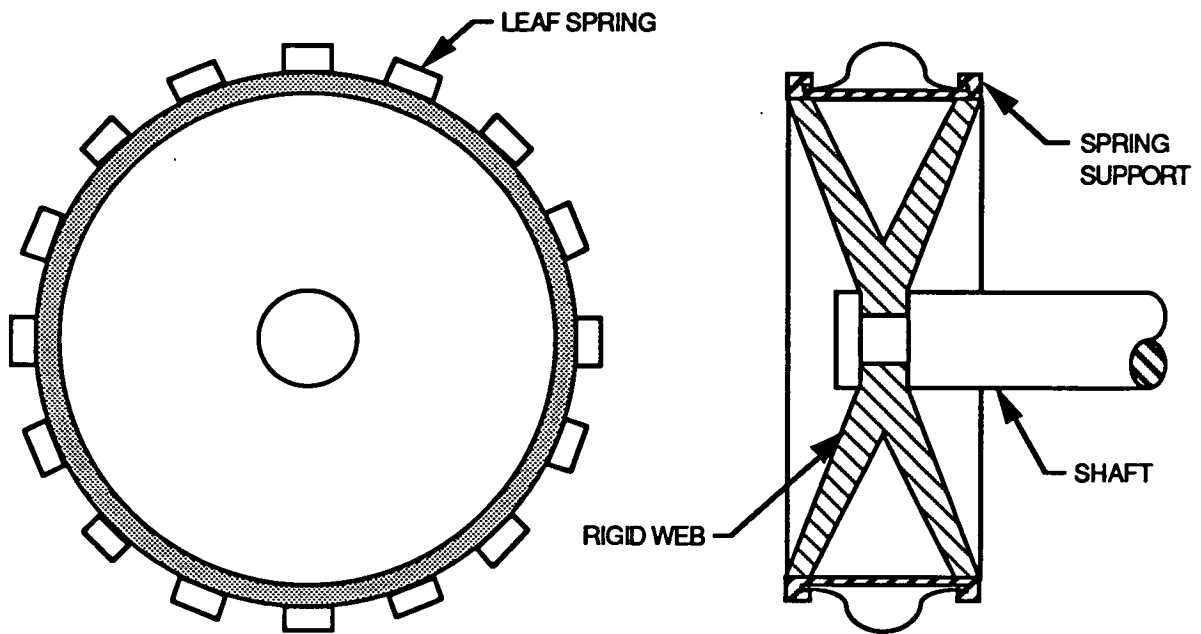
Figure 16 : The Leaf Wheel

The Leaf Wheel requires a thickness of 0.03 cm to give the desired deflection. While the sliding springs will introduce axial deflection, tracking will remain straight.

Like the other designs, mass for this design can be reduced by removing unnecessary material from the hub and web areas. The leaf springs may be designed to provide near linear radial compliance, provided the deflections are small. The Leaf Wheel can be designed to be energy

31

efficient. Axial deflection will be negligible, if both sides of the springs deflect equally. In the worst case, a spring with one end pushed against one of the retainers, will not cause axial deflection to exceed design specifications. Tangentially, deflection will be minimal with the use of wide leaf springs. Reliability for the design may be poor, because a strong tangential load can dislodge a spring element from its retainers.

The main advantage of this design is the provision for an overload spring without the weight penalty of additional springs. A disadvantage of this design is that like the Spoke Wheel, the Leaf Wheel has spring members on the perimeter of the wheel which causes an uneven compliance due to their discrete spacing. Also, axial deflections cannot be eliminated because of the need to provide clearance for small spring deflections. In addition, the placement of the spring surface at the contact area may cause accelerated wear of the spring material, as well as making it susceptible to snagging or tearing on rough surfaces.

2.12 Alternative Nine : Continuous Coil Wheel

The Continuous Coil Wheel employs a continuous-coil type of radial construction (Figure 17). A continuous flat coil of spring steel is wound radially around the circumference of a dished wheel rim. Each winding is held against the base of the rim by passive loops. These loops allow the system to store energy from the wheel's radial deflection in the torsional deflection of the coil. A thin strip of material, also held by passive loops,

encloses the circumference of the wheel providing a continuous contact surface.
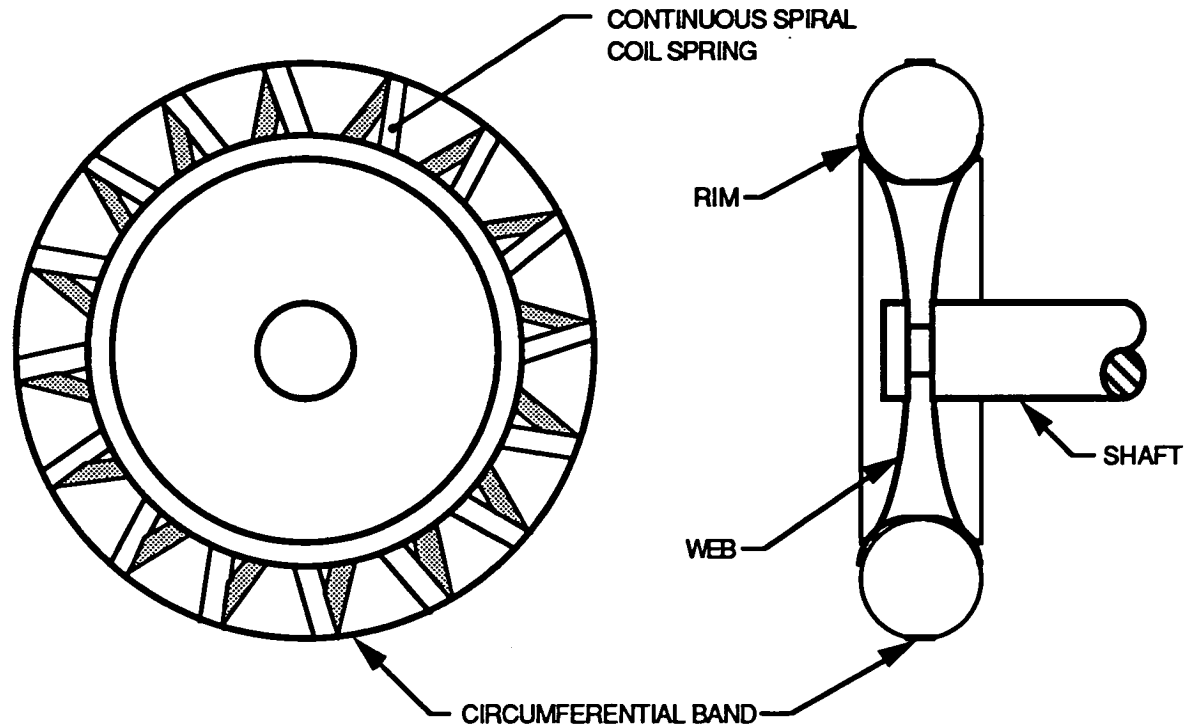
Figure 17 : The Continuous Coil Wheel

A cross-sectional thickness of 0.02 cm will give the desired spring constant. The near-radial construction of this design will provide true running with low energy requirements.

The thin coil material, in conjunction with the hollow hub, will allow a low mass design. Radial deflection will be linear and meet the design criteria. Axial deflection for this design will be low, due to the hemispherical support of the coil provided by the rim. Tangential deflection of the wheel is minimized, by the use circumferential band. Reliability will

be low because the loops which prevent tangential deflection are exposed to abrasive wear.

The main advantages of Alternative Nine, as discussed above, are low mass, linear radial deflection, limited axial and tangential deflection, and low energy requirements. The circumferential outer band of the wheel will also serve as a wear surface, protecting the spring portion from abrasive wear. The main disadvantage of the Coil Spring Wheel is that if one coil fails, the entire wheel fails. Two additional disadvantages of this design are its complexity and low reliability.

2.13 Alternative Ten: Double-J Wheel

The Double-J Wheel uses several segmented contact areas, or shoes, and a rigid hub connected by curved-end cantilever leaf springs (Figure 18). The short curved ends of the springs are attached to the hub, with the straight end connected to the shoes. The curved ends deflect radially and axially when loaded. Leaf springs, 0.2 cm square, will provide the desired deflection. Tracking will be straight since the spring will not deflect axially.

Mass will be high because of the thick springs and shoes. Radial deflection, like the other designs, will be linear as long as deflections are not extreme. Design formulas are available which can theoretically reduce axial deflection to zero. Also, tangential deflection will be low because the square cross section will resist deflection in this direction. Reliability will be low because of the complexity of the design.

The main advantage of the Double-J Wheel is that the dimensions of the cantilever leaf springs can be manipulated to minimize axial deflection. However, this advantage is offset by the high mass of the design and the uneven compliance caused by sequential loading. Another disadvantage is that the spring elements of this design are more susceptible to fatigue failure due to their greater thickness.
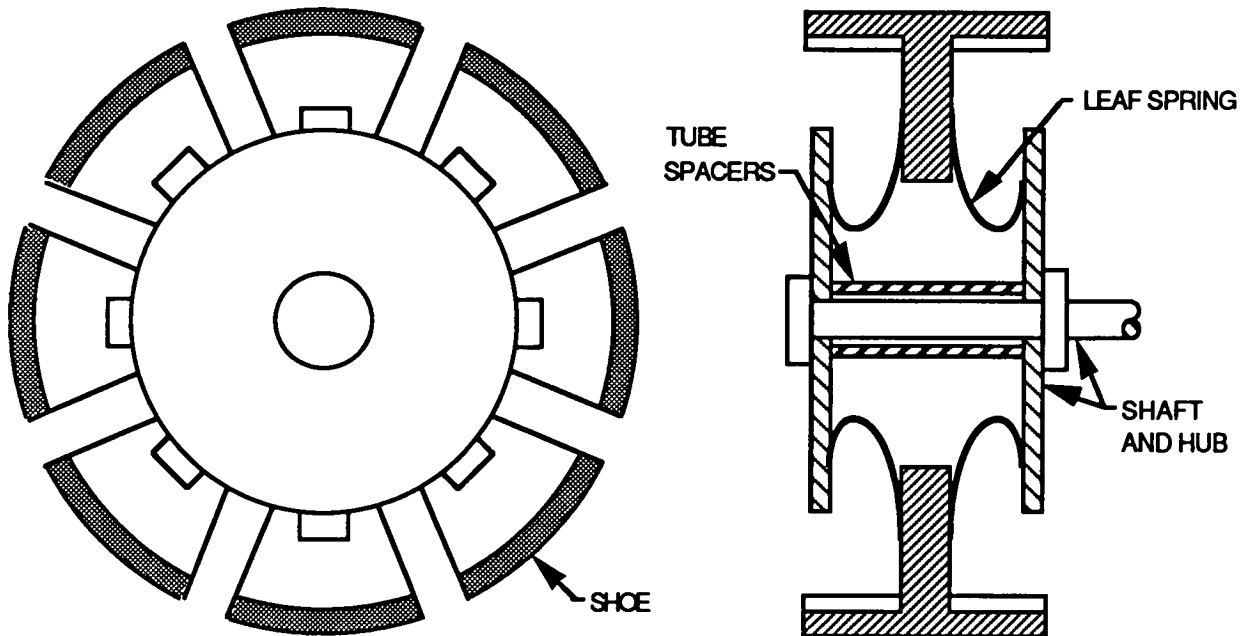
Figure 18: The Double-J Wheel

III. Design Solution

3.1 Evolution of the Hybrid Wheel

The design solution evolved from the top three alternative designs chosen from the decision matrix. The decision matrix (Appendix E) weighted the design criteria by relative importance and allowed the design team to quantify how closely each idea adhered to these criteria. The top ideas chosen from the decision matrix process were the V-Wheel, Sigma Wheel, and Tab Wheel. The design solution, or Hybrid Wheel, was made by combining the best features of these three wheel designs. The evolution of the Hybrid Wheel is shown in Figure 19.

V-Wheel   Double Sigma Wheel   Hybrid Wheel
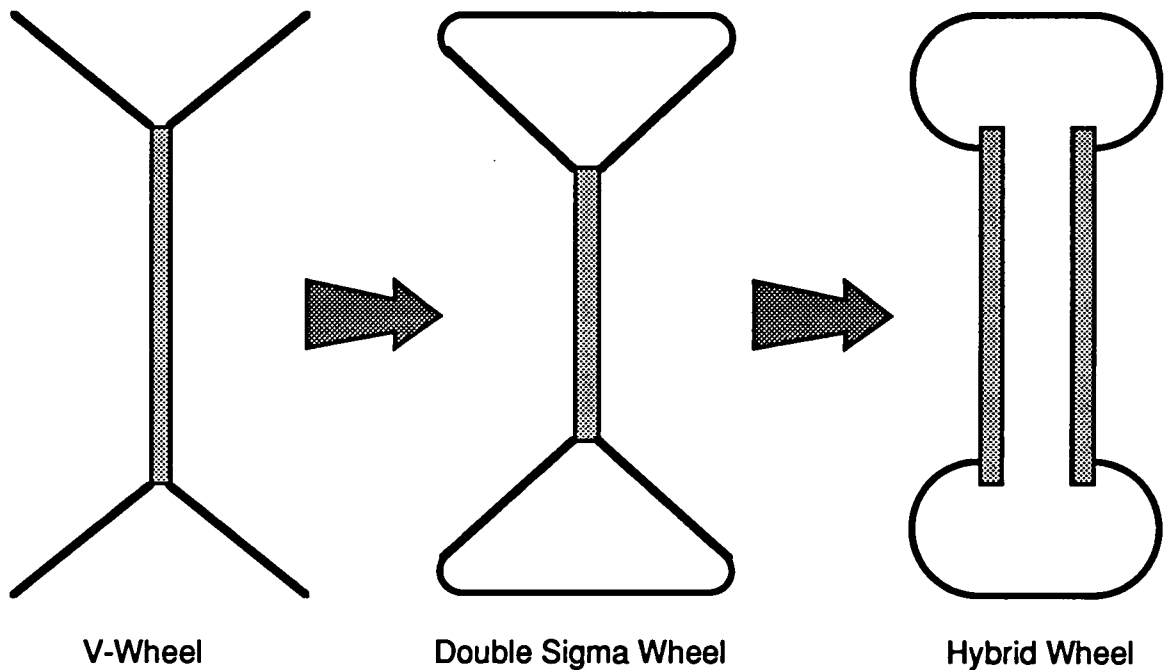
Figure 19 : Evolution of the Hybrid Wheel

The V-Wheel was considered highly promising for use on hard surfaces, but the design team felt that it would not perform well in soft, abrasive sand. To prevent excessive wear at the thin edges, a flat wear surface was added that enclosed the V section. This wear surface gave the wheel a cross-section that resembled a doubled Sigma Wheel. The doubled Sigma Wheel would be susceptible to axial deflection about its center. To remedy this problem, the legs of the triangular cross-section were moved to the outer edges of the hub, strengthening the wheel against side loading. Also, the contact surface was rounded to improve radial deflection, causing the design to resemble the Tab Wheel.

Simple FEA models indicated that the Tab Wheel was weak axially. It was felt that axial deflection of the Hybrid Wheel could be minimized if the side wall were joined perpendicularly to the hub (Figure 20). The modification of the side wall angle led to the present configuration of the Hybrid Wheel.
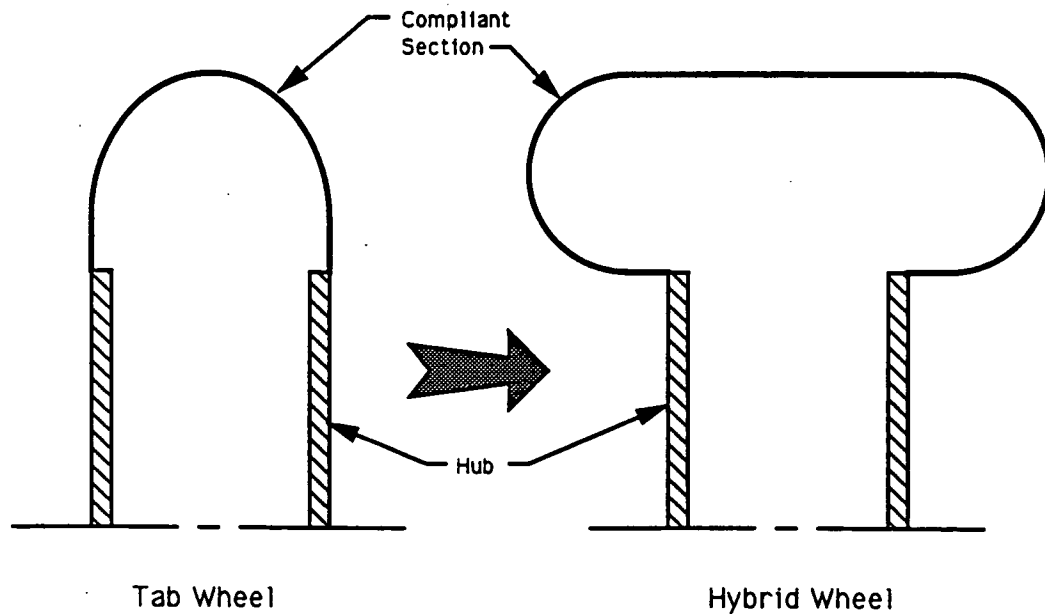
Figure 20 : Hybrid wheel cross-section

3.2 Determination of Wheel Width

3.2.1 Bekker Analysis

The first step toward designing the Hybrid Wheel was determining its geometry. The diameter was given as part of the design criteria but the wheel width would depend upon the characteristics of the martian soil. Dr. M. G. Bekker was the first to develop mathematical models describing the interaction of different soils and terrains with wheeled and tracked vehicles. Almost all reports and papers relating to wheel/soil interaction found by the design team referenced the work of Bekker. The design team began their analysis using techniques developed by Bekker to determine the proper width of the Hybrid Wheel.

Since there is little specific information about martian sand, the design team was asked to choose a set of soil values with which to evaluate wheel/soil interactions [6]. Yuma sand was chosen because it was used to evaluate LRV wheels and its properties have been well defined. The Bekker soil values for dry Yuma sand are shown in Table 2 [13].

Data gathered from the Viking missions indicates that the martian sand has a crusty surface layer [4]. Since the strength and uniformity of this crust is unknown, the design team assumed that the rover would break the crust and operate in loose sand. This assumption presented the worst-case scenario for wheel operation.

For dry sand, the width must be large enough that the wheel does not sink into the sand, but not so wide that the wheel begins to push, or bulldoze, the sand in front of it. It has been found that bulldozing will occur when the wheel sinkage to wheel diameter ratio is greater than 0.06 [14].

Table 2.

Dry Yuma Sand Values for Use With Bekker Analysis [13]

MC (%)	k_ϕ (kN/m^2)(cm^{-n})	k_c (kN/m)(cm^{-n})	n	c (kPa)	p (degrees)
0.5	11.41	-0.01	0.91	0	27.5

MC is Moisture Content, k_ϕ is the frictional modulus soil of soil deformation, kc is the cohesive modulus of soil deformation, n is the exponent of soil deformation, c is the coefficient of cohesion, and p is the angle of soil friction.

Reactive forces in the martian soil will depend upon the weight and width of the wheel. The vertical force is called floatation, and the horizontal forces are called traction and motion resistance (Figure 21). Energy requirements are determined by the interaction of the soil with the contact surface of the wheel as well as its weight, diameter, and width.
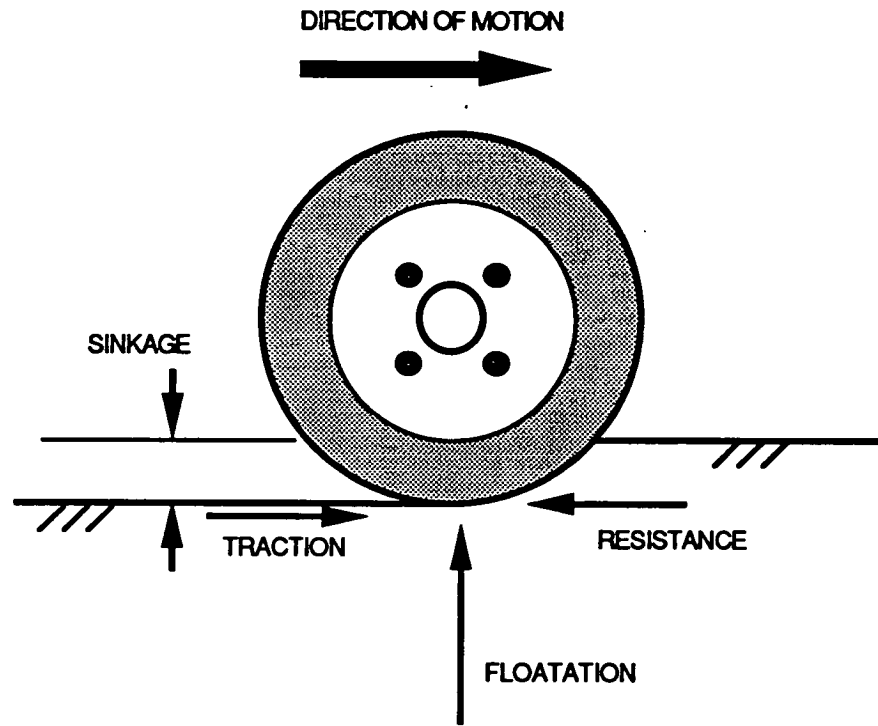
Figure 21 : Terminology associated with wheel/soil interaction

Safe wheel load is the normal load on the wheel that is needed to maintain complete contact between the soil and the wheel and is represented by the equation [7] :

$$Ws = A \left(c\, N_c + \gamma z\, N_q + 0.5\, \gamma b\, N_\gamma \right) \tag{1}$$

Where W_s is safe wheel load, A is contact patch diameter, c is the coefficient of cohesion, γ is density, z is sinkage, and b is width. N_c, N_q, and N_γ are soil constants that are dependent on the angle of soil friction. Equation (1) is simplified for Yuma sand because the coefficient of cohesion is zero. If it is assumed that the weight seen by the wheel is the safe load,

and the contact patch is circular, the equation can be solved for wheel width when sinkage is zero. Equation (1) then takes the form :

$$W_S = (\pi \, b^3 \, \gamma \, N_\gamma) / 8 \qquad (2)$$

Equation (2) gives a width of 4.4 cm (Appendix F).

Sinkage z is given by the formula [12] :

$$z = [\, 3W / (3\text{-}n) \, (k_c + bk_\phi) \, D \,]^{\, 2 / 2n+1} \qquad (3)$$

Where W is the load, n is the exponent of sinkage, k_c is the cohesive modulus of soil deformation, k_ϕ is the frictional modulus of soil deformation, and D is wheel diameter. Sinkage predictions for dry sandy soils using this equation are not as accurate as those made for soils that contain clay. Light loads also reduce the accuracy of the predictions [12]. Equation (3) and the relationship for bulldozing were used to find that bulldozing would begin at a width of 1.04 meters (Appendix F). This value indicates that the calculated width is well below the bulldozing threshold.

A device called a bevameter (BEkker VAlue meter) is used to perform soil tests from which k_c and k_ϕ are derived. Calculations made using equation (3) are more accurate for large wheel diameters because of the way the soil parameters are derived. Predictions for wheels smaller than 50.8 cm in diameter are less accurate with decreasing diameter because the sharp curvature of the contact area was not considered in the derivation of the equations or in the bevameter tests [12].

41

As stated above, Bekker's equations were not intended for lightly loaded wheels smaller than 50.8 cm in diameter. There has been little work done on wheels smaller than 50.8 cm, so the design team initially used this analysis for determining wheel geometry. However, the design team did not have a great deal of confidence in the results of this analysis because it was not intended for this application. For this reason, a more specific analysis was used.

3.2.2 WES Analysis

The design team used dimensionless analysis developed by the Mobility and Environmental Division of the U.S. Army Engineer Waterways Experiment Station (WES) in Vicksburg, Mississippi. WES developed dimensionless parameters for the evaluation of proposed LRV wheel designs.

The design team felt that the calculated width resulting from this method would be more accurate than the Bekker analysis because the WES experiments are more specifically related to the design constraints of the Hybrid Wheel. While no experiments on 12.7 cm wheels were performed by WES, empirical data was gathered for wheels of 39 cm in diameter. In addition, a cone test was used instead of a bevameter to derive soil values that could be applied to narrow wheels [15]. Experiments were performed on a broad range of lightly loaded wheels in Yuma sand and it has been found that the resulting parameters can be applied to a wide range of wheels with a diameter to wheel ratio between 1.0 and 2.5 [16].

Three relationships were used to calculate wheel width [15] :

$$P/W = \alpha - 5.50 / 1.92 \, \alpha + 37.20 \qquad (3)$$

$$\alpha = G \, (\, b \, d \,)^{3/2} \, \delta / (W \, h) \qquad (4)$$

$$P_{opt} / W_{opt} = 0.166 \qquad (5)$$

Where P is pull, W is load, G is soil penetration gradient, b is width, d is diameter, δ is deflection, h is section height, and the opt subscript denotes optimum.

A width of six cm was calculated using the above equations. Assumptions and calculations are shown in Appendix G. This width gives a diameter to width ratio of 2.1. The design team considers this width more reliable than the Bekker width, but since the wheel diameter falls outside of the range of the wheels tested by WES, it does not consider the WES width completely accurate.

Experiments similar to those performed by WES could be performed to find the appropriate width, but experiments of that nature are beyond the scope of this project. With this in mind the design team chose to use the width calculated using WES analysis.

3.3 Material Selection

The design team selected a composite material for the Hybrid Wheel because of its superior strength-to-weight ratio over cryogenic metals. For comparison, a 67% Kevlar filled epoxy composite tensile specimen gives a

57% mass savings over an equivalent specimen constructed of 6061-T6 aluminum. A calculation of the strength to weight comparison of the two materials is given in Appendix H. Table 3 offers a comparison of specific tensile strengths of selected candidate materials.

Table 3.

Specific Tensile Strengths of Material Candidates

Material	Kevlar / Epoxy Composite	6061-T6 Al	SS 304
Specific Tensile Strength (km)	260E3	35E3	64E3

The versatility of composite construction comes from the number of geometrical and material parameters available to the designer. Fiber aspect ratio, fiber volume fraction, damping and stiffness properties of the matrix and fiber materials, fiber orientation, laminate stacking sequence, and fiber length may be varied to give the desired composite properties. The compliance and damping of the composite may be engineered into the design, and may be made directionally dependent by altering the parameters mentioned above [17].

Composite construction allows directionally dependent strength for a constant material thickness, due to the anisotropic material properties. In a composite construction the matrix and filler may be adjusted to provide precise material characteristics. Composite constructions may also be designed to give an appreciable amount of viscoelastic damping through hysteresis of the resin matrix. Damping occurs primarily due to shear

concentrations at the ends of the reinforcing fibers being distributed into the resin. The use of discontinuous fibers increases the damping characteristics of the composite structure [17].

Pre-tensioned filament winding of the reinforcing fiber in the desired orientation will provide higher strength from a given member. The pre-tensioning of the filament requires that an input load first take the member out of tension before it can be loaded compressively [18].

Kevlar 49, an aramid fiber, was chosen over glass or graphite fibers as the reinforcing fiber for the composite filler because of its excellent toughness, low density, and damping characteristics (Table 4). The morphology of Kevlar fiber is somewhat different than other organic fibers, giving unique mechanical properties that prove beneficial to composite construction. Aramid fibers have a higher tensile strength due to the strong covalent bonds oriented along the longitudinal fiber axis. The alignment of these bonds yield a rod-like structure, with aromatic rings inducing high rigidity by forcing extension rather than folding of the polymer chains. The relatively weak hydrogen bonds joining the aramid polymeric chains make them weak in shear. The difference in the strength of these bonds gives Kevlar its anisotropic mechanical properties. It should be noted that Kevlar is ductile, unlike graphite or glass fibers which are very brittle. Research suggests that a 67% fiber volume in a plastic resin matrix gives the highest tensile strength [19].

The selection of a resin for the composite material was based upon several criteria. These criteria included durometer hardness, tear strength, and compression set %. The durometer hardness of a plastic serves as an indicator of the material's toughness and wear resistance.

The determination of this value is defined by ASTM standard D-2240. Tear strength of a plastic resin is determined using a tensile test in accordance with ASTM standard D-624. Compression set % is a measure of the materials' ability to retain its elasticity after prolonged exposure to both static and cyclic compressive stresses. The procedure for determining compression set % is given by ASTM-D 395, procedure B. This property is especially important to determine the resin performance under cyclic loading resulting from the rolling of the wheel.

Table 4

Comparison of candidate fiber materials [20]

Fiber	Kevlar 49	E-Glass	Graphite
Specific fiber toughness ($Pa/g/cm^3$)	145	85	48
Density (g/cm^3)	1.44	2.55	1.75
Vibrational loss factor (10E-4)	180	29	17

Materials with a Shore-A durometer reading between 80 and 95 and tear strength values above 300 kN/m were recommended for this application. Materials with a compression set % less than 50 were also recommended [21].

The use of composite structures in cryogenic conditions initially appeared unworkable due to the lack of test data for toughness and wear mechanisms. However, research into the cryogenic behavior of plastic

resins indicates clear trends which make special hypotheses for cryogenic conditions unnecessary. It has been shown that wear and toughness characteristics of composite materials actually show an improvement with decreasing temperatures [22, 23].

Composite resins may be divided into the two broad categories of thermosets and thermoplastics. Thermosets offer very high strength at the expense of toughness and ductility. Thermoplastics have lower strengths but offer good toughness and compliance characteristics.

Thermoset plastics have a glass transition temperature (T_g) at which they become very brittle, with near zero elongation at rupture. This is due to the covalent bonding, or cross-linking, between the long polymer chains in the resin (Figure 22). Exposure to decreasing temperatures shortens the chains, thus increasing the density of the cross-links and the brittleness of the plastic. The T_g of all the thermoset resins investigated by the design team was either above or inside of the temperature range found on Mars. With this in mind, the team decided against the use of thermoset resins, because the desired spring constant of the wheel requires a thin cross-sectional area. The possibility of brittle failure of the wheel upon a high impact load made this type of resin a poor choice [24].

The second broad category of resins are thermoplastics, differing from thermosets in that they do not cross-link. Thermoplastic resins trade the ultimate strength of thermosets for superior toughness and compliance. Thermoplastics are divided into two sub-categories; amorphous and semi-crystalline. The strength of amorphous thermoplastics comes from the entanglement of randomly distributed long chain polymers (Figure 23). Semi-crystalline thermoplastics have

crystalline regions interspersed throughout their structure. This crystallinity provides improved resistance to chemical attack at the expense of toughness. The amorphous resins offer the highest toughness and ductility values for plastics but have the lowest values for tensile modulus [24].
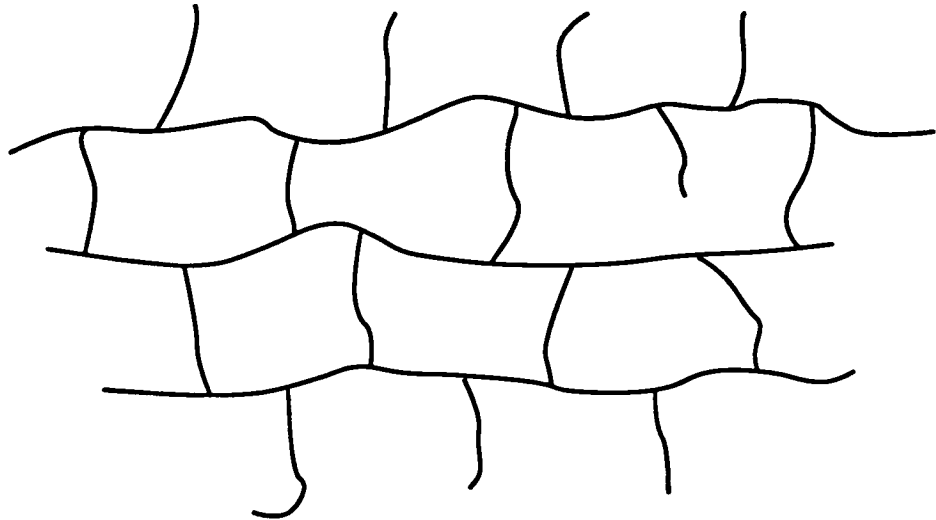

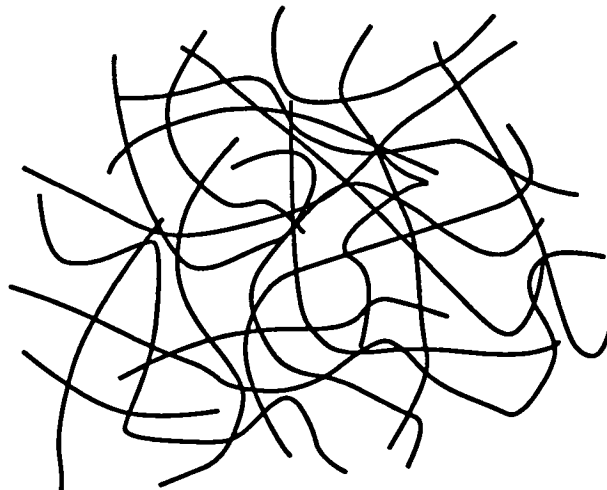Figure 22 : Cross-linking thermoset plastic polymers

Figure 23 : Thermoplastic long chain polymers

Amorphous thermoplastic resins were determined by the group to be the best choice for the wheel because of their high toughness and good ductility. Chemical attack is not an issue for this application and the low strength can be used to provide radial compliance for the composite wheel.

Of the amorphous thermoplastics considered, polyurethane elastomer type resins had the best general properties. Dow Chemicals' Pellathane 2103-80WC thermoplastic resin was chosen for its outstanding toughness and wear properties. Pellathane 2103-80WC offered the best compromise between toughness, tear strength, and compression set. This resin also has excellent wear properties, and compared to other resins, a low specific gravity (1.10) [21].

3.4 Finite Element Modeling

The design team used MSC/PAL2 software (PAL) to determine the relative deflections of the wheel in the radial, axial, and tangential directions. This finite element analysis (FEA) software made it possible to quickly change the shape and thickness of a Hybrid Wheel model, without having to actually build and test many different wheels.

Before the PAL software was used to determine the deflection of a complex model with unknown results, a simpler model was tested to verify the accuracy of this technique. The deflection of a leaf spring was analyzed using standard formulas and finite element modeling. The results of both techniques were compared and it was found that the deflections differed by 140%. Leaf springs with a deflection to length ratio less than 0.3 are more

accurately modeled as flexible beams [25]. Beams exceeding this ratio are non-linear and cannot be analyzed on the PAL program [26].

The MSR wheels will carry a static load of three Newtons on Mars and deflections are not expected to be so great in normal operation that they become non-linear. For this reason a simply loaded beam (Figure 24) was analyzed using FEA and standard formulas. The results of these two methods differed by 5.3% (Appendix I). Due to the fewer degrees of freedom in the FEA model, the FEA results were lower. The small difference was not considered to be great enough to prevent the use of FEA modeling for evaluation of the Hybrid Wheel [26].

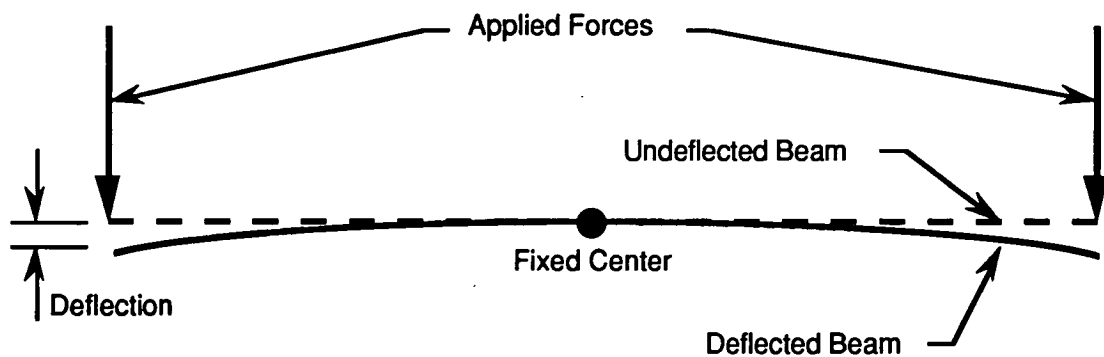Figure 24 : Beam model used for validation of FEA analysis

The loads used for FEA were determined from the angle of soil friction of the Yuma Sand, which is approximately equal to its angle of repose. The angle of repose represents the greatest angle a pile of sand in static equilibrium would make with a horizontal surface [6]. Theoretically, the steepest dune of Yuma sand will be 27.5 degrees.

The FEA models were evaluated using static loads because only the maximum torque on the wheel was specified. Torque for normal operation was needed to determine the tangential forces on the wheel. However, the velocity of the wheel is sufficiently small, and the load so light, that the dynamic loads may be approximated with a static loading condition.

The static loads were determined by analyzing the wheel on level ground and while climbing and crossing a 27 degree incline (Appendix I). The static loads for a 27 degree incline are shown in Table 5. Deflections were determined by applying the axial or tangential loads along with the radial load to the FEA models.

Table 5

Static Loads for 27 Degree Incline
(Newtons)

Radial	Axial	Tangential
2.7	1.4	1.4

The Hybrid Wheel was modeled using the material properties of aluminum. Aluminum was used instead of the chosen composite material for several reasons. When the FEA analysis began, the wheel material was not specified and aluminum was chosen as a representative cryogenic material so that analysis could begin. After the composite material was chosen, it was found that PAL could not be used for anisotropic materials and the MSC/NASTRAN program would have to be used instead. This software would greatly increase the amount of computer time needed to

51

analyze a single model and would limit the total number of different models that could be investigated. The design team also felt that the increase in time might prevent the team from obtaining any conclusive results. For these reasons aluminum was used for all the FEA models. Cross-sectional thickness ranged from 0.0075 to 0.0150 cm.

Radial deflection is defined as the difference in compliant section height between the deflected and undeflected condition. A radial deflection range between 10 and 22.5% was chosen for the Hybrid Wheel. WES research indicates that changing deflection within this range has little effect on wheel performance [5]. Below this range the wheel behaves rigidly and traction decreases. Above this range, energy consumption increases dramatically due to hysteresis and non-linear deflections.

Each of the models discussed below were evaluated using a variety of cross-sectional thicknesses. Only the results from each series of evaluations are discussed. Complete results are given in Appendix I.

The Hybrid Wheel was halved symmetrically and modeled with a continuous sidewall cross-section as shown in Figure 25. The model was halved along its vertical axis to reduce the size of the model file, and thus computer run time. It was found that the continuous sidewall made the design too stiff so material thickness was reduced from 0.01 to 0.005 cm.

Reducing the material thickness did not improve deflection appreciably, so segments of material were removed from the sidewall (Figure 26). Radial deflection then fell into the desired range with a material thickness of 0.01 cm, however axial deflection was greater than 10% of the radial value.
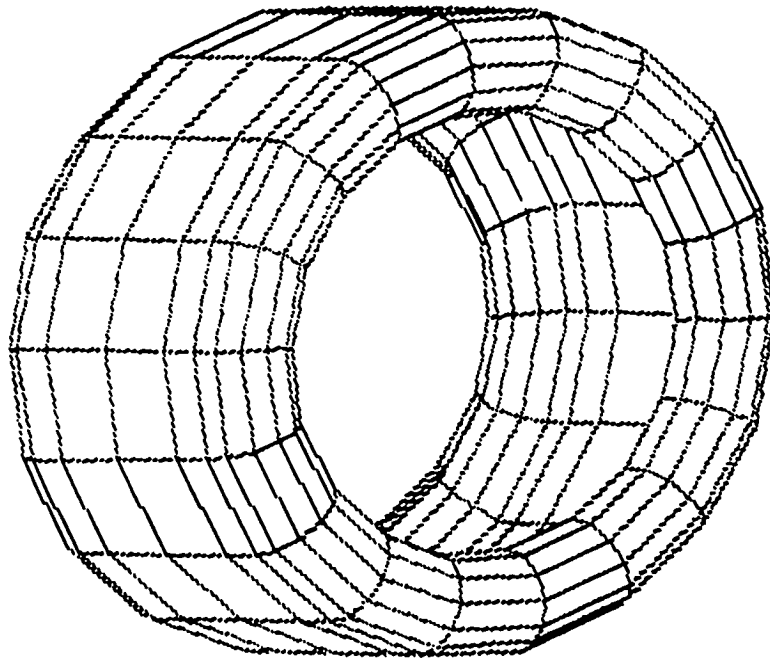
Figure 25 : FEA model of continuous sidewall Hybrid Wheel
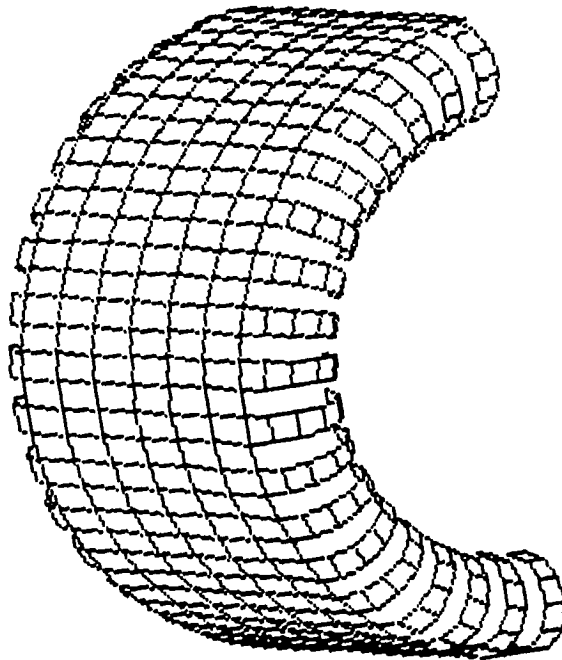
Figure 26 : FEA model of slotted sidewall Hybrid Wheel

The design team then modeled the two dimensional sidewall under radial, and then axial loads. The PAL models located the areas of greatest stress. Figures 27 and 28 show photographs of the PAL results. The spectrum of colors illustrates the magnitude of stress. Purple indicates the highest degree of compressive stress and red indicates the highest degree of tensile stress.
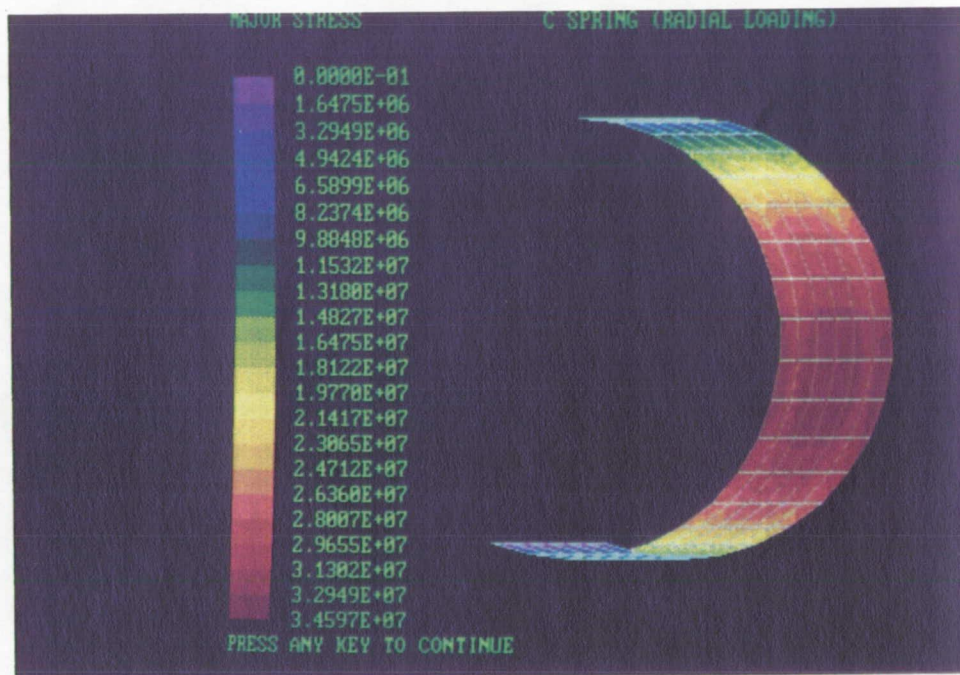
Figure 27 : Photograph of two-dimensional PAL results for sidewall under radial loading
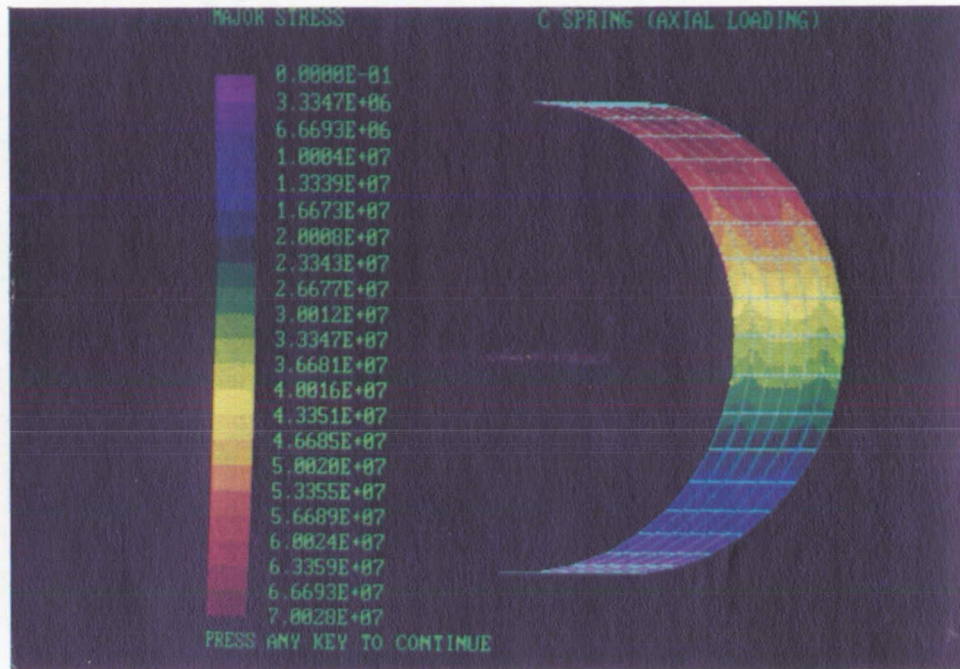
Figure 28 : Photograph of two-dimensional PAL results for sidewall under
axial loading

It was hoped that changing material thickness in the appropriate
areas of the sidewall would decrease the deflection in the axial direction
without affecting radial deflection. This method proved ineffective because
the three dimensional model did not behave in the same manner as the two
dimensional model. In the two dimensional model the highest stresses due
to axial and radial deflection occur in different areas of the cross-section.
The three dimensional model places the sidewall in shear as well as
compression causing the highest stresses to occur in the same area (Figure
29). Increasing the thickness in particular areas of the Hybrid Wheel
would affect both radial and axial deflection. These results led the design
team to conclude that the round sidewall of the Hybrid Wheel would have

an inherently high axial deflection. The design team decided to abandon the circular sidewall in favor of a design with higher axial strength.
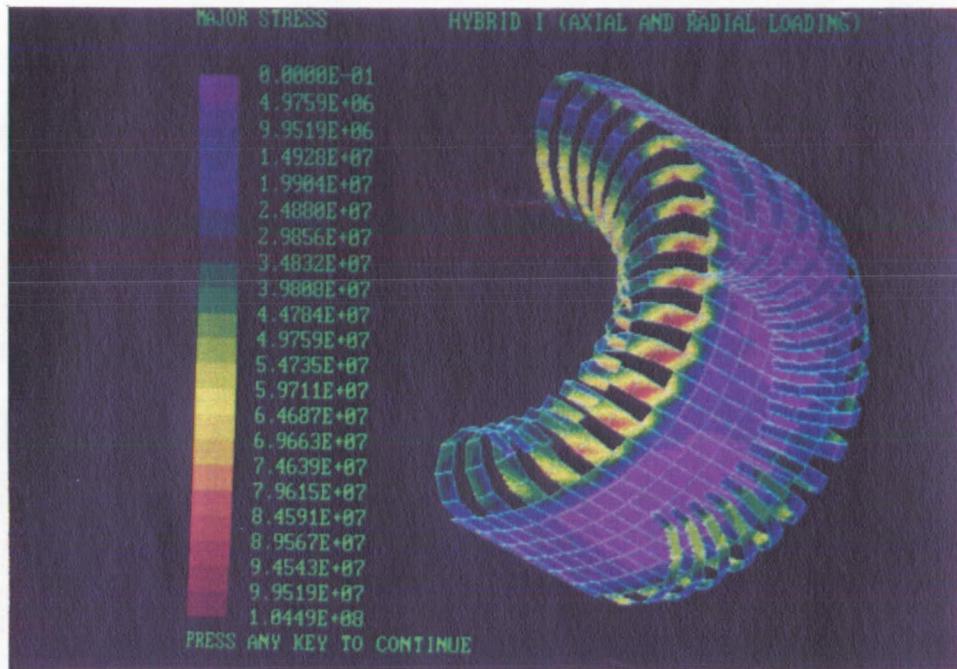
Figure 29 : Photograph of three-dimensional PAL results for Hybrid I
under radial and axial loads

The cross-section of the wheel was changed to reduce axial deflection (Figure 30a). The new model was called the Hybrid II to avoid confusion. The pointed sidewall of the Hybrid II reduced axial deflection from over 100% to 30% of radial deflection. This change made the wheel too stiff in the radial direction. To improve the radial compliance, the pointed ends of the sidewalls were replaced with small radii (Figure 30b). Radial deflection improved to 13.4%, and axial deflection was reduced to 20% of radial deflection. To further improve radial deflection, the straight contact

surface was made convex and the portions connecting the sidewall to the hub were made concave (Figure 30c). Radial deflection increased to 20% and the axial to radial percentage (A/R) decreased to 17%. The radii at the tips of the sidewall were then changed to a short straight section (Figure 30d). Radial deflection increased to 30%, but the subsequent increase in axial deflection caused A/R to improve only slightly. It was found that further adjustments to the sidewall caused axial deflections to increase.

The design team decided to investigate the effects of altering the portion of the cross-section connecting the sidewall to the hub. The radii at the tips replaced the straight sidewall, the contact surface remained rounded, and the portions connecting the sidewall with the hub were made concave (Figure 30e). These changes produced a 32% radial deflection and an A/R of 16%. Radial deflection was reduced to 13% by flattening the contact surface and changing the thickness of the material. This design gave an A/R of 16%. Tangential deflection for this design was found to be 17%.

The short time allowed for this project prevented the design team from evaluating additional configurations. The Hybrid II does not meet the 10% axial and tangential deflection criteria when climbing a 27 degree slope. However, the Hybrid II can transversely cross a 16 degree slope, and climb a slope of 17 degrees without violating the design criteria. For comparison, the Hybrid I could not transversely cross even a one degree slope without violating the design criteria. Figures 30 and 31 show how deflection of the Hybrid II changes in the three principle directions as the angle of incline increases. Figures 32 and 33 show the deflection ratios of

the final configuration. The final dimensions of the Hybrid II model are given in Appendix J and the final configuration is shown in Figure 34.
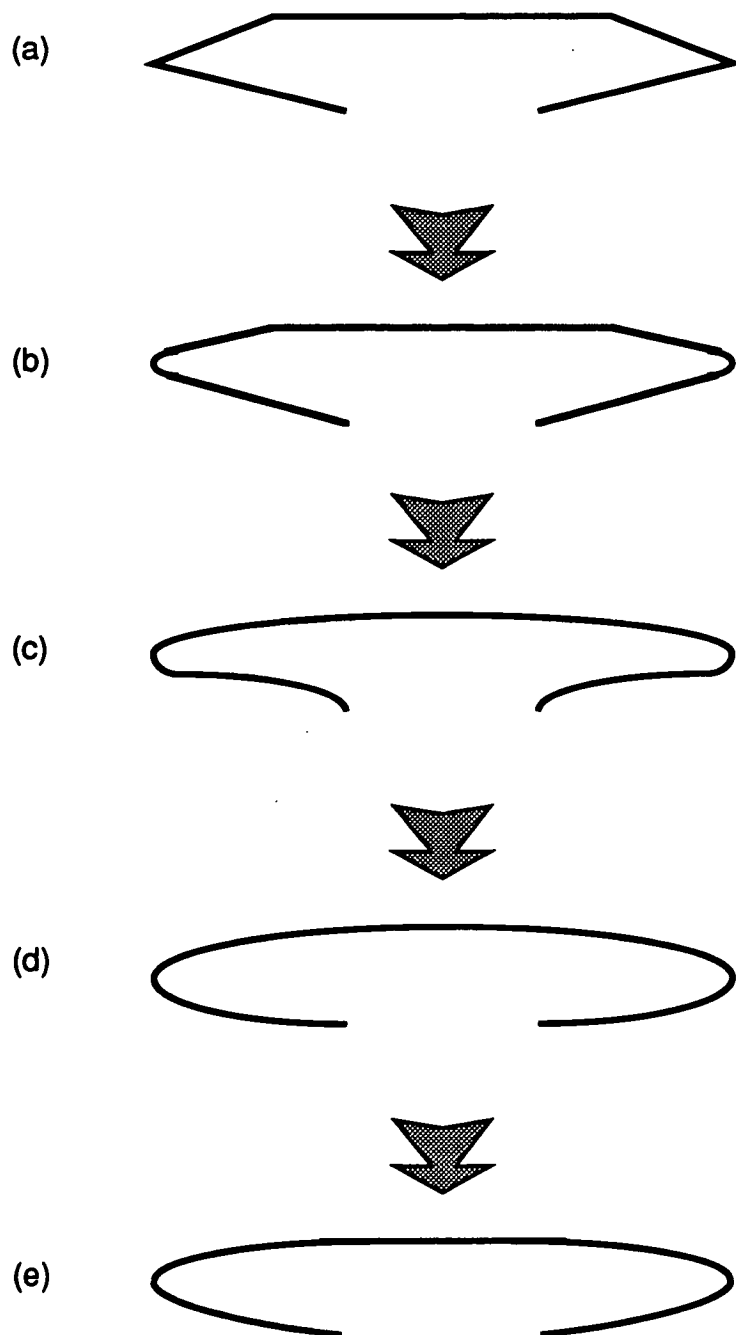
Figure 30 : Progression of Hybrid II cross-section development

The FEA modeling enabled the design team to reduce the axial deflection from 300% to 17% of the radial value. The Hybrid II Wheel does not meet the deflection criteria using an isotropic material. It is anticipated that further analysis on NASTRAN will allow the manipulation of the directional properties of the composite material as well as the shape of the wheel to further reduce the axial and tangential deflections.
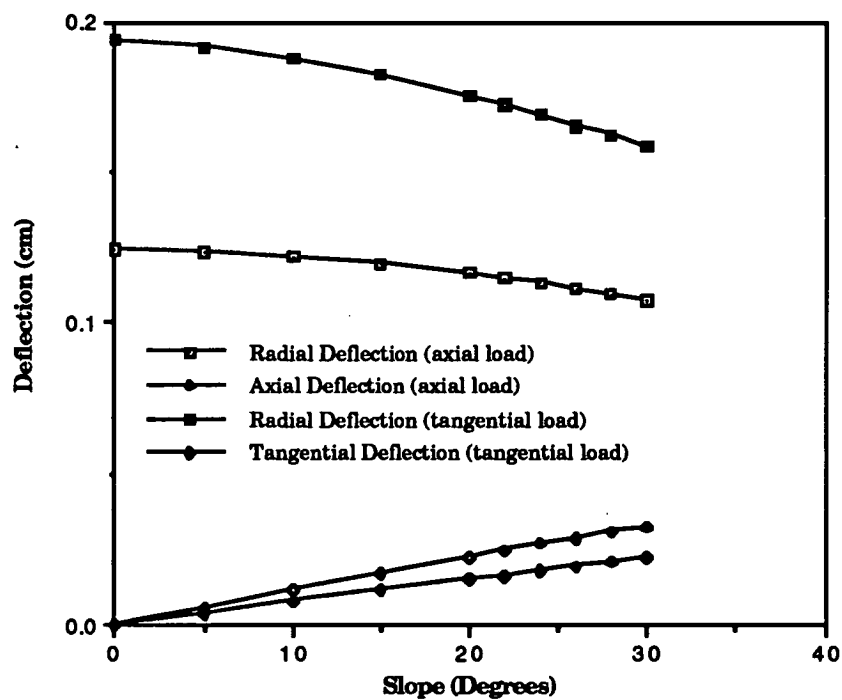
Figure 31 : Change in axial, tangential, and radial deflection for Hybrid II as a function of slope
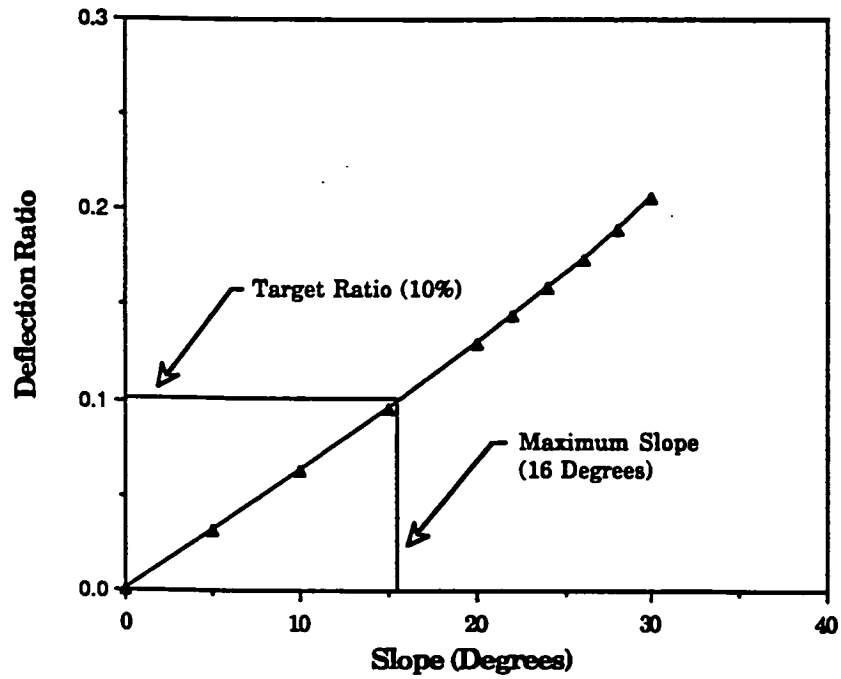
Figure 32 : Axial/radial deflection ratio as a function of slope for Hybrid II
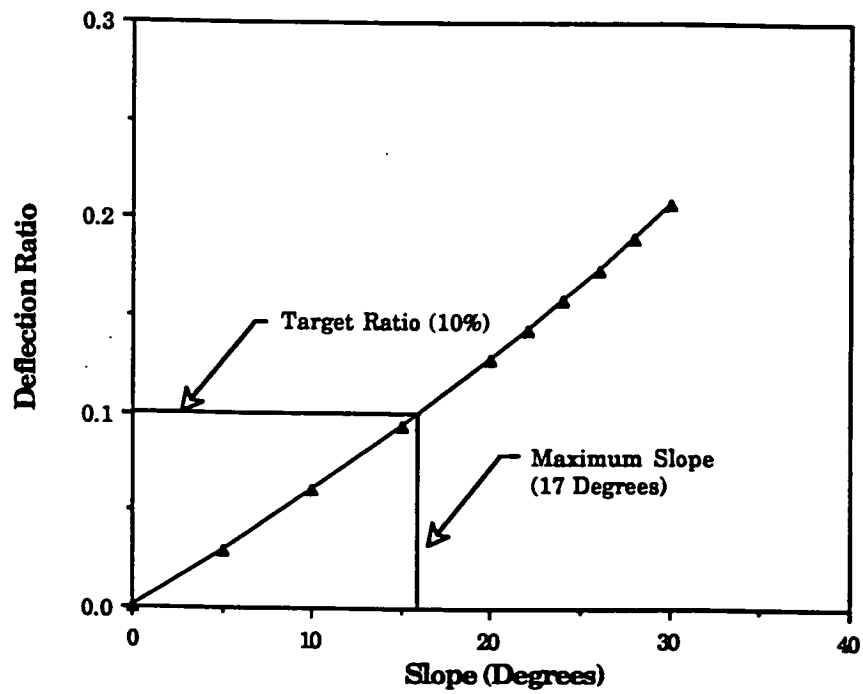
Figure 33 : Tangential/radial deflection ratio as a function of slope for
Hybrid II
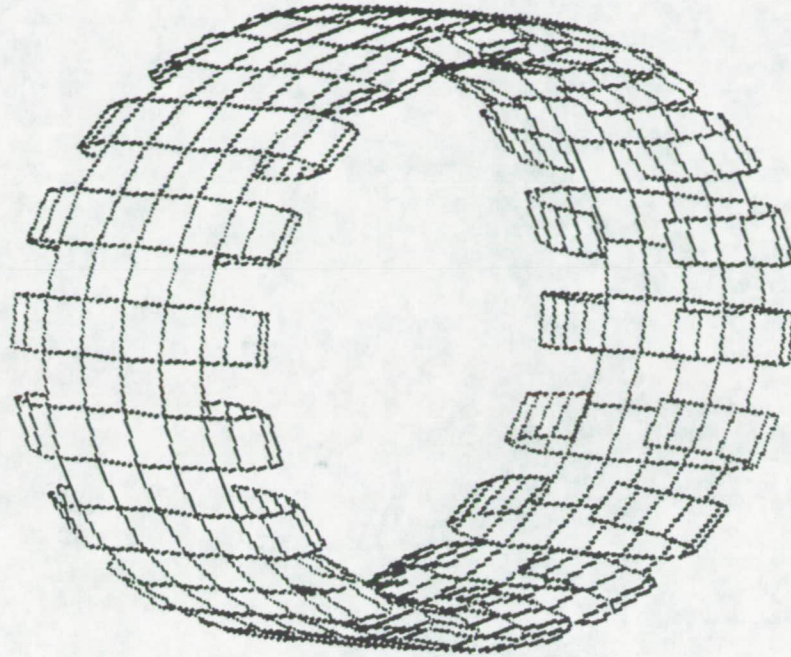
Figure 34 : Final configuration of the FEA Hybrid II wheel model

3.5 Cost

Material and assembly cost for the wheel will be a small fraction of the total cost. The largest expense will come from testing and development of the rover wheel. WES estimated these costs to be approximately $280,000 [27]. This figure includes the building and testing of the prototype, as well as development and testing of a martian soil simulant. Cryogenic testing of the Pellethane will start at $2000 and could go as high as $20,000 [21]. Miscellaneous costs include additional engineering time and injection wheel molds. The actual cost per wheel will depend upon the test results and the number of wheels needed. The design team estimates the total cost of the project to be $600,000 (Appendix K).

IV. Conclusion and Recommendations

4.1 Conclusion

The design team developed the geometry of the Hybrid Wheel using a combination of non-dimensional and finite element analysis techniques. Although this shape will require further refinement through empirical testing and iteration of the modeling process, a suitable shape for the wheel has been determined. The PAL models clearly illustrate the importance of choosing the correct wheel cross-section, and its role in controlling deflection.

4.2 Recommendations

Wheel geometry is strongly dependent upon soil properties. Before wheel optimization may begin, a soil approximating the mechanical properties of martian sand must be found or manufactured. A soil with the correct properties are needed in order to evaluate the performance of the Hybrid II wheel. Evaluation procedures based on the methods utilized by WES are recommended.

Empirical testing of 12.7 cm wheels in the martian soil simulant is required for a more accurate derivation of the correct wheel dimensions. The information contained in this report concerning wheel deflection and width was based upon a compilation of different analytical solutions. The coefficients appearing in these analytical solutions were derived through

empirical testing of large wheels. Although analysis based on the larger wheels was used in this report, further testing on 12.7 cm wheels will give more accurate results.

Single and multi-wheel testing should be performed to optimize the geometry of the wheels. Multi-wheel testing is recommended to determine the effects of a wheel following in the track of a preceding wheel. If the front wheels break the surface crust, the conditions encountered by the rear wheelsets will be dramatically different.

The Pellethane resin chosen for the composite construction of the Hybrid Wheel was the most suitable material found by the group. Another type of resin, liquid silicone rubber (LSR), shows promise as a replacement for the Pellethane. LSR is a much better choice than the Pellethane if it is used above its T_g. LSR exhibits elastic behavior at cryogenic temperatures until hitting its transition temperature, at which point it behaves like quartz glass. The design team decided against the use of LSR because the low temperature on Mars is below 130K and the T_g of LSR is approximately 160K. If the wheel were operated below this transition temperature, it would behave as a rigid member. Although brittle failure would not be a problem given the design thickness and load, the compliance of the wheel would be lost. Preliminary research at Dow Corning indicates that the T_g of their Silastic 598 LSR resin can be lowered to near 140K by the addition of a phenyl stabilizer [28]. The design team recommends investigating the possibilities of lowering the T_g of this material to 130K. It may be possible to use this material if the mission is limited to the more temperate regions of the planet.

Material testing at cryogenic temperatures is recommended regardless of the resin chosen. Fatigue, wear, thermal cycling, and the effects of radiation should be investigated to ensure that the material will perform reliably over its lifespan.

The selection of an anisotropic material for the final design exceeds the capabilities of the PAL software. The design team recommends the use of NASTRAN software to further analyze the Hybrid Wheel. The model file assembled for the PAL program may be imported into NASTRAN, with the addition of a compliance matrix added to define the anisotropic material properties. The NASTRAN model will take into account the composite material's directionally dependent properties, and allow manipulation of these properties to further reduce axial and tangential deflections.

References

1. Clayton R. Koppes, *JPL and the American Space Program: A History of the JPL*, New Haven, New York, 1982.

2. Carol Stoker, *The Case for Mars III: Strategies for Exploration-Technical*, Science and Technology Series Vol. 75, American Astronautical Society, San Diego, California, 1987.

3. Carol Stoker, *The Case for Mars III: Strategies for Exploration-Technical*, Science and Technology Series Vol. 74, American Astronautical Society, San Diego, California, 1987.

4. R E. Smith, G. S. West, *Space and Planetary Environmental Criteria Guideline for Use in Space Vehicle Development*, NASA, 1982.

5. G. Turnage, D. Banks, *Lunar Surface Mobility Studies Past and Future*, U.S. Army Waterways Experimental Station, Vicksburg, Mississippi, 1989.

6. D. Bickler, Jet Propulsion Laboratory, 4800 Oak Grove, Pasadena, California 91109, (818) 354-5488, Sept. 1991, personal conversation.

7. M. G. Bekker, *Off-the-Road Locomotion*, The University of Michigan, Ann Arbor, Michigan, 1960.

8. C. Ruoff, B. Wilcox, G. Klein, "Designing a Mars Surface Rover," Aerospace America. November 1985. Vol. 54.

9. D. Van Nostrand, *Principles of Guided Missile Design,* Princeton, New Jersey, 1962.

10. G. Pahl, W. Beitz, *Engineering Design, a Systematic Approach*, Springer-Verlag, London, 1988.

11. H. Franklin, The University of Texas at Austin, Mechanical Engineering Machine Shop, Austin, Texas 78712-1063, (512) 471-5388, November 1991, personal conversation.

12. M. G. Bekker, *Introduction to Terrain-Vehicle Systems*, The University of Michigan, Ann Arbor, Michigan, 1969.

13. D. Frietag, A. Green, K. Melzer, *Performance Evaluation of Wheels for Lunar Vehicles*, U.S. Army Waterways Experimental Station, Vicksburg, Mississippi, 1970.

14. G. Sitkei, *The Bulldozing Resistance of Towed Rigid Wheels in Loose Sand*, The Journal of Terramechanics, Pergamon Press, New York, New York,Vol. 23, 1966.

15. G. Turnage, *Performance of Soils Under Tire Loads*, U.S. Army Waterways Experimental Station, Vicksburg, Mississippi, 1972.

16. T. Patin, *Performance of Soils Under Tire Loads ; Extension of Mobility Prediction Procedures to Rectangular-Cross-Section Tires in Coarse Grained Soil*, Technical Report No. 3-666, April, U.S. Army Waterways Experimental Station, Vicksburg, Mississippi, 1972.

17. S. Lee, *International Encyclopedia of Composites*, Vol. 2, VCH Publishers, New York, New York, 1990.

18. G. Rylander, The University of Texas at Austin, Mechanical Engineering Department, Austin, Texas 78712-1063, (512) 471-3044, November 1991, personal conversation.

19. S. Lee, *International Encyclopedia of Composites*, Vol. 1, VCH Publishers, New York, New York, 1990.

20. "Kevlar - The Uncommon Material for Uncommon Solutions," Brochure No. H-05500-I, Du Pont Company, G-51400, Wilmington Delaware 19880-0023.

21. R. Oertel, Dow Chemical Company, Plastics TS&D, Midland, Michigan, 48667, October 1991, personal conversation.

22. K. Freidrich, *Friction and Wear of Polymer Composites*, Elsevier Publishing, New York, New York, 1986.

23. G. Luben, *The Handbook of Composites*, Van Norstrand Reinhold Publishing, 1982.

24. M. Callaghan, *Use of Resin Composites for Cryogenic Tankage*, Cryogenics, Vol. 31, April, 1991.

25. A. Wahl, *Mechanical Springs*, Second Edition,Mcgraw-Hill,New York, 1963

26. A. Traver, The University of Texas at Austin, Mechanical Engineering Department, Austin, Texas 78712-1063, (512) 471-3059, November 1991, personal conversation.

27. D. Willoughby, U.S. Army Waterways Experimental Station, Vicksburg, Mississippi, (601) 634-2447, November 1991, personal conversation.

28. K. Larson, Applications Engineer, Dow Corning Corporation, Midland, Michigan, 48686-0995, November 1991, personal conversation.

Appendix A
Patent List

Shown below is a listing of the relevant patents found by the design team. Most of these patents were found under the heading, 'spring wheel'. Copies of two patents that resemble alternative designs are also included. The quality of the original copies was poor. If better copies are desired, the reader can contact the U.S. Patent Office.

Patent Number	Title
3,424,259	Vehicle with Inclined Wheels
3,459,454	Elliptical Wheel
3,465,804	Cushioned Wheel
3,620,278	Hybrid Pneumatic-Mechanical Variable Configuration Wheel
3,746,112	Directionally Stable Self Propelled Vehicle
3,746,331	Annular Springs
3,746,658	Flexible Sectional Wheel
3,763,910	Resilient Wheel
3,814,157	Non-Pneumatic Vehicle Wheel
3,821,995	Vehicle with Composite Wheel
3,876,255	Wheels for a Course Stable Self-Propelling Vehicle Movable in any Desired Direction on the Ground or Some Other Base
3,957,101	Punctureproof Tire
4,026,342	Spring Wheel Having an Overload Stop
4,031,937	Unitary Tire Wheel
4,093,299	Articulated Railway Service Wheel and Unitary Railway Hub and Axle
4,240,483	Spoked Wheel
4,535,827	Molded Shock-Absorbing Wheel Assembly
4,549,590	Resilient Wheels
4,553,577	Wheel Structure with Resilient Spokes
4,635,990	Resilient Wheel of a Railway Car

Patent Number	Title
4,739,810	Convoluted Cone Wheel
4,782,875	Ground Engaging Wheels for Vehicles
4,785,899	Vehicle with Spherical Shaped Wheels for Steering and Speed Control Purposes
4,867,217	Nonpneumatic Elastic Tire
4,878,525	Epicycloid Rolling Resistance Abatement
4,919,489	Cog-Augmented Wheel for Obstacle Negotiation
4,919,490	Vehicle Wheel
4,963,083	Composite Metal-Elastomer Styled Wheels and Method and Apparatus for Molding the Same

United States Patent [19]

Hawes

[11] 3,763,910

[45] Oct. 9, 1973

[54] **RESILIENT WHEEL**

[76] Inventor: **Edward M. Hawes**, 32418 Birkshire, St. Clair Shores, Mich. 48082

[22] Filed: **Dec. 23, 1971**

[21] Appl. No.: 211,589

[52] U.S. Cl. 152/14, 152/92
[51] Int. Cl. B60b 9/06
[58] Field of Search 152/14, 92

[56] **References Cited**
UNITED STATES PATENTS

,146,289   7/1915   Shook 152/92

854,655   5/1907   Krell 152/92
2,403,690   7/1966   Stanley 152/92

Primary Examiner—James B. Marbert
Attorney—Donald P. Bush

[57] **ABSTRACT**

A wheel in which the load bearing portion adapted to engage the ground is essentially in the form of a multiplicity of spring convolutions. In a preferred form these convolutions form parts of a continuous helically coiled spring bent to extend around the periphery of the central portion of the wheel.
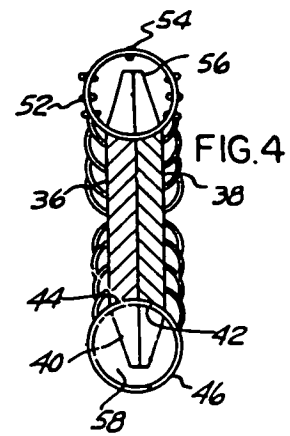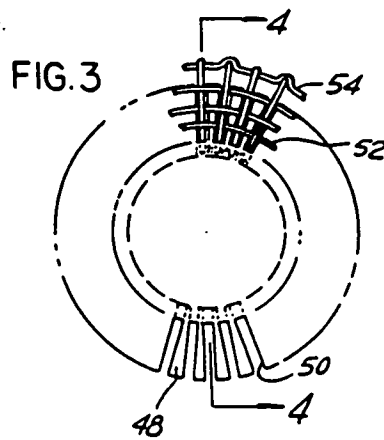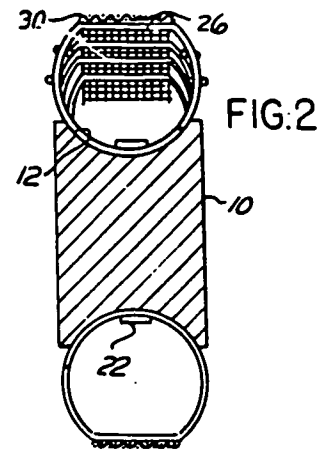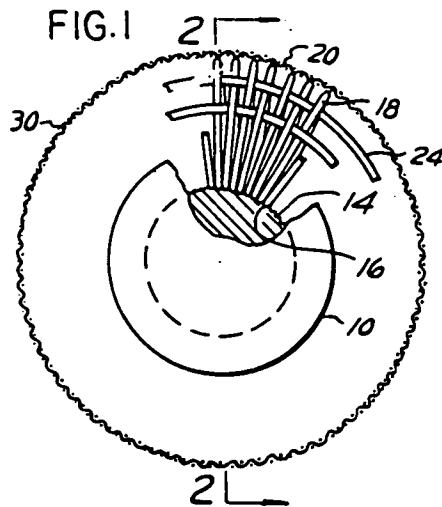
14 Claims, 7 Drawing Figures

FIG.1

FIG:2

FIG.3

FIG.4

FIG.5

FIG.6

FIG.7

1
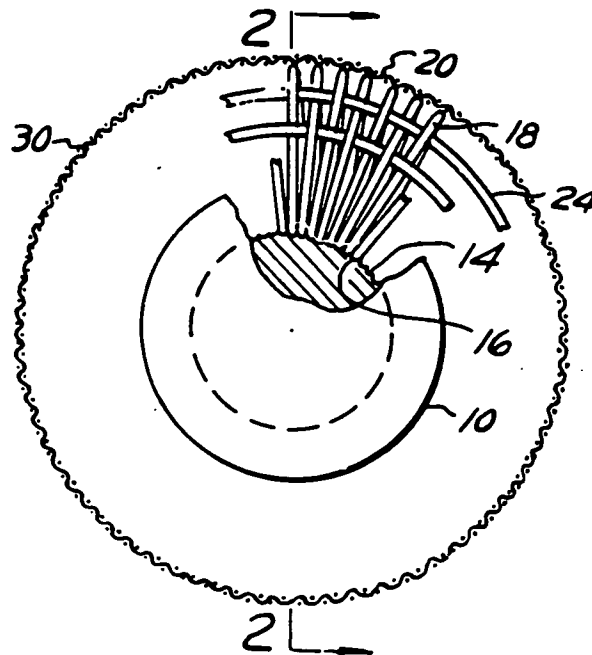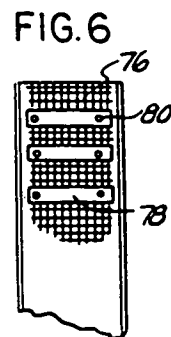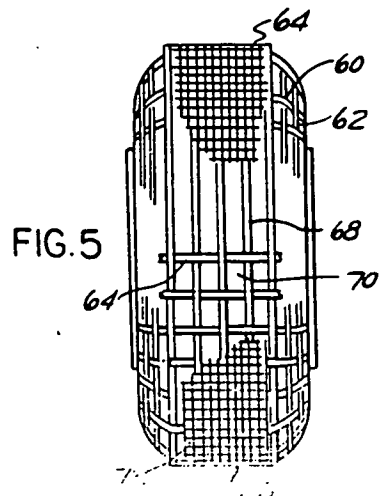
RESILIENT WHEEL

BRIEF SUMMARY OF THE INVENTION

The present invention relates to a wheel intended generally for use on sand, loose dirt, mud, or other similar terrain.

In its simplest form the invention comprises a wheel having a circular central portion and provided with a tread or ground engaging load supporting surface in the form of a multiplicity of spring convolutions. Conveniently, these spring convolutions may be provided by bending a helically coiled spring around the periphery of the wheel in the position normally occupied by the tire.

Since the spring convolutions at the outer periphery of the wheel are spaced apart they become embedded into the loose material of the terrain which therefore enters into the annular space defined by the complete series of convolutions. In a preferred form of the invention the supporting wheel is provided with a tapered peripheral portion which extends substantially into the annular space defined by the complete series of spring convolutions, the radially inwardly diverging sides serving to guide the material forced into the spring assembly by ground pressure outwardly as the wheel turns, thus tending to keep the interior of the spring or the annular space defined by the spring, substantially clear of ground material.

Preferably, means are provided extending around the spring assembly tending to maintain the adjacent convolutions against individual circumferential displacement so as to maintain the designed spacing therebetween under service conditions. In addition, the convolutions may be designed to define a substantially cylindrical outer surface which in turn establishes a great area of contact with the ground, and further, reduces excessive wear centrally of the spring convolutions.

In some cases it is desirable to cover the outer peripheral envelope defined by the spring convolutions with a relatively coarse screen material, which will contribute to support of the spring structure in sand, soft ground, mud, or the like.

Finally, traction may be increased by providing transversely extending ground engaging cleats.

BRIEF DESCRIPTION OF THE DRAWINGS

FIG. 1 is a fragmentary more or less diagrammatic elevational view of a wheel assembly constructed in accordance with the present invention.

FIG. 2 is a fragmentary sectional view on the line 2—2, FIG. 1.

FIG. 3 is a fragmentary elevational view of another embodiment of the invention, with parts broken away.

FIG. 4 is a sectional view on the line 4—4, FIG. 3.

FIG. 5 is a side elevational view of a wheel assembly representing a further embodiment of the present invention.

FIG. 6 is a fragmentary elevational view illustrating the application of cleats to the tread structure.

FIG. 7 is a fragmentary end view of the structure shown in FIG. 6.

DETAILED DESCRIPTION

Referring first to FIGS. 1 and 2, the central portion of the wheel assembly is indicated diagrammatically at 10 as a generally circular block having a peripheral annular groove 12 extending therearound. It will of

2

course be understood that in practice the wheel proper will be provided with the usual structure permitting attachment to rotatable wheel supporting structure, but this forms no part of the present invention and is omitted for the purpose of simplifying the present disclosure.

As previously indicated in FIG. 1 the peripheral annular groove 12 is formed with its surface suitably corrugated as indicated at 14 to receive the inner portions 16 of the individual convolutions 18 of the spring structure. The spring structure initially may be in the form of a helically coiled straight spring in which the adjacent convolutions are somewhat spaced apart. The helical spring then is bent to extend circumferentially around the wheel portion 10 with the result that the inner portions 16 of the convolutions are brought toward each other. As illustrated in FIG. 1, the inner portions 16 of the convolutions may be brought into actually circumferential engagement or alternatively, they may remain slightly spaced apart. In any case, due to the curvature of the coil spring into a circular shape, the outer portions of the spring convolutions as indicated at 20 are moved apart to a separation greater than occurs in the straight helical spring.

Any suitable means may be provided for establishing a permanent connection between the inner convolution portion 16 and the interfitting corrugated surface of the wheel 10. For example, the individual convolutions may be welded or brazed in place. Alternatively, a mechanically engaging mounting ring indicated at 22 may extend around and engage the inner surfaces of the inner convolution portions 16. The ring 22 may have end structure adapted to overlap and to receive camming means effective to tighten the ring so as to press the inner convolutions of the spring into the corrugations 14. The structure illustrated in FIGS. 1 and 2 includes a multiplicity of circumferentially extending rings 24 which as shown are interlaced back and forth between adjacent convolutions, the adjacent rings 24 being disposed at opposite sides of each particular convolution, as best illustrated in FIG. 1. Again, the rings 24 may be permanently attached to the spring convolution in the position shown by suitable means such for example as welding, brazing, or the like.

The individual spring convolutions, as best seen in FIG. 2, are preferably not completely circular, but each includes a radially outer straight portion 26 adapted to have theoretical contact from end to end with the terrain when the structure is employed in supporting a vehicle. It will be appreciated that the complete envelope described by the multiplicity of straight convolution portions 26 is essentially cylindrical.

As best seen in the Figures, the extreme outer periphery of the spring tire assembly is provided with a relatively coarse screen structure 30 which in turn may be attached to the straight convolution portions 26 by suitable means such for example as welding, brazing or the like.

With the structure as above described, it will be apparent that when supporting a vehicle, and particularly a heavy vehicle, on soft terrain such as sand, loose dirt, mud or the like, the resilient wheel is capable of supporting the load, and due to the tying together of adjacent spring convolutions, the load will be distributed over a multiplicity of convolutions without permitting displacement of individual spring convolutions. The amount of penetration of the resilient wheel

3

into the terrain may be controlled by dimensions of the parts, particularly the coarseness of the screen 30 where such screen is provided.

In the simplest possible case the spring convolutions may be completely circular and the tying rings 24 and the screen 30 may be omitted. Alternatively, the tying rings 24 may be provided and the screen 30 omitted, or the screeen 20 may be provided and the tying ring 24 omitted, in which case the screen serves the dual function of controlling penetration and also tying adjacent convolutions together to prevent lateral displacement of individual convolutions.

The resilient wheel structure provided by bending the helically coiled spring into a circular or annular configuration, supported on the periphery of the inner wheel portion, also provides great stability against lateral displacement, particularly when the inner portion of the spring assembly is received in an annular channel of arcuate cross-section, as best illustrated in FIG. 2.

Referring now to FIGS. 3 and 4 there is illustrated a further embodiment of the present invention. In this case the inner wheel portion indicated generally at 34, is composed of two circular or preferably annular elements 36 and 38 which are brought together in assembly and united to form a unitary structure. The peripheral portions 40 of the rings 36 and 38 are tapered and are slotted, the bottoms of the slots as indicated at 42 being of arcuate cross-section so as to receive and closely interfit with the inner portions 44 of the spring convolutions 46. With this arrangement the inner convolution portions 46 are fully supported against circumferential movement by the material 48 intermediate and defining the slots 50 which receive the individual spring convolutions. In assembly, the coil spring may be bent into the circular configuration shown and the two wheel portions 36 and 38 assembled by movement toward each other into the position illustrated in FIG. 4. The ends of the helically coiled spring may be united by suitable means such for example as welding, or by reception in a tubular connecting element (not shown).

As best seen in FIG. 4 the slots 50 are radial and are of a uniform width such as to receive the wire of the convolutions of the spring. As a result, the material 48 intermediate adjacent convolutions is tapered and of outwardly increasing circumferential dimension.

As best seen in FIG. 3, the convolutions 46 of the spring may be fully circular although it is also contemplated that they may be straight across their outer peripheral port. on in the same manner as the straight portions 26 of the spring shown in FIG. 2. Again, the convolutions are interconnected by rings indicated at 52 which are preferably interleaved intermittently inwardly and outwardly of the convolutions, as best illustrated in FIG. 3. As indicated in these Figures, three rings are provided at each side of the resilient wheel assembly and a single ring 54 is provided centrally of the wheel at its outer periphery.

The construction illustrated in FIGS. 3 and 4 provides the radially outwardly extending tapered wheel portion indicated in its entirety at 56 which extends substantially into the hollow interior of the resilient wheel support structure. This wheel portion 56 ... extending into the hollow in- ... ...

4

ground pressure as the vehicle moves over the terrain.

While in FIGS. 3 and 4, no screen such as the screen 30 of FIGS. 1 and 2 is illustrated, it will of course be appreciated that if desired screen material of this type may be applied over the outer transversely curved peripheral surface of the resilient wheel assembly

FIG. 5 is a side elevation of a wheel somewhat similar to that shown in FIG. 2, in which the convolutions of the main wheel supporting structure are indicated at 60 and are interleaved with annular wire rings 62 substantially similar to the rings 52 disclosed in FIG. 3, and the rings 24 disclosed in FIG. 1. In this case the radially outer portion of each convolution is relatively straight as indicated at 64 so as to provide a substantially cylindrical envelope 66, of the general configuration illustrated in FIG. 2. In this case however, the generally flat convolution portions are interlaced with circumferentially extending rings 68 which are provided in over and under relation to define the generally recticulate form best illustrated at 70. In many cases this will be the final condition of the wheel assembly although it is contemplated that if desired a relatively coarse screen as indicated at 72, may be provided to overlie the interlaced spring convolutions, and circular tie rings 68. This will in general be a matter of choice depending upon the terrain for which the resilient wheel is designed.

Referring to FIGS. 6 and 7 there is illustrated a further modification which may be applied generally to any of the wheel previously described. In these Figures the wheels are illustrated as supplied around their outer periphery with the screen material 76 and to provide for increased traction transversely extending cleats 78 are provided with may be attached by any suitable means such for example as rivets or threaded fasteners indicated diagrammatically at 80. While in FIGS. 6 and 7 the transversely extending cleats are indicated as straight and as applied to the cylindrical outer wheel surface such as illustrated in FIGS. 2 and 5, it will be appreciated that the cleats may be arcuately curved if desired and applied to the outer transversely curved surface of the wheel such as the wheel illustrated in FIGS. 3 and 4, particularly when supplied with screen material thereover.

The resilient spring structure provided at the periphery of the wheel assembly is not only effective to support the load and to provide traction, but it is effective to withstand the tangential force applied when the wheels provided with the resilient spring portions at the periphery are driving wheels. This function is enhanced where adjacent convolutions are interconnected by the tie rings illustrated in the several embodiments of the invention.

Conveniently, the springs employed to provide the adjacent spring convolutions may be formed from spring wire of circular cross-section suitably compounded and tempered to produce adequate wear resistance, resilience, and strength to withstand the anticipated loads due to the weight of the vehicle, tangential force applied in driving the wheels, and lateral and other forces applied as a result of turning of the vehicle and/or turning of the wheels relative to the vehicle as in steering.

In all cases, the outer portions of the convolutions provide an annular series of circumferentially generally transversely extending ...
ground engaging elements
... ...

1. A resilient vehicle wheel assembly comprising a rigid central wheel portion, and a ground engaging load sustaining drive transmitting resilient portion in the form of a series of circumferentially spaced spring wire convolutions extending around the periphery of the assembly and providing an annular series of circumferentially spaced, generally transversely extending, resiliently supported ground engaging elements.

2. An assembly as defined in claim 1 in which said convolutions are parts of a helically coiled wire spring bent into overall annular shape.

3. An assembly as defined in claim 2 comprising in addition means securing the radially inner portions of each convolution to the outer periphery of the central wheel portion.

4. An assembly as defined in claim 3 in which the periphery of the central wheel portion is slotted to leave radially outwardly extending fingers intermediate the slots, said fingers being shaped to assist in expelling ground material forced into the interior annular space defined by said spring convolutions.

5. An assembly as defined in claim 1 comprising in addition annular means connected to each convolution to form tie supports preventing relative circumferential displacement between adjacent convolutions.

6. An assembly as defined in claim 5 in which said annular means comprises wires connected to the side portions of said convolutions.

7. An assembly as defined in claim 6 in which said wires are disposed in alternate inside and outside relation with the series of spring convolutions.

8. An assembly as defined in claim 7 which comprises in addition a screen tread portion secured around the outer periphery of the assembly.

9. An assembly as defined in claim 5 in which said an-

nular means comprises a screen tread portion secured around the outer periphery of the assembly.

10. An assembly as defined in claim 9 comprising in addition a multiplicity of separate transversely extending cleats secured to the peripheral portion of said assembly outwardly of the screen tread portions.

11. A group engaging vehicle wheel for use on soft loose terrain such as loose sand, soil, and the like comprising a rigid rim, a multiplicity of resilient support elements extending outwardly from both edges of said rim, said elements being curved to present outwardly convex surfaces at both sides of said wheel, and an outer ground engaging tread portion comprising a multiplicity of elongated circumferentially spaced tread elements operatively connected to and supported by said support elements.

12. A wheel as defined in claim 11 wherein the spacing between adjacent tread elements is greater than the width of said tread elements measured in a circumferential direction.

13. A wheel as defined in claim 11 in which said ground engaging tread portion comprises a multiplicity of elongated spaced tread elements extending at an angle to said first mentioned tread elements, and connected thereto to form therewith an open mesh structure having openings through which particulate terrain material may pass.

14. A vehicle wheel assembly for use on soft loose terrain such as sand, soil, and the like comprising a rigid rim, a ground engaging drive transmitting tread portion including a series of circumferentially spaced spring wire elements, and means connecting said tread portion to said rim and resiliently supporting said tread portion in spaced surrounding relation to said rim.

* * * * *

40

45

50

55

60

65

[54] SPRING WHEEL HAVING AN OVERLOAD STOP

[76] Inventor: James D. Wormley, 11010 Palmeras Drive, Sun City, Ariz. 85351

[22] Filed: Nov. 17, 1975

[21] Appl. No.: 632,535

[52] U.S. Cl. 152/18; 152/19; 152/73

[51] Int. Cl.² B60B 9/04

[58] Field of Search .... 301/5 R, 8; 152/18–19, 152/73, 76, 79

[56] References Cited

UNITED STATES PATENTS

847,099	3/1907	Nelson	152/73
1,001,753	8/1911	Goldsmith	152/19
1,040,426	10/1912	Sanders	152/19 X
1,049,129	12/1912	Moore	152/73 X
1,130,762	3/1915	Pirtle	152/19 X

FOREIGN PATENTS OR APPLICATIONS

803,743	4/1951	Germany	152/73
16,010	8/1895	United Kingdom	301/8
10,195	5/1906	United Kingdom	152/73

Primary Examiner—Robert B. Reeves
Assistant Examiner—Charles A. Marmor
Attorney, Agent, or Firm—Edward Hoopes, III

[57] ABSTRACT

A wheel comprising a hub element, a rim element, a plurality of substantially circular bands of flexible material spaced about the hub element interposed between and bearing against both of the elements, the axes of the bands being parallel to the axes of the elements, and fastening devices fastening the bands of flexible material to the elements, each fastening device being mounted at its end portions on one of the elements and at its mid-portion engaging one of the bands on the inner peripheral surface thereof only to clamp the band against the element, the bands of flexible material being spaced apart so as at all times to act freely individually and flexing to provide a cushioning effect when the wheel rolls over rough terrain.
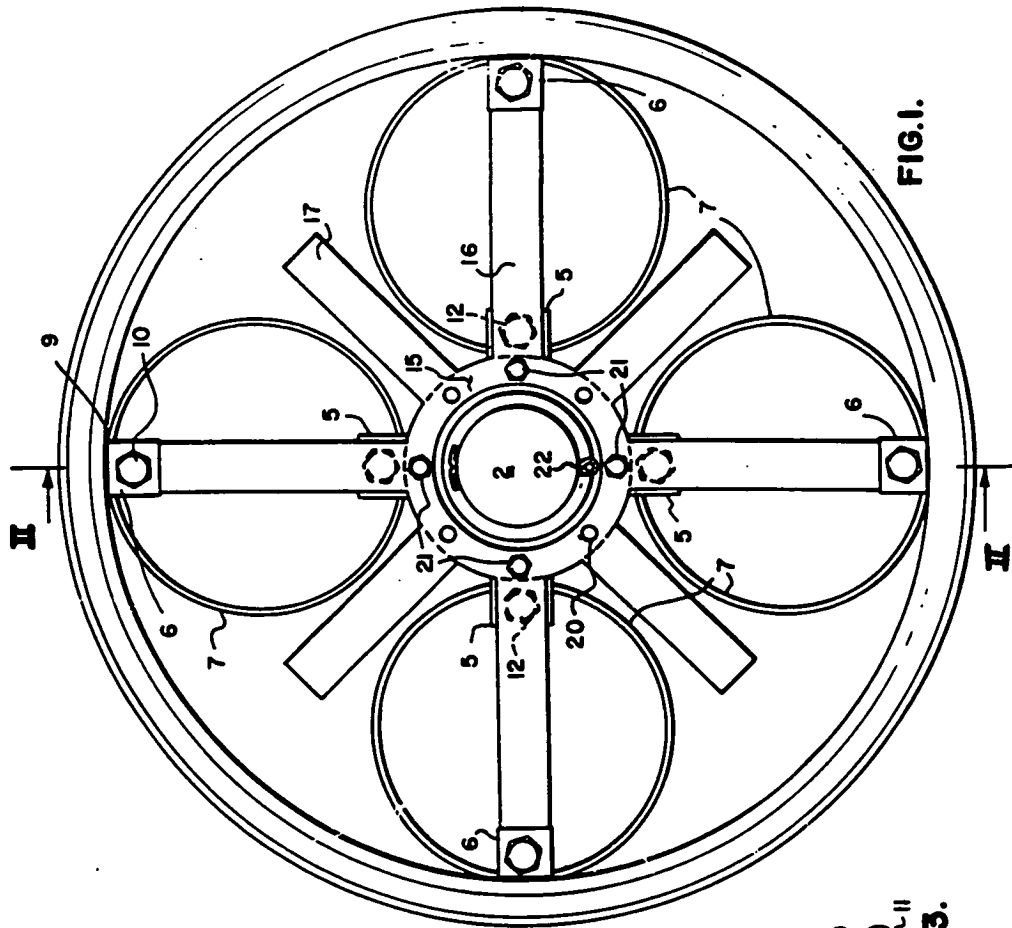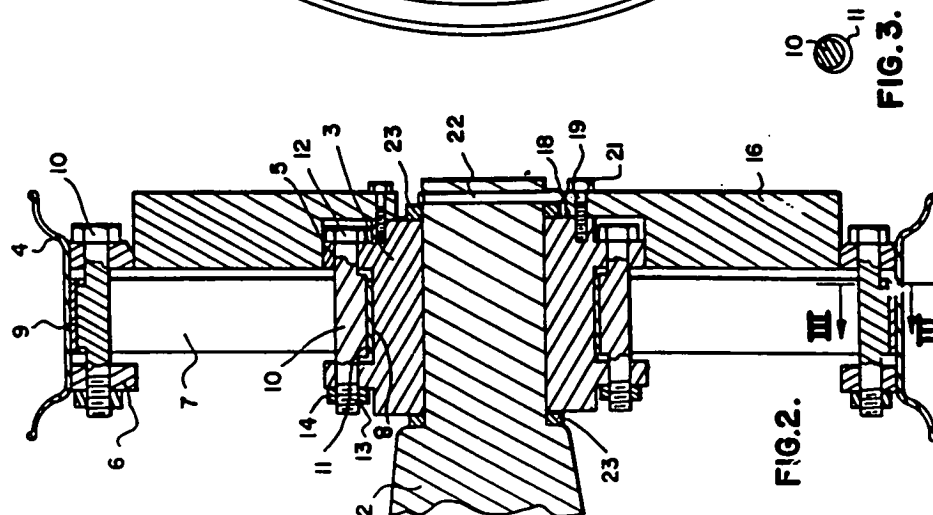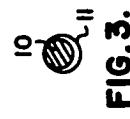
2 Claims, 3 Drawing Figures

FIG.I.
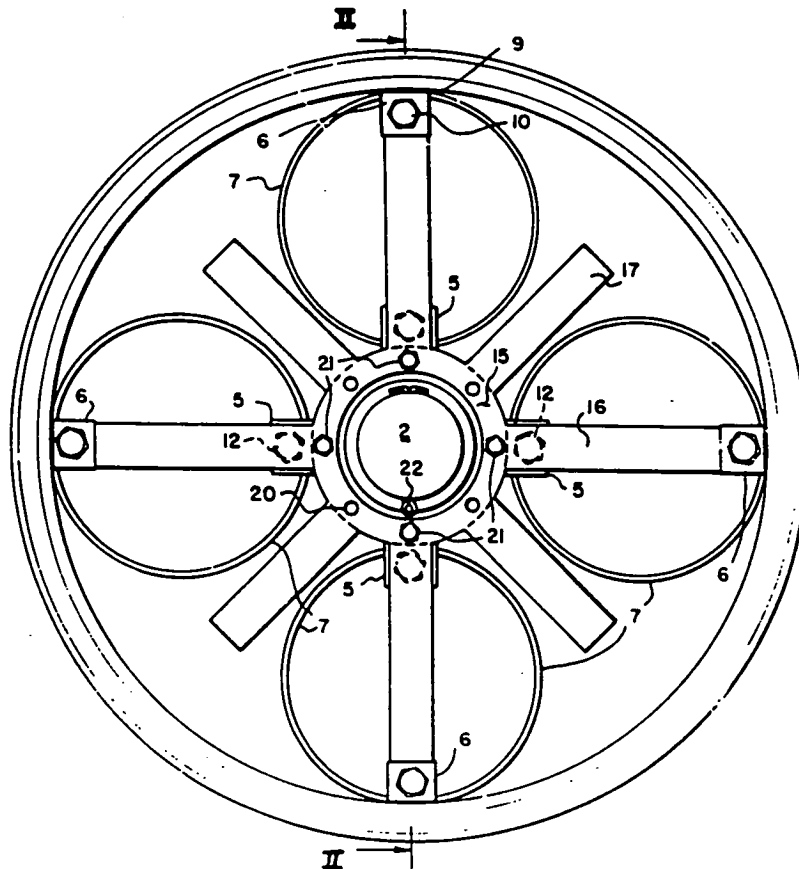
FIG.3.

FIG.2.

SPRING WHEEL HAVING AN OVERLOAD STOP

This invention relates to a wheel of the type having bands of flexible material interposed between the hub and rim to provide a cushioning or springing effect when the wheel rolls over rough terrain. The invention has to do particularly with the provision of improved means for fastening the bands to the hub and rim whereby important new and useful results are achieved, and also with the provision of means operable when a cushioning or springing effect is not desired to rigidly connect the hub and rim to provide in effect a conventional wheel.

Heretofore in wheels having bands of flexible material interposed between the hub and rim the bands have been maintained in place by rivets, bolts or screws penetrating the bands. When a band is punctured to provide a hole for a fastener such as a rivet, screw or bolt an area of stress concentration during springing cycles is created around the edge of the hole and around the head of the fastener or fastener-keeper reducing the strength, durability and springiness of the band and also the ability of the band to withstand side thrust forces. Also band replacement is rendered difficult and in some cases impossible.

I have obviated the disadvantages above stated by the provision of novel means for fastening the bands to the hub and rim elements. I provide fastening devices each mounted on one of the hub and rim elements and engaging one of the bands on the inner peripheral surface thereof only to clamp the band against the element. Preferably each fastening device passes within the band and is carried by the hub element or rim element at opposite sides of the band. Each fastening device may engage the band across the full width of the inner peripheral surface thereof. Each fastening device may have a lateral protuberance within the band which engages the band on the inner peripheral surface thereof only, desirably in substantial line contact parallel to the axis of the band.

I also desirably provide the wheel with means operable when the cushioning effect is not desired to rigidly connect the hub element and rim element to provide in effect a conventional wheel. Such means may include spoke-like members positionable to maintain the hub element and rim element in relatively fixed position. Desirably a device is provided which is fastenable to the hub element in a plurality of positions in one of which the hub element and rim element are rigidly connected and in another of which the hub element and rim element are not rigidly connected. The device may have means predeterminedly limiting the extent of flexing of the bands when the device is fastened to the hub element in the position in which the hub element and rim element are not rigidly connected.

Other details, objects and advantages of the invention will become apparent as the following description of a present preferred embodiment thereof proceeds.

In the accompanying drawings I have shown a present preferred embodiment of the invention in which

FIG. 1 is a face view of a wheel embodying the invention;

FIG. 2 is an axial cross-sectional view taken on the line II—II of FIG. 1; and

FIG. 3 is a detail cross sectional view taken on the line III—III of FIG. 2.

Referring now more particularly to the drawings, there is shown an axle designated generally by reference numeral 2 on which is rotatably mounted a wheel constructed in accordance with my invention. The wheel comprises a hub 3 and a rim 4. In the form shown the hub 3 has four pairs of axially opposed outwardly extending radial projections 5 and the rim 4 has four pairs of axially opposed inwardly extending radial projections 6. Each pair of projections 5 on the hub is in radial alignment with one of the pairs of radial projections 6 on the rim. Disposed within each of such sets of radial projections 5 and 6, as clearly shown in FIG. 2, is a circular band 7 of flexible or yieldable material which may be spring steel, plastic or other material having the requisite flexing or yielding property. Each band 7 abuts against the hub 3 at 8 and abuts against the rim 4 at 9 (FIG. 2). A fastening device in the form of a pin 10 is mounted in each of the pairs of projections 5 and 6 and passes within the band 7 which is disposed between those projections as clearly shown in FIG. 2. Each pin 10 has a lateral protuberance 11 within the band which is adapted to engage the band on the inner peripheral surface thereof across the full width of the band to clamp the band against the hub or rim. Each pin 10 has a head 12 at one end and is threaded at 13 at the opposite end to receive a nut 14 whereby the pin may be tightened in place. Before the nut is tightened the pin is turned so that the protuberance 11 extends radially outwardly of the band to tightly clamp the band to the hub or rim in substantially line contact parallel to the axis of the band.

The structure thus far described constitutes a yieldable wheel in which the bands flex to provide a cushioning effect when the wheel rolls over rough terrain. The bands are maintained in place without puncturing them to provide a hole for a fastener such as a rivet, screw or bolt which would create an area of stress concentration during yielding or springing cycles as above referred to. Also my wheel construction facilitates replacement of a band if a band after prolonged use loses its elasticity or becomes damaged or if a band of different width or other characteristics is to be installed.

As above stated, I provide means operable when the cushioning effect is not desired to rigidly connect the hub and rim of the wheel to provide in effect a conventional wheel. In the form shown such means comprises a spider 15 having a plurality of radially extending arms of different lengths. In the form shown the spider 15 has four relatively long arms 16 and four relatively short arms 17. As shown in FIG. 1 the arms 16 are spaced apart 90° and the arms 17 are spaced apart 90°, each arm of one length being exactly half way between adjacent arms of the other length.

The hub 3 is provided with four internally threaded bores 18 spaced apart 90° about the axis of the hub. The spider 15 has two sets of bores, these comprising bores 19 spaced apart 90° and bores 20 also spaced apart 90°. The bores 20 are exactly half way between adjacent bores 19. The bores 19 and 20 of the spider 15 are at the same distance radially outwardly from the axis of the wheel as are the bores 18 of the hub.

In the drawings the spider 15 is shown as being connected with the hub 3 by screws 21 which extend through the bores 19 of the spider and thread into the bores 18 of the hub. With the spider thus connected to the hub the longer arms 16 of the spider have their outer ends abutting the inner ends of projections 6 of

3

the rim so that the arms 16 prevent flexing or yielding of the bands 7 and in effect convert the wheel into a conventional rigid wheel.

When the wheel is to be converted from a conventional rigid wheel into a flexible or yieldable wheel the bolts 21 are removed and the spider is rotated 45° and is fastened to the hub by introducing the bolts 21 through the bores 20 of the spider and into the threaded bores 18 of the hub. This places the shorter arms 17 in alignment with projections 6 of the rim. When the wheel is not under load there is a space between the outer end of each arm 17 and one of the projections 6 of the rim so that the bands 7 are permitted to yield to a predetermined extent. The bands 7 yield until the outer ends of the arms 17 engage projections 6 of the rim whereafter further yielding of the bands is prevented. The length of the arms 17 may be determined so as to limit flexing or yielding of the bands to an extent within their elastic limit.

In the form shown when the shorter arms 17 of the spider are in radial alignment with projections 6 of the rim the longer arms 16 of the spider will engage the rim intermediate projections 6 at the same time as the outer ends of the arms 17 will engage projections 6 so actually my result can be obtained without utilizing the shorter arms 17 at all, relying on engagement of the longer arms 16 with the rim intermediate projections 6 of the rim to limit flexing of the bands within the elastic limit thereof. However, I prefer to employ a spider with both long and short arms as shown in FIG. 1 since both sets of arms will engage the rim at the same time creating a stronger and more stable wheel.

The wheel is maintained in place on the axle by a keeper 22 with washers 23 disposed about the axle at opposite faces of the hub 3 as shown in FIG. 2.

While I have shown and described a present preferred embodiment of the invention it is to be distinctly understood that the invention is not limited thereto but

4

may be otherwise variously embodied within the scope of the following claims.

I claim:

1. A wheel comprising a hub element, a rim element, a plurality of substantially circular bands of flexible material spaced about the hub element interposed between and bearing against both of said elements, the axes of the bands being parallel to the axes of said elements, fastening means fastening the bands of flexible material to said elements, the bands of flexible material being spaced apart so as to at all times act freely individually and normally flexing to provide a cushioning effect when the wheel rolls over rough terrain, and means within the confines of the wheel operable when such cushioning effect is not desired to rigidly connected the hub element and rim element to provide in effect a conventional wheel, said last mentioned means including substantially radial spoke-like members of different lengths selectively fastenable to the hub element in a first position in which the outer ends of the longer spoke-like members engage the rim element to rigidly connect the hub element and rim element and a second position in which the hub element and rim element are not rigidly connected and the outer ends of the shorter spoke-like members engage the rim element after predetermined flexing of the bands to limit the extent of such flexing.

2. A wheel as claimed in claim 1 in which the rim element has inwardly extending radial projections and said last mentioned means include substantially radial spoke-like members of different lengths selectively fastenable to the hub element in a first position in which the outer ends of the longer spoke-like members engage said inwardly extending radial projections to rigidly connect the hub element and rim element and a second position in which the hub element and rim element are not rigidly connected and the outer ends of the shorter spoke-like members engage said inwardly extending radial projections after predetermined flexing of the bands to limit the extent of such flexing.

* * * * *

45

50

55

60

65

Appendix B
Specification List And Function Structure

This appendix contains the specification list and function structure used to generate the alternative designs described in this report. A *D* or a *W* preceeds each specification indicating whether it is a desired requirement or merely a wish.
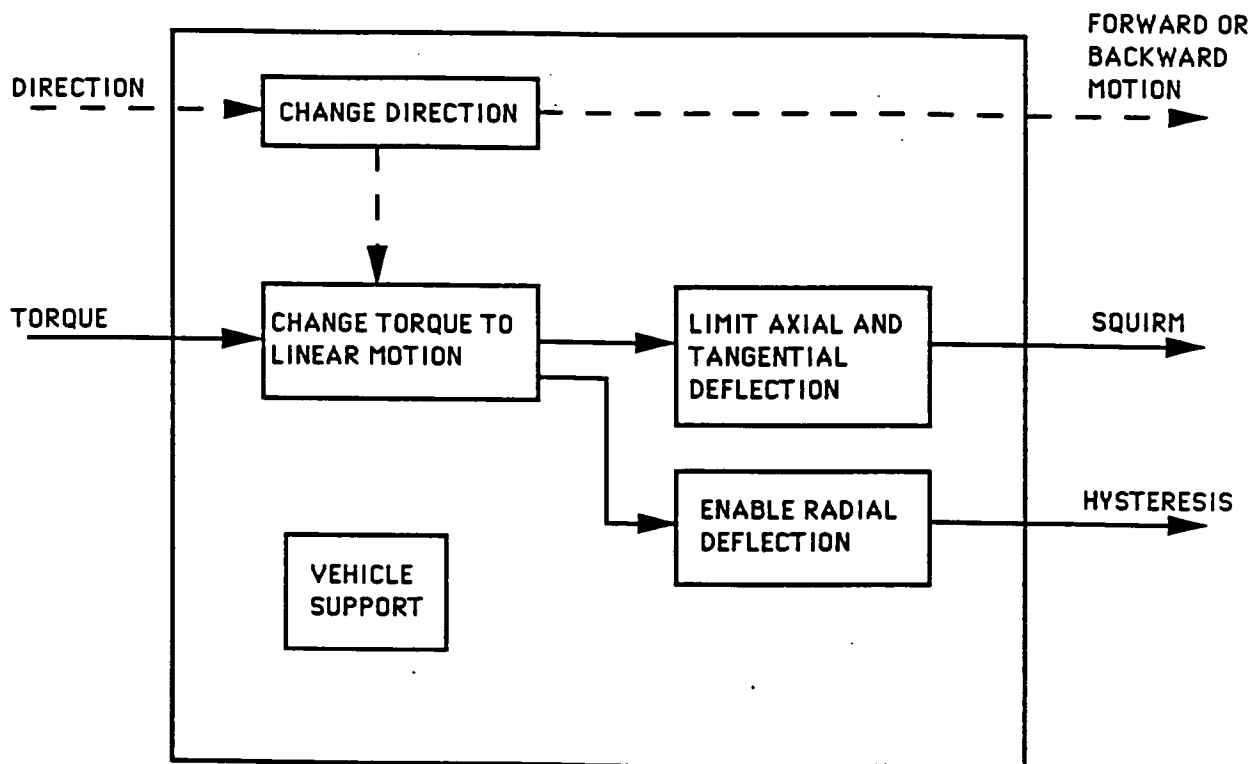
Specification List

D	1. Low mass
W	2. Collapsible
D	3. Cryogenic
D	4. 2.5 million cycles
D	5. Radiation exposure
D	6. Low pressure atmosphere
D	7. Abrasion resistant
D	8. Linear deflection in radial direction
D	9. Axial and tangential deflection no more than 10% of radial deflection
D	10. Resist wedging into smaller areas
D	11. 12.7 cm diameter
W	12. Damping
D	13. Low contact pressure
D	14. Forward and backward operation
D	15. High reliability for components
D	16. Infinite fatigue life
D	17. Maximum velocity will be 10 cm/s
D	18. Simple design- small number of components, low complexity
D	19. Must function with minor component damage
D	20. Cost is not a design factor
D	21. 'Good' traction in sand and rock
D	22. Squirm is minimized

D   23. Quantity of wheels needed will be number of rovers times six wheels per rover plus number needed for testing and evaluation

D   24. Components subject to surface wear will not puncture tear or cut

D   25. Maintenance free

D   26. Must survive two meter fall onto hard flat surface

D   27. Tire operation cannot damage rover

D   28. Reliability can only be improved by increasing mass after tolerances, manufacturing operations,quality control, etc have been optimized

W   29. Easily assembled

D   30. Fastening devices or adhesives must have same material properties as the materials being joined

Function structure

DIRECTION

CHANGE DIRECTION

FORWARD OR
BACKWARD
MOTION

TORQUE

CHANGE TORQUE TO
LINEAR MOTION

LIMIT AXIAL AND
TANGENTIAL
DEFLECTION

SQUIRM

ENABLE RADIAL
DEFLECTION

HYSTERESIS

VEHICLE
SUPPORT

Appendix C

Designs Not Evaluated

Designs not investigated by the design team are briefly described in this appendix.

Gun-Clip Wheel
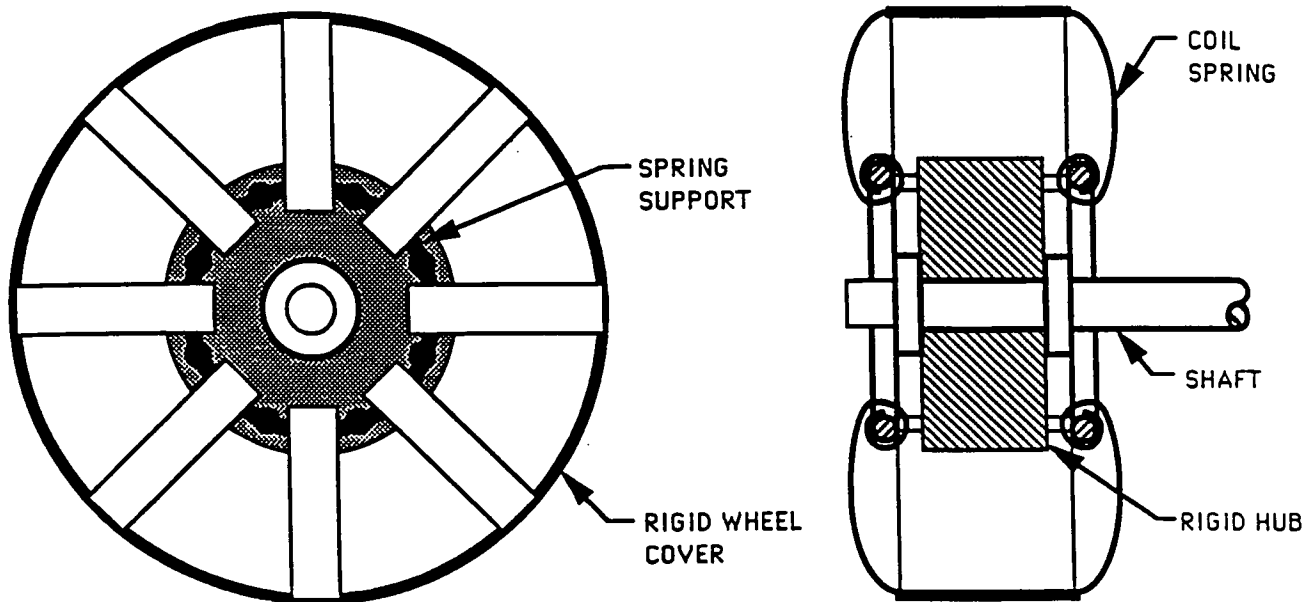
The Gun-Clip Wheel uses negator springs to suspend a rigid hub from the top of the wheel wear surface. The negator springs are flat coil springs resembling those found in the magazine clip of an automatic weapon. This design would resist tangential deflection, due to the orientation of the flat springs but this design would be weak axially.

Flexible Hoop Wheel
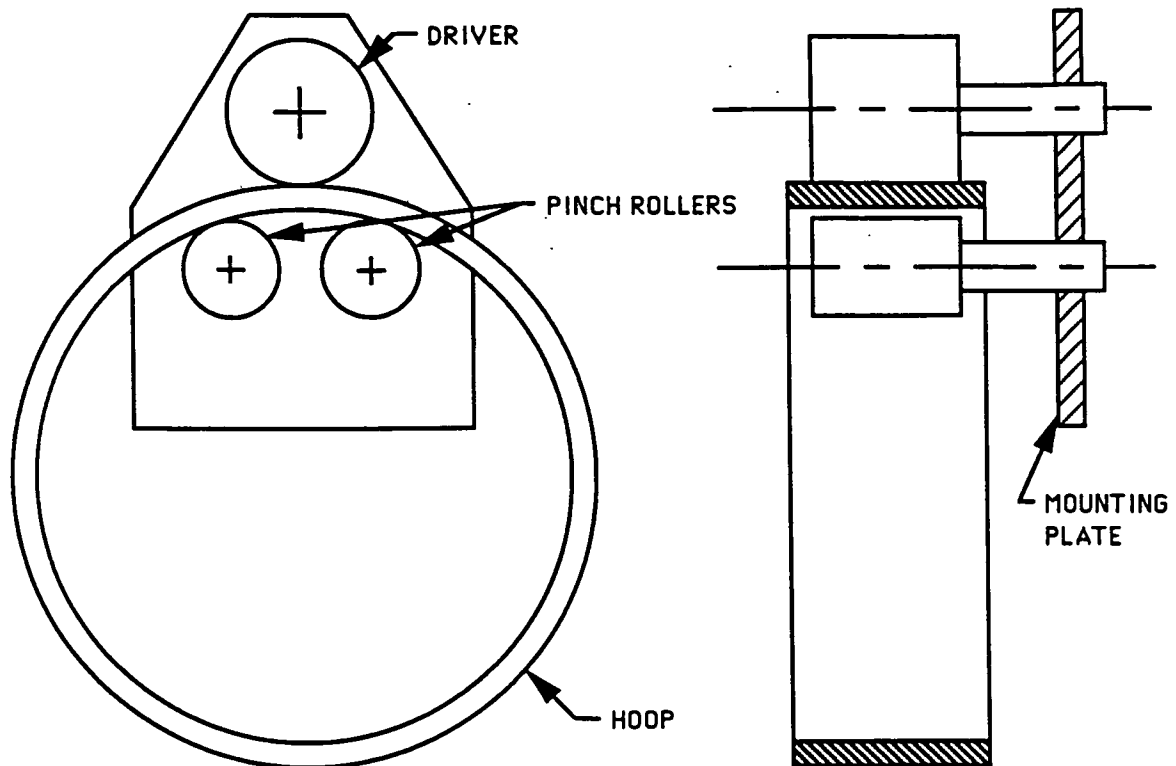
The Flexible Hoop Wheel utilizes a drive roller and a set of pinch rollers at the top of a flexible hoop. Advantages of this design are good ground clearance, and a large amount of radial deflection, with low axial deflection provided by the geometric axial stiffness of the hoop. Tangential deflection would pose a problem, unless the wheel were additionally constrained. The friction drive would also be susceptible to abrasive wear, and slippage under high loads.

Spring at Hub

FLEXIBLE SPRING TUBE

SHAFT

RIGID HUB AND RIM
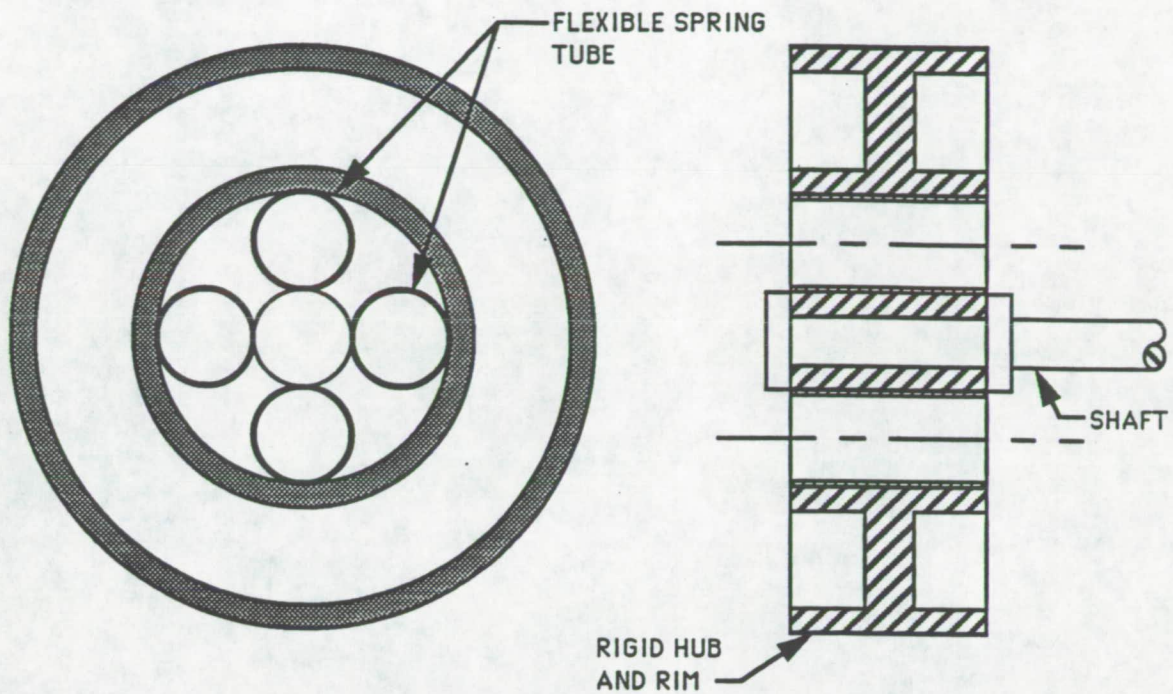
This wheel is similar to the Hoop Spring Wheel, with the hoops relocated to the hub the differentiating feature. The movement of the springs to the hub area should limit both radial and tangential deflections. Axial deflection will be small for both designs, due to the geometric strength of the springs in the axial direction. This design was determined to be inferior to the Hoop Spring Wheel due to its higher mass, and limited deflection potential.

Paddle Wheel

THREE PADDLE
RIGID HUB

RIGID WHEEL
COVER

SHAFT

ROLLER
FOLLOWERS
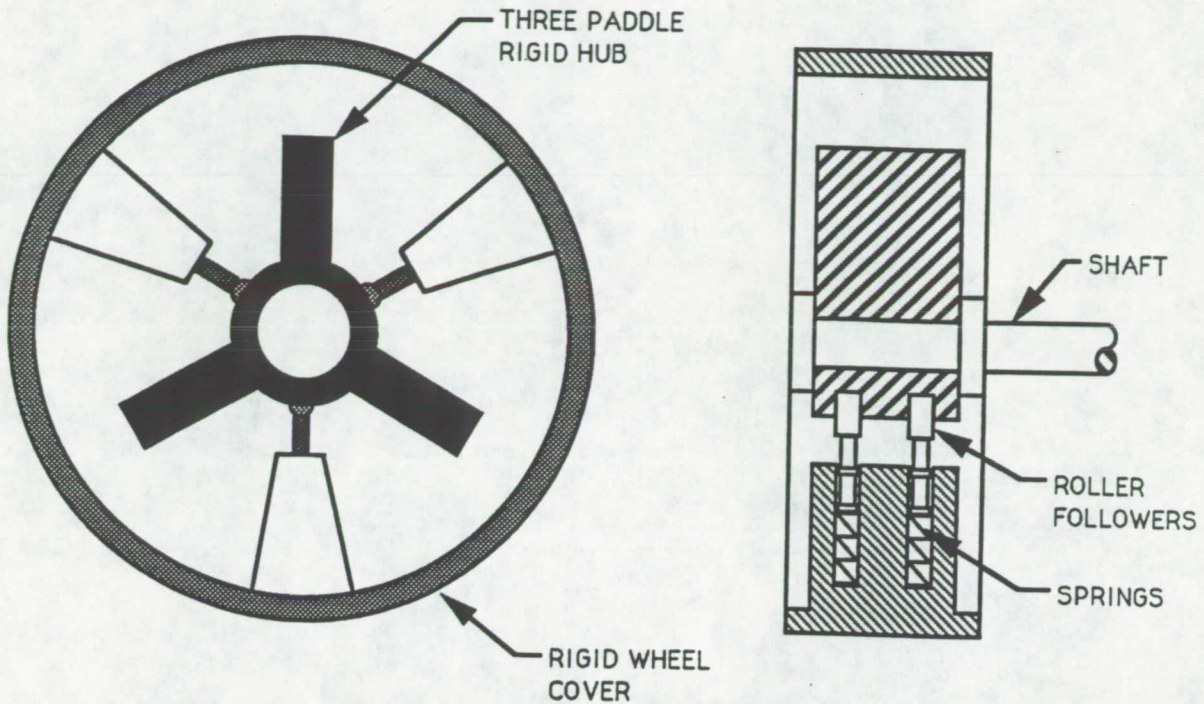
SPRINGS

The paddle wheel uses a spring and damper piston/cylinder arrangement to provide both compliance and damping to the wheel. Three symmetrically spaced cylinders connected to the inner rim of the wheel support the hub. Axial deflection is eliminated with the use of roller followers riding in grooves machined into the circumference of the hub. Three "paddles" extend outward from the hub on 120 degree centers. Torque is transmitted through the contact of the paddles and the cylinder walls. Advantages of this design include linear radial compliance and no appreciable axial deflection. Disadvantages of the design include large amounts of tangential deflection, and a high design mass.

C-2

Frictional Damping Wheel
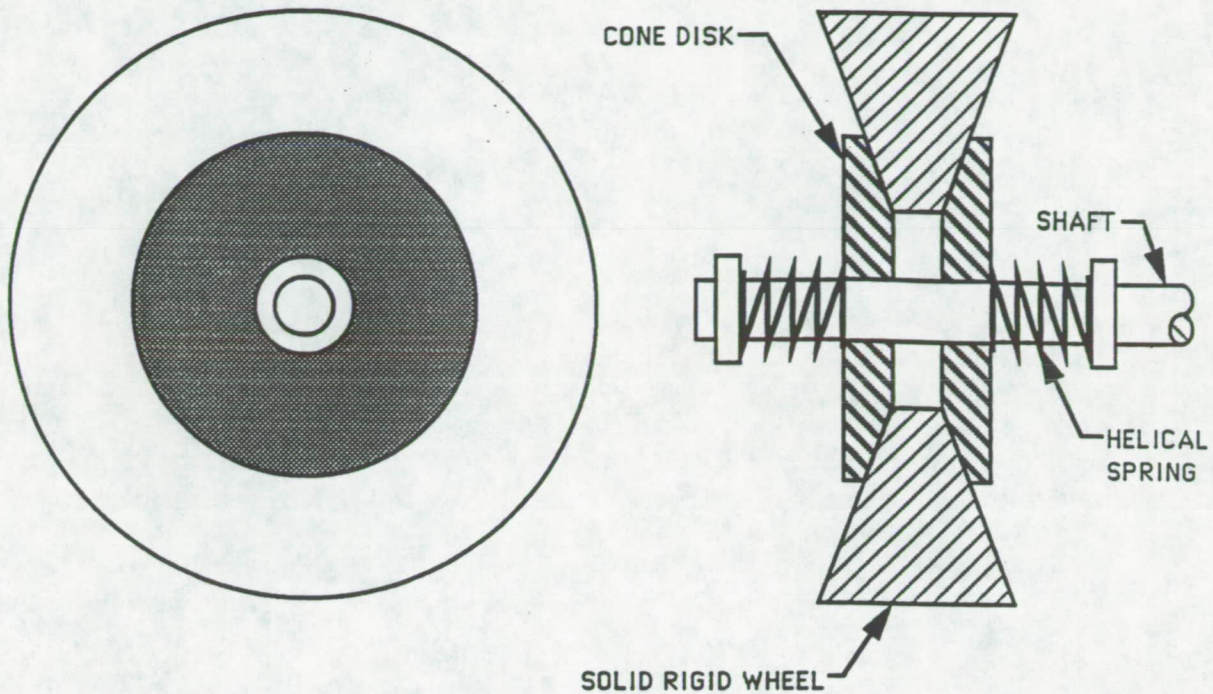
This design is comprised of a conic section solid revolute suspended by a mating conic disk on either side. Coil springs forcing the conic disks together keep the revolute centered as the wheel rotates. When deflected, the revolute contact surface forces the conic disks apart, storing deflection energy in the springs. This design operates in much the same way as a constantly variable transmission. Torque is transmitted through the mating surface due to spring tension. Once deflected the springs restore the wheel components to their concentric orientation. Advantages for this design are linear radial deflection, and frictional damping provided by the mating surface. Disadvantages of the design include a high design mass, high energy consumption, and axial and tangential deflection directly linked to the radial spring rate. Abrasive wear of the frictional surfaces may also pose a problem.

J-Spring Wheel

RIGID
HUB

J SPRING

SHAFT

RIGID WHEEL
COVER
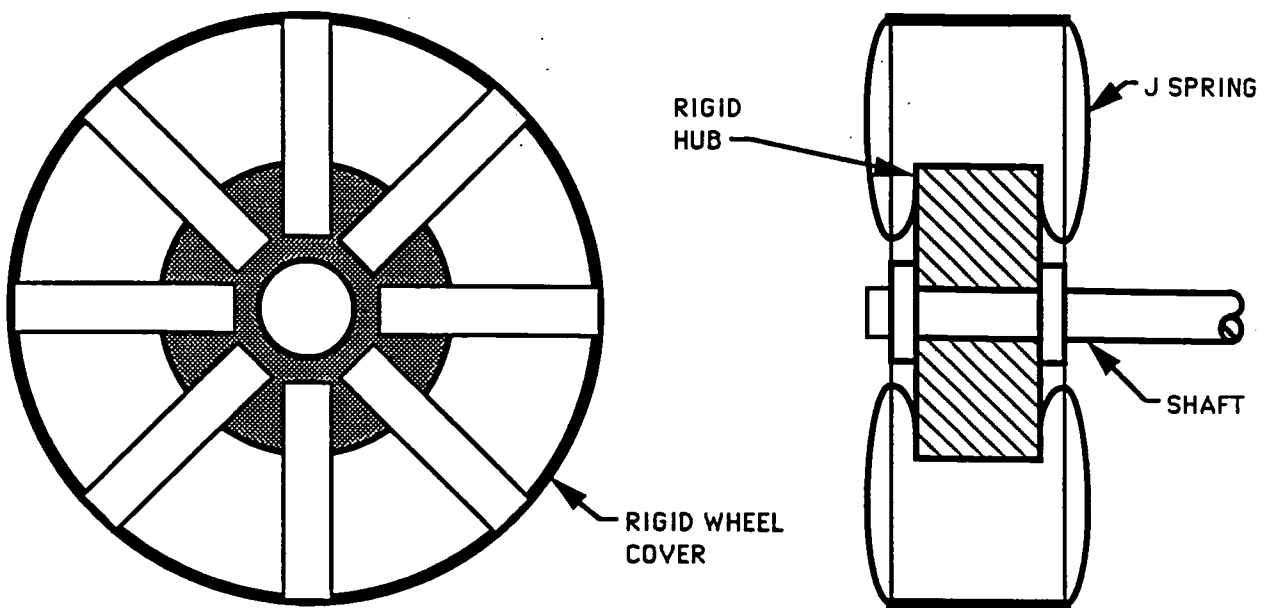
The J-Spring Wheel is similar to the Double-J Wheel mentioned in the Alternative Designs section of this report. This design uses curved cantilever springs (J-springs) to give the wheel its compliance. These springs connect the rigid contact surface segments to the hub. The advantage of the j-spring is that its dimensions may be engineered to give near zero axial deflection. Tangential deflection should be low for this design due to the high mass moment of inertia the springs have on edge. Disadvantages for this design are high mass, and low radial deflection, as well as a sinusoidal spring rate as the wheel rolls, due to the segmented contact surface and discrete spring spacing.

Cone Wheel

RIGID HOLLOW
DOUBLE CONE

SHAFT

GROUSERS
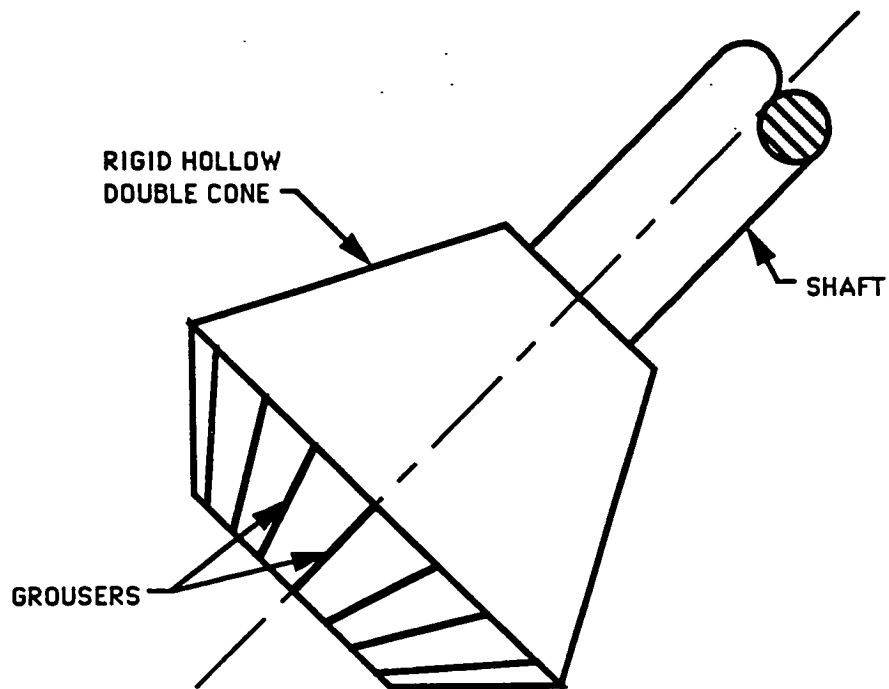
This design is novel in its approach by the use of an oblique axle transmitting torque to a conic-section contact surface. Ground clearance for this design will be good, however the design team felt this configuration would be very stiff, as well as inefficient. The offset axle will consume more energy than an equivalent horizontal design, placing a considerable thrust load on the support bearings. Further, the conic section will generate steering forces normal to the direction of movement as the wheel rolls, consuming additional energy and further loading the support bearings.

Appendix D
Feasibility Analysis

This appendix contains the feasibility calculations for the design alternatives. Assumptions and formulas are given for each design as needed.

Spring Thickness Calculations

X = deflection

F = Force

K = spring constant = $\frac{F}{X}$

$E_{steel} = 207 \times 10^9 \, P_a$

g (earth) = $9.81 \, m/s^2$

for $X = \frac{F}{K} = \frac{3.1065 \, N}{.001 \, M}$

$X = .001 \, M \rightarrow K = 3106.5 \, N/M$
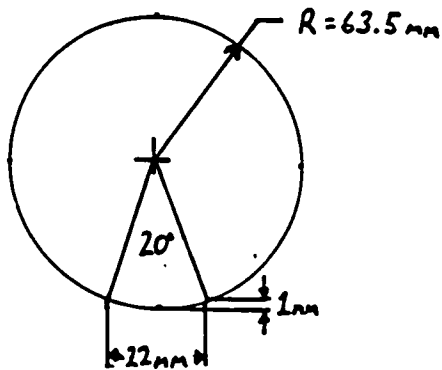
ASSUME

1) 1mm static deflection (for Mars)
2) $F = 3.1065 \, N$
3) $K = 3106.5 \, N/M$
4) Material is steel

for Circular Geometry:

R = 63.5 mm

20°

1mm

22mm

Alternative One: 1-Piece Wheel

Assume:

1) Wheel cut into 10 sections
2) Only 1 element supporting wheel
3) element may be modeled as a cantilever beam tilted @ an angle of 15°
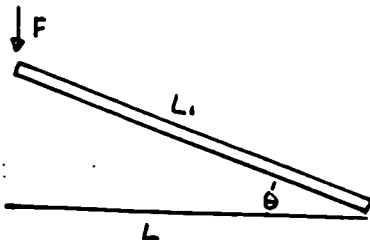
$F_1 = F\cos\theta = 3N$

$F = 3.1065 \, N$

b = width = $.03148 \, m$

E = Young's Modulus for steel = $207 \times 10^9 \, P_a$

$\theta = 15°$

$L = 0.05 \, m$

$L_1 = L/\cos\theta = .0483 \, m$

F

L_1

θ

L

F_1

L_1

D2

1-Piece Wheel (continued)

FLEXIBLE SEGMENT

SHAFT

LOAD
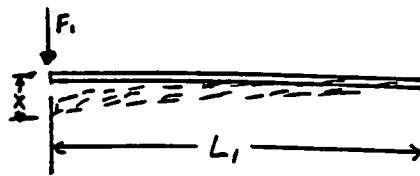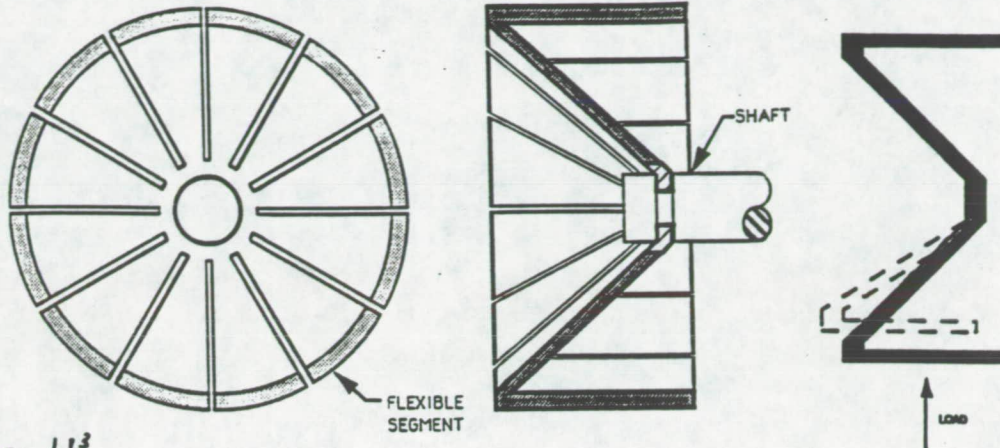
$$I = \frac{bt^3}{12} =$$

$$y_1 = \frac{F_1 L^3}{12 EI}$$

$$y_1 = \frac{F_1 L_1^3}{E b t^3} \quad \rightarrow \quad y = y_1 \cos\theta = \frac{F_1 L_1^3}{E b t^3} \cos\theta$$

$$y = \frac{(3.1065N)\cdot(0.05m)^3}{(207\times10^9 \, N/m^2)\cdot(.03148\,m)\cdot\cos(15°)\cdot t^3} = 1mm \quad \rightarrow \quad t = 0.000395\,m$$

$$\boxed{t = 0.0395\,cm}$$

Alternative Two: V-Wheel

Assumptions:

1) Force is equally distributed between the two sides of the "V"

2) The Wheel is modeled as a continuous beam

3) A section of the wheel is 1/18 of the total, to make equivalent of 20° bending only

RETAINER

ONE PIECE RIGID HUB

SHAFT

CONE SHAPED LEAF SPRING
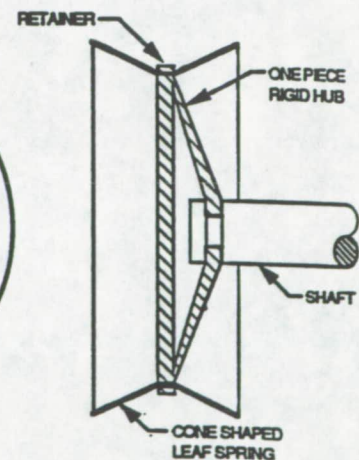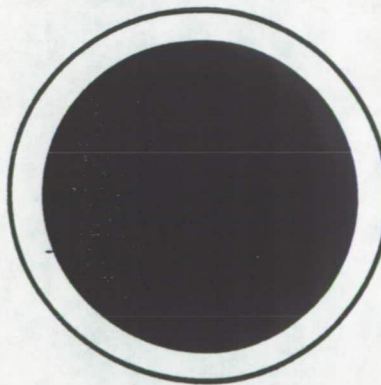
V-Wheel (continued)

Assume values for modeling:

$L = 2.5\,cm = 0.025\,m$

$b = 0.0209\,m$

$F = 1.553\,N$

$\theta = 20°$
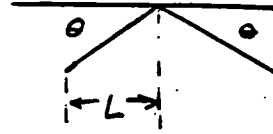
$$Y = \frac{FL^3}{E\,bt^3\cos\theta} = \frac{(1.553\,N)(2.5cm)^3}{(207\times10^9\,N/m^2)(0.0209\,m)(\cos20°)\,t^3}$$

$$Y = \frac{5.969 \times 10^{-15}\,m^4}{t^3}$$

$$t = 0.00018\,m = \boxed{0.018\,cm}$$

Alternative Three: Corrugated Spring Wheel

Assumptions used for modeling:

1) Corrugated spring may be modeled as a leaf spring

2) Top + bottom of wheel each deflect 0.5mm

3) There are 20 complete waves = ($\smile$) of spring

Assume for modeling values:

$F = 3.1065\,N$

$L = 0.00997\,m$

$b = 0.05\,m$

$E = 207 \times 10^9\,Pa$
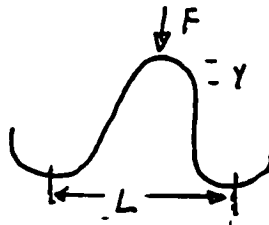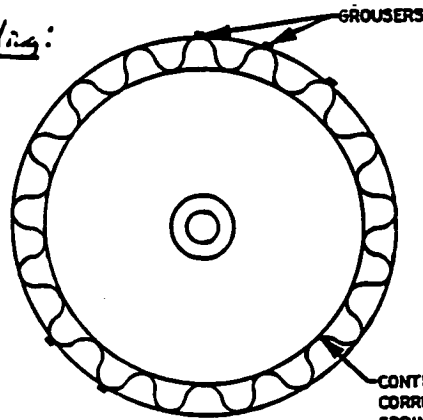
For small deflection ONLY! use

$$Y = \frac{FL^3}{4E\,bt^3}$$

$$Y = \frac{(3.1065N)(.00997\,m)^3}{(4)(207\cdot10^9\,N/m^2)(.05m)(t^3)} = .001\,m$$

$$t = 5.3 \times 10^{-5}\,m$$
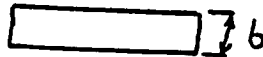
$$\boxed{t = 0.0053\,cm}$$

Alternative Four: Tab Wheel

Assumptions used for modeling:
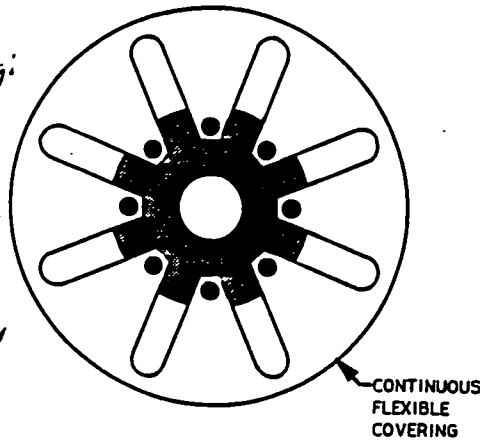
1) 10 sections (9 tabs) for total wheel
2) deflection a horizontal contact surface only
3) No interference between elements

Values used in model:

$L = 0.05\,m$

$b = 0.0399\,m$

$F = 3.1065\,N$

FASTENER

SPOOL HUB AND SHAFT

CONTINUOUS FLEXIBLE COVERING
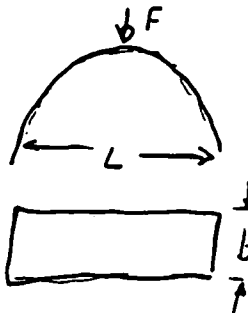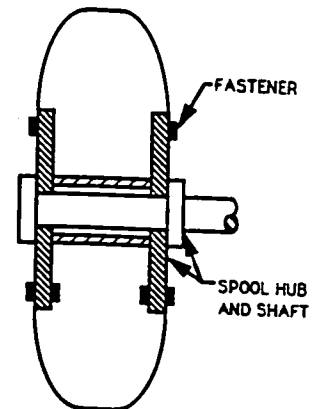
$$y = \frac{FL^3}{4Ebt^3} = 0.001\,m$$

$$y = \frac{(3.1065\,N)(0.05\,m)^3}{(4)(207 \times 10^9 \frac{N}{m^2})(0.0399\,m)\,t^3}$$

$$\boxed{t = 0.0227\,cm}$$

Alternative Five: Mesh Wheel

Assumptions for modeling:

1) Weave may be approximated as a solid sheet of mat'l
2) dimensions for sheet the same as alternative four

METAL WEAVE

RIGID HUB

SHAFT

FLEXIBLE FABRIC BAG

$$y = \frac{FL^3}{4Ebt^3}$$

$$y = \frac{(3.1065\,N)(0.05\,m)^3}{(4)(207 \cdot 10^9 \,^N/_{m^2})(0.0399\,m)\,t^3} = 0.001\,m$$

$$y = 1.175 \times 10^{-14} \quad \rightarrow \quad t = 0.0227\,cm$$
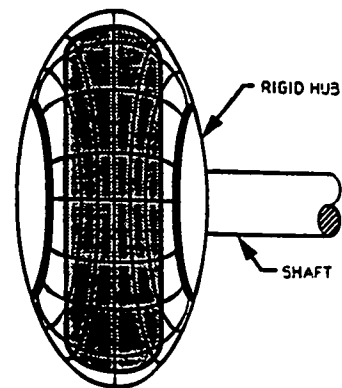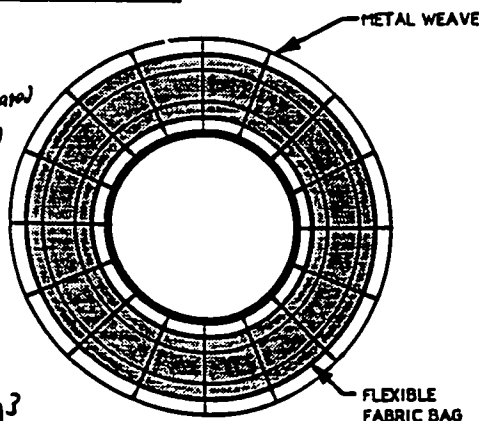
Note: weave may be assumed weaker (more easily deflected) than sheet, so the thickness will be less than 0.0227 cm, the value found from this model.

Alternative Six: Hoop Spring Wheel

Assumptions used for Modeling:

1) Negligible interference between hoops
2) Force is shared equally between springs above & below axle
3) No other springs carry load
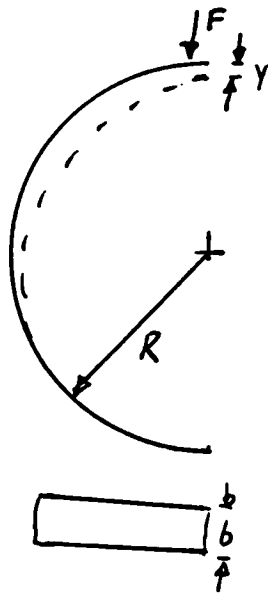4) hoop modeled as two hemispherical hoop springs
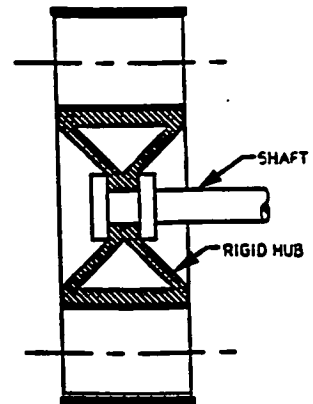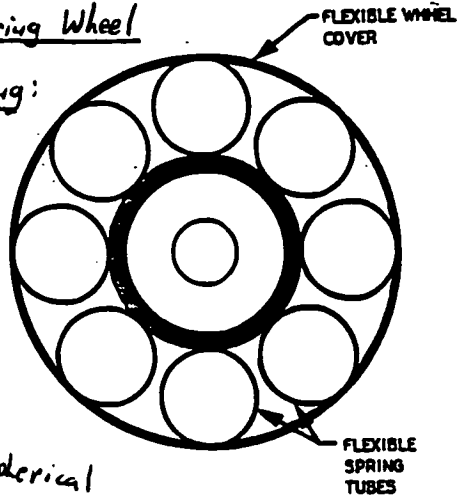
Values used in Model:

$R = 1.588 \, cm = 0.01588 \, cm$
$b = 5 \, cm = 0.05 \, m$
$E = 207 \times 10^9 \, Pa$
$F = 0.776 \, N$
$Y = 0.001 \, m$

$$Y = \frac{\pi F R^3}{2 E I}$$

$$.001m = \frac{\pi (.776 N)(0.01588 m)^3 \, 12}{(2)(207 \times 10^9 \, N/in^2)(.05)}$$

$$\cdot \frac{1}{t^3} \Rightarrow t = 0.00017 \, m$$

$$\boxed{t = 0.0177 \, cm}$$

Alternative Seven: Spoked Wheel

Assumptions used in modeling:

1) 16 equally spaced springs (leaf springs)
2) pinned @ sides ∴ ∅ Axial deflection as a result of Radial deflection
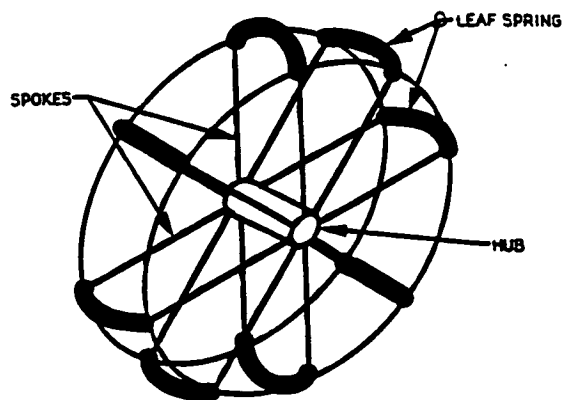
Values used in model:

$L = 5 \, cm = 0.05 \, m$
$b = 1.246 \, cm = 0.01246 \, cm$
$F = 3.1065 \, N$

$$Y = \frac{F L^3}{4 E b t^3}$$

$$Y = \frac{(3.1065 N)(0.05 m)^3}{(4)(207 \times 10^9 \, N/m^2)(0.01246 m) t^3}$$
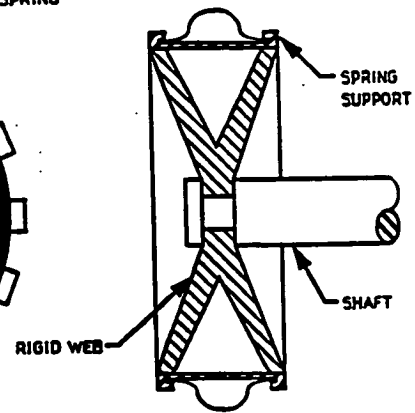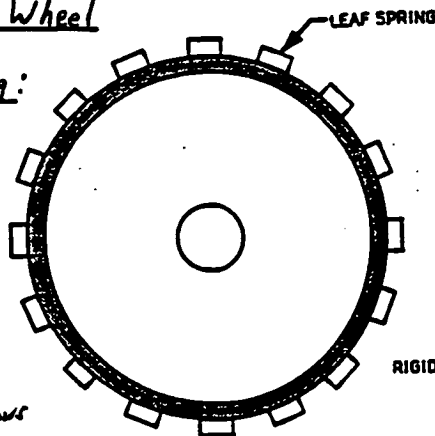
$$\boxed{t = 0.0335 \, cm}$$

Alternative Eight: Leaf Wheel

Assumptions used in modeling:

1) Spring elements behave much like those of the spoke wheel
2) There are 16 equally spaced leaf spring elements

Note: deflection calculations are identical to those of the spoke wheel.

$$Y = 0.001\,m = \frac{FL^3}{4Ebt^3} \rightarrow \boxed{t = 0.0335\,cm}$$

(diagram labels: LEAF SPRING, SPRING SUPPORT, SHAFT, RIGID WEB)

Alternative Nine: Continuous Coil Wheel

Assumptions used in modeling:
1) Model coil as hoop element
2) Assume 3 coils in contact with ground
3) Use 3 cm wide wheel

Values used in Model:

$R = 1.5\,cm = 0.015\,m$
$b = 0.008\,m$
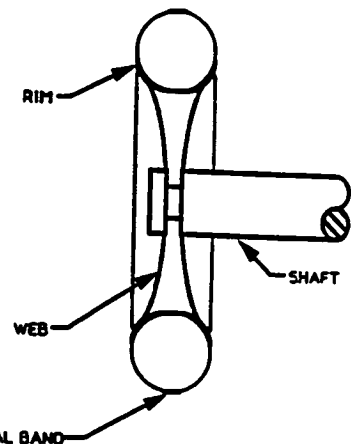$E = 207 * 10^9\,P_a$
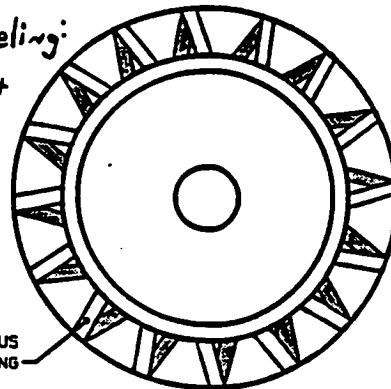$F = 3.1065\,N$
$Y = 0.001\,m$
$F' = 0.51775\,N = F/3$

(diagram labels: RIM, SHAFT, WEB, CONTINUOUS COIL SPRING, CIRCUMFERENTIAL BAND)

Note: Equation is the same as alternate eight. i.e. $Y = \frac{FL^3}{4Ebt^3}$

$$\boxed{t = 0.0185\,cm}$$

Alternative Test: Double-J Wheel

Assumptions used in Modeling:
1) 8 equally spaced feet
2) Load is equally divided between 2 springs

Values used in model:

$L = 0.00026\,m$
$R = 0.01524\,m$
$b = 1.0\,cm$
$F = 1.553\,N$
$E = 207 \times 10^9\,Pa$
$Y = 0.001\,m$
$C_{10} = 11$ ⊛

SHOE

TUBE SPACERS

LEAF SPRING

SHAFT AND HUB
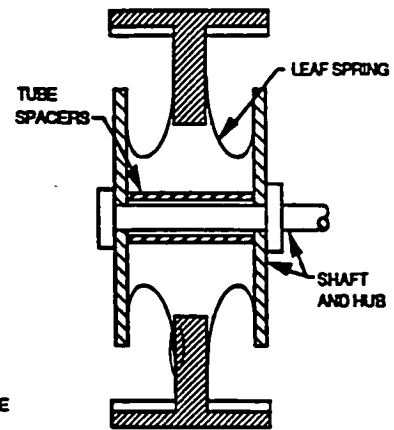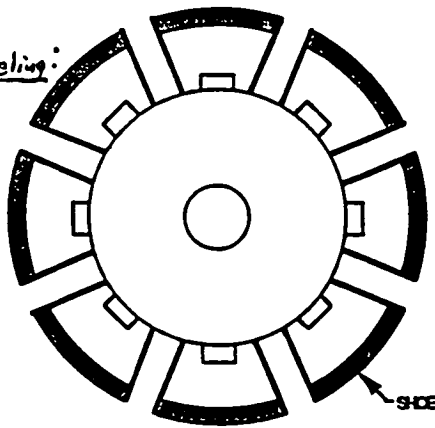
$$Y = \frac{F R^3 C_{10}}{EI} = 0.001 = \frac{(1.553\,N)(0.01524\,m)^3 (11)(12)}{(207 \times 10^9\,N/m^2)(0.01m)(t^3)}$$

⊛ From <u>Mechanical Springs</u> by A.M Wahl

$$\boxed{t = 0.07\,cm}$$

Appendix E

Decision Matrix

The decision matrix used to select the design solution is shown below.

PARAMETERS / WEIGHT FACTOR / DESIGNS	MASS	RADIAL DEFLECTION	ENERGY EFFICIENCY	RELIABILITY	TOTAL
	0.4	0.15	0.25	0.20	1.0
TAB WHEEL	8 / 3.2	8 / 1.2	7 / 1.75	10 / 2.0	8.15
SIGMA WHEEL	10 / 4.0	8 / 1.2	7 / 1.75	10 / 2.0	8.95
V-WHEEL	10 / 4.0	8 / 1.2	8 / 2.0	10 / 2.0	9.2
SPOKE WHEEL	8 / 3.2	8 / 1.2	4 / 1.0	4 / 0.8	6.2
LEAF WHEEL	4 / 1.6	8 / 1.2	6 / 1.5	4 / 0.8	5.1
CORRUGATED SPRING WHEEL	4 / 1.6	4 / 0.6	9 / 2.25	5 / 1.0	5.45
DOUBLE SPRING WHEEL	2 / 0.8	8 / 1.2	7 / 1.75	2 / 0.4	4.15
HOOP AT WEB WHEEL	6 / 2.4	8 / 1.2	7 / 1.75	4 / 0.8	6.15
CONTINUOUS COIL WHEEL	6 / 2.4	8 / 1.2	7 / 1.75	2 / 0.4	5.75
MESH WHEEL	6 / 2.4	8 / 1.2	2 / 0.5	7 / 1.4	5.5

Appendix F

Width Calculations Using Bekker Analysis

Width was calculated using formulas developed by Dr. M.G. Bekker. The answer is compared to the width at which bulldozing begins.

$$w_s = A \left(c N_c + \gamma z N_q + \tfrac{1}{2} \gamma b N_\gamma \right)$$

- A = CONTACT AREA
- c = COEFFICIENT OF COHESION
- γ = DENSITY
- b = WIDTH
- D = DIAMETER OF CONTACT PATCH
- N_γ = SOIL COEFFICIENT

ASSUME: $c = 0$ FOR DRY SAND
$z = 0$

$$w_s = A \left(\tfrac{1}{2} \gamma b N_\gamma \right)$$

ASSUME CIRCULAR CONTACT PATCH

WIDTH = DIAMETER OF CONTACT PATCH

$$A = \frac{\pi b^2}{4}$$

$$\therefore w_s = \frac{\pi b^2}{4} \cdot \frac{1}{2} \gamma b N_\gamma$$

$$= \frac{\pi b^3}{8} \gamma N_\gamma \implies b = \sqrt[3]{\frac{8 w_s}{\pi \gamma N_\gamma}}$$

$$b = ?$$
$$w_s = \frac{5 \, kg}{6 \, WHEELS} * \frac{1000 \, g}{kg}$$
$$\gamma = 1.5 \, g/cm^3$$
$$N_\gamma = 17$$

$$\left. \right\} \quad b = \sqrt[3]{\frac{8 (5/6) \, kg \cdot \frac{1000 \, g}{kg}}{\pi (1.5 \, g/cm^3) \, 17}}$$

$$\boxed{b = 4.36 \text{ cm}}$$

BULLDOZING $= \dfrac{Z}{0} = 0.06$

$Z =$ SINKAGE

$D =$ DIAMETER OF WHEEL

$Z = (0.06)(0.127m) = 0.00762m$

WHEEL SINKS THIS FAR AND IT WILL BULLDOZE.

BEKKER EQN. FOR SINKAGE

$$Z = \left[\dfrac{3W}{(3-n)(K_c + bK_\phi)\sqrt{D}}\right]^{2/2n+1}$$

$Z =$ SINKAGE $= 0.00762$

$W =$ WEIGHT $= 3.0248N$

$n =$ EXPONENT OF SOIL DEFORMATION $= 0.91$

$K_c =$ MODULUS OF SOIL DEFORMATION DUE TO COHESION $= -0.01\left(\dfrac{KN}{m}\right)(m^{-n})$

$K_\phi =$ MODULUS OF SOIL DEFORMATION DUE TO FRICTIONAL ELEMENTS

$\quad = 11.41\left(\dfrac{KN}{m^2}\right)(m^{-n})$

$D =$ DIAMETER $= 0.127m$

$\hat{\jmath} = \dfrac{2n+1}{2}$

$$Z^{\hat{\jmath}} = \left[\dfrac{3W}{(3-n)(K_c + bK_\phi)\sqrt{D}}\right]$$

$$b = \dfrac{\left(\dfrac{3W}{Z^{\hat{\jmath}}(3-n)\sqrt{D}}\right) - K_c}{K_\phi}$$

$$b = \frac{\left(\dfrac{3(3.0248\ N)}{(.00762)^{\frac{2(.91)+1}{2}}(3-.91)\sqrt{1.127}}\right) - \left(-0.01 \times 10^3\right)}{11.41 \times 10^3}$$

$$= 1.035\ m$$

∴ BULL DOZING OCCURS AT WIDTHS GREATER THAN 1.035 m. THIS IS GREATER THAN 4.36 cm SO WIDTH WILL NOT GIVE A PROBLEM.

NOTE: 4.36 cm IS FOR ZERO SINKAGE

Appendix G

Width Calculations Using WES Analysis

Width was calculated using formulas developed by WES. The answer is validated by checking to see if the calculated width to diameter ratio falls within the correct range.

$P = PULL$

$w = LOAD$

$G = SOIL\ PENETRATION\ RESISTANCE\ GRADIENT$

$b = WIDTH$

$d = DIAMETER$

$\delta = DEFLECTION$

$h = COMPLIANT\ SECTION\ HEIGHT$

$$\frac{P}{w} = \frac{\alpha - 5.50}{1.92\alpha + 37.20}$$

$$\alpha = \frac{G(bd)^{3/2}}{w} \cdot \frac{\delta}{h}$$

$$\frac{P}{w} = \frac{\frac{K_1}{w} - 5.50}{1.92 \frac{K_1}{w} + 37.20} \qquad K_1 = G(bd)^{3/2} \cdot \frac{\delta}{h} = \alpha w$$

$$\frac{P}{w} = \frac{K_1 - 5.50\,w}{1.92 K_1 + 37.20\,w}$$

$$P = \frac{K_1 w - 5.50\,w^2}{1.92 K_1 + 37.20\,w}$$

$$\frac{dP}{dW} = \frac{(1.92K_1 + 37.20W)(K_1 - 11.00W) - (K_1W - 5.50W^2)(37.20)}{(1.92K_1 + 37.20W)^2} = 0$$

$$1.92K_1^2 - 21.12K_1W + 37.20K_1W - 409.20W^2 - 37.20K_1W +$$

$$204.60W^2 = 0$$

$$W_{opt} = \frac{21.12K_1 \pm \sqrt{(21.12K_1)^2 - 4(-204.60)(1.92K_1^2)}}{2(-204.60)}$$

$$= 0.0582 K_1$$

ASSUME $W_{opt} =$ LOAD ON WHEEL $= 3.0248$ N

$$W_{opt} = 0.0582 K_1$$

$$K_1 = \frac{3.0248}{0.0582} = 51.9725 \text{ N}$$

$$K_1 = \alpha W \Rightarrow \alpha = \frac{K_1}{W} = \frac{51.9725 \text{ N}}{3.0248 \text{ N}} = 17.1821$$

$$K_1 = G(bd)^{3/2} \cdot \frac{s}{n}$$

$$51.9725 \text{ N} = (.54 \times 10^6) b^{3/2}(.127)^{3/2}(.15)$$

$$b^{3/2} = 0.01476$$

$$b = 0.5857 \text{ m} = 5.8587$$

$$= 5.8 \text{ cm} \approx \boxed{6 \text{ cm}}$$

NOTE: ROUNDED UP TO EVEN NUMBER FOR EASE OF
USE IN FEA ANALYSIS AND TO BE ON SAFE
SIDE. WE ARE BELOW BULL DOZING WIDTH (1.01m)

EQUATIONS ARE VALID WHEN

$$1 < \frac{d}{b} < 8$$

$$\frac{d}{b} = \frac{12.7 \text{ cm}}{6 \text{ cm}} = 2.1$$

∴ WIDTH IS VALID

Appendix H

Calculation and Comparison of Tensile Strength-to-Weight of a

Kevlar Composite and Aluminum

In this appendix, the tensile strength-to-weight of a Kevlar filled (67% by volume) epoxy resin composite is compared to the tensile strength-to-weight of 6061-T6 aluminum.

Definition of terms:

E = Young's Modulus
ρ = density
V = volume
m = mass

Material Property Values:

$E_c = 81.8 \ GPa$
$\rho_{Kevlar} = 1.44 \ g/cm^3$
$\rho_{epoxy} = 1.27 \ g/cm^3$

$E_A = 70 \ GPa$
$\rho_A = 2.78 \ g/cm^3$

① For an equivalent spring rate: $E_c V_c = E_A V_A$ ∴ $\dfrac{E_A}{E_c} = \dfrac{81.8 \ GPa}{70 \ GPa} = \dfrac{V_c}{V_A}$

$\dfrac{V_c}{V_A} = 0.855$ ← this indicates that for a given spring rate, 85% of the

$\boxed{V_c = 0.855 \ V_a}$

Volume of an Aluminum Wheel would be needed if made of composite.

② Calculate necessary mass: $m = \rho V$, $\rho_c = (0.33)(1.27 \ g/cm^3) + (0.67)(1.44 \ g/cm^3)$

$\rho_c = 1.38 \ g/cm^3$ → $m_c = (1.38 \ g/cm^3)(0.855 \ V_a)$, $m_A = (2.78 \ g/cm^3)(V_a)$

③ ratio of necessary masses of materials for a given spring rate:

$\dfrac{m_c}{m_A} = \dfrac{(1.38 \ g/cm^3)(0.855 \ V_A)}{(2.78 \ g/cm^3)(V_a)} = 0.42$ → $m_c = 0.42 \ m_A$

$1 - .42 = 0.58$

thus, the composite has only 42% the mass of the Aluminum member. this equates to a $\boxed{58\% \ Mass \ reduction}$ by using composite construction in place of aluminum.
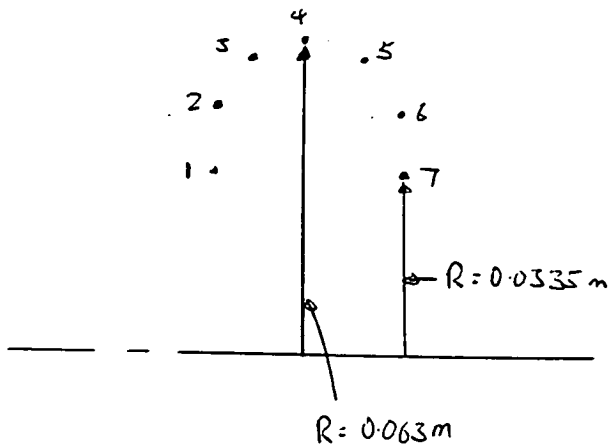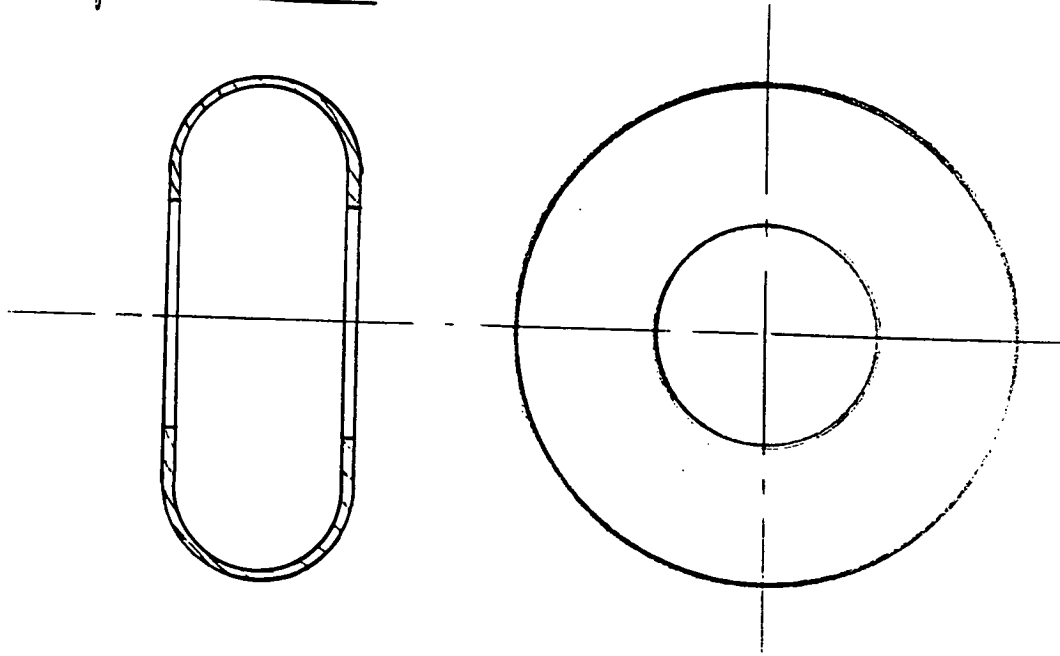
Appendix I
FEA Test Model

The procedure and models used to validate the FEA technique are described in this section. Also, the procedure and models used to evaluate and develop the Hybrid I and Hybrid II wheels are described.

A simple model of a wheel was first tried out on PAL2 to see if modeling is possible.

Simple Model

5 .   4   . 5

2 .   . 6

1 .   . 7

←R = 0.0335 m

R = 0.063 m

The profile of the simple wheel was modeled by 7 circular nodal points

The model file is:

```
C          TEST MODEL OF WHEEL
C          THE MODEL IS A FULL TORUS SHAPED WHEEL

TITLE WHEEL

NODAL POINT LOCATIONS 3
1,0.0335,0,0.03 THROUGH 36,0.0335,350,0.03
37,0.0485,0,0.0259 THROUGH 72,0.0485,350,0.0259
73,0.05948,0,0.015 THROUGH 108,0.05948,350,0.015
109,0.0635,0,0 THROUGH 144,0.0635,350,0
145,0.05948,0,-0.015 THROUGH 180,0.05948,350,-0.015
181,0.0485,0,-0.0259 THROUGH 216,0.0485,350,-0.0259
217,0.0335,0,-0.03 THROUGH 252,0.0335,350,-0.03

MATERIAL PROPERTIES 207E9,79E9,7.7E6,.3,313.7E9
QUADRILATERAL PLATE TYPE 1,1,0.005
GENERATE CONNECTS 1,217,252,36,1
CONNECT 1 TO 36 TO 72 TO 37
CONNECT 37 TO 72 TO 108 TO 73
CONNECT 73 TO 108 TO 144 TO 109
CONNECT 109 TO 144 TO 180 TO 145
CONNECT 145 TO 180 TO 216 TO 181
CONNECT 181 TO 216 TO 252 TO 217
ZERO
TA 1,2,3,4,5,6,7,8,9,10,11,12,13,14,15,16,17,18
TA 19,20,21,22,23,24,25,26,27,28,29,30,31,32,33,34,35,36
TA 217,218,219,220,221,222,223,224,225,226,227,228,229,230
TA 231,232,233,234,235,236,237,238,239,240,241,242,243,244
TA 245,246,247,248,249,250,251,252

END DEFINITION
```
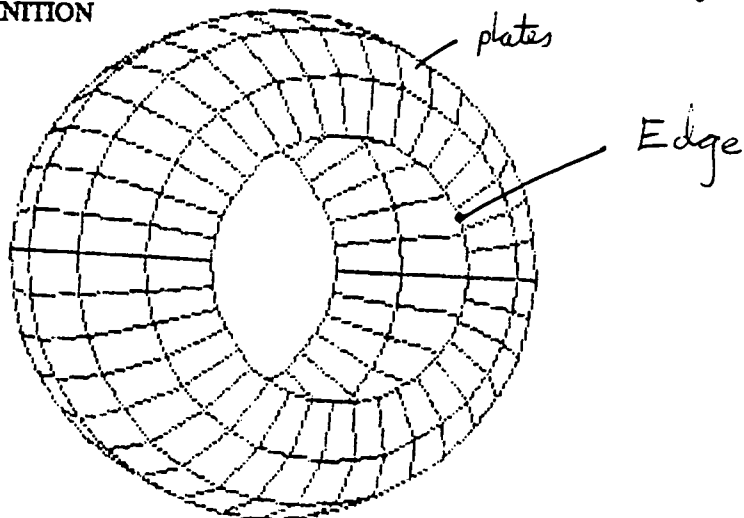
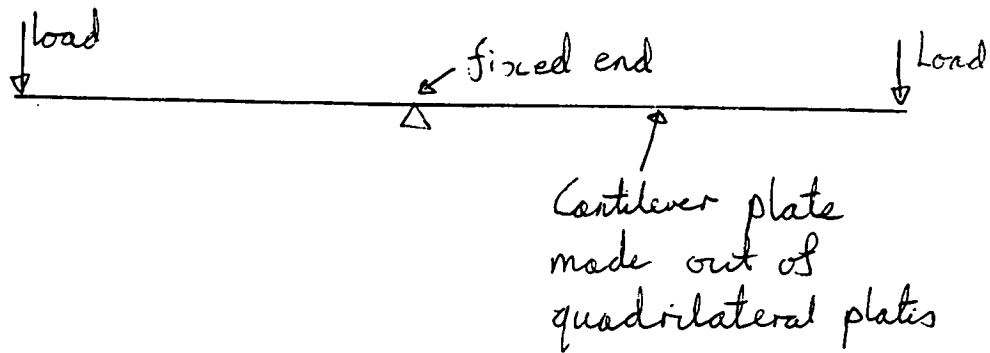*Define — Nodal Points*

Connect nodal points

Fix all point at Edge

plates

Edge

Result : Using quadrilateral plates to model the simple was successfull.

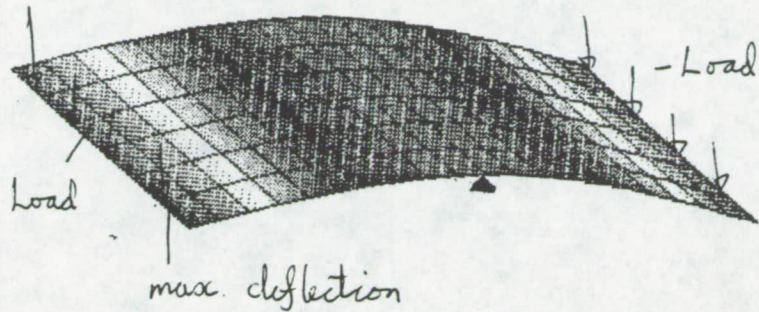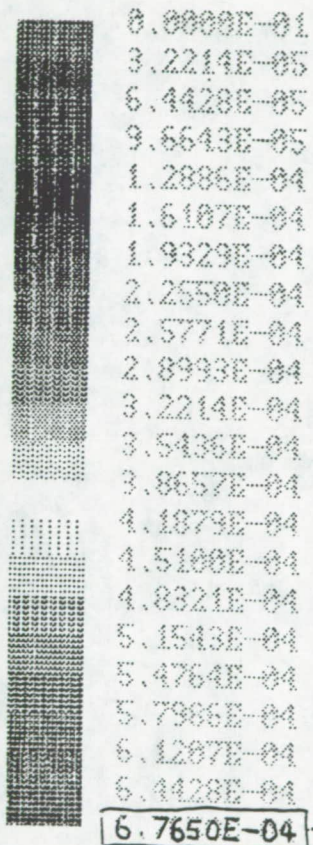A model of a simple cantilever plate was tested to see the accuracy of PAL 2.

load ↓   ← fixed end   ↓ Load

Cantilever plate
made out of
quadrilateral plates

Form our test model, we found that the accuracy was around 5% error.

Values Used : $E = 70E9 \; P_a$

$L = 0.05 \; m$

$P = 6 \; N$

$t = 0.001 \; m$

$$\text{Deflection} = \frac{PL^3}{3EI}$$

$$= \frac{6 \times 0.05^3 m \times 12}{3 \times 70 \times 10^9 \times 0.06 \times 0.001^3}$$

$$= 7.142 \times 10^{-4} \, m$$

TRANS. DEFL. Y

8.0000E-01
3.2214E-05
6.4428E-05
9.6643E-05
1.2886E-04
1.6107E-04
1.9329E-04
2.2550E-04
2.5771E-04
2.8993E-04
3.2214E-04
3.5436E-04
3.8657E-04
4.1879E-04
4.5100E-04
4.8321E-04
5.1543E-04
5.4764E-04
5.7986E-04
6.1207E-04
6.4428E-04

6.7650E-04 — max deflection

Load

max. deflection

—Load

$$\text{Error} = \frac{7.142 - 6.765}{7.142} \times 100$$

$$= 5.278\%$$

Result : Error is acceptable.

The wheel to model is the Tab wheel shown below:
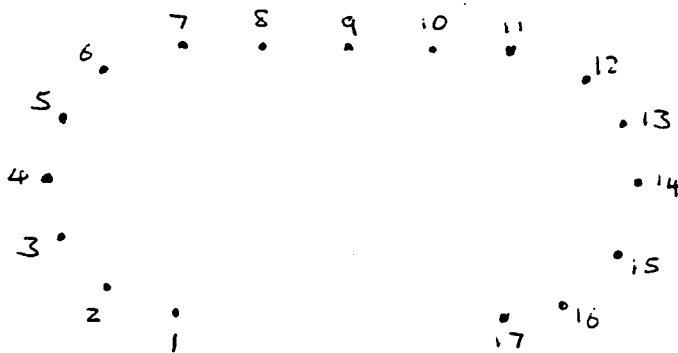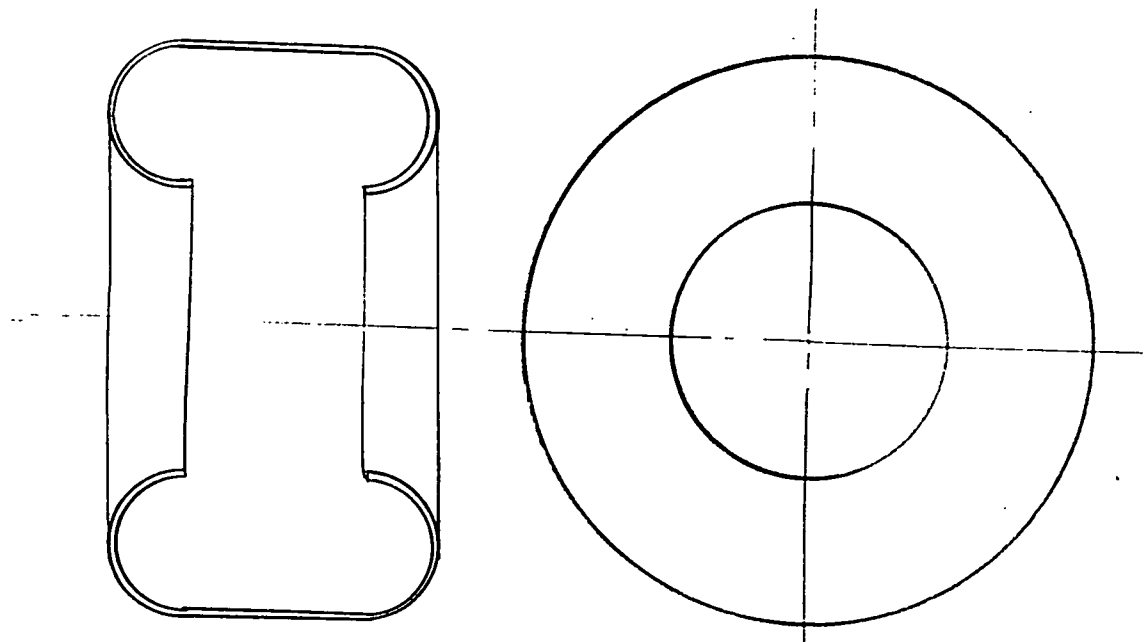
The profile of the Tab wheel was modelled by 17 circular points.

TITLE TAB-WHEEL
C   FIRST MODEL OF WHEEL
C   DIAMETER OF WHEEL = 12.70 cm
C   DIAMETER OF HUB = 8.70 cm
C   WIDTH OF WHEEL = 8.00 cm
C   THICKNESS   = 0.04 cm
C   YOUNG MODULUS   = 207E9 Pa *Modulus of Steel.*
C   LOAD FILE IS T1LOAD.TXT

1. NODAL POINT LOCATIONS 3
2. 1,0.0435,0,0.03 THROUGH 18,0.0435,340,0.03
3. 19,0.0448,0,0.035 THROUGH 36,0.0448,340,0.035
4. 37,0.0485,0,0.0387 THROUGH 54,0.0485,340,0.0387
5. 55,0.0535,0,0.04 THROUGH 72,0.0535,340,0.04
6. 73,0.0585,0,0.0387 THROUGH 90,0.0585,340,0.0387
7. 91,0.0621,0,0.035 THROUGH 108,0.0621,340,0.035
8. 109,0.0635,0,0.03 THROUGH 126,0.0635,340,0.03
9. 127,0.0635,0,0.02 THROUGH 144,0.0635,340,0.02
10. 145,0.0635,0,0 THROUGH 162,0.0635,340,0
11. 163,0.0635,0,-0.02 THROUGH 180,0.0635,340,-0.02
12. 181,0.0635,0,-0.03 THROUGH 198,0.0635,340,-0.03
13. 199,0.0621,0,-0.035 THROUGH 216,0.0621,340,-0.035
14. 217,0.0585,0,-0.0387 THROUGH 234,0.0585,340,-0.0387
15. 235,0.0535,0,-0.04 THROUGH 252,0.0535,340,-0.04
16. 253,0.0485,0,-0.0387 THROUGH 270,0.0485,340,-0.0387
17. 271,0.0448,0,-0.035 THROUGH 288,0.0448,340,-0.035
18. 289,0.0435,0,-0.03 THROUGH 306,0.0435,340,-0.03

Each line will define a single circular band of point

MATERIAL PROPERTIES 207E9,79E9,7.7E6,.3,313.7E9
QUADRILATERAL PLATE TYPE 1,1,0.0004
GENERATE CONNECTS 1,289,306,18,1
CONNECT 18 TO 1 TO 19 TO 36
CONNECT 36 TO 19 TO 37 TO 54
CONNECT 54 TO 37 TO 55 TO 72
CONNECT 72 TO 55 TO 73 TO 90
CONNECT 90 TO 73 TO 91 TO 108
CONNECT 108 TO 91 TO 109 TO 126
CONNECT 126 TO 109 TO 127 TO 144
CONNECT 144 TO 127 TO 145 TO 162
CONNECT 162 TO 145 TO 163 TO 180
CONNECT 180 TO 163 TO 181 TO 198
CONNECT 198 TO 181 TO 199 TO 216
CONNECT 216 TO 199 TO 217 TO 234
CONNECT 234 TO 217 TO 235 TO 252
CONNECT 252 TO 235 TO 253 TO 270
CONNECT 270 TO 253 TO 271 TO 288
CONNECT 288 TO 271 TO 289 TO 306

This will make the last connections to form the wheel
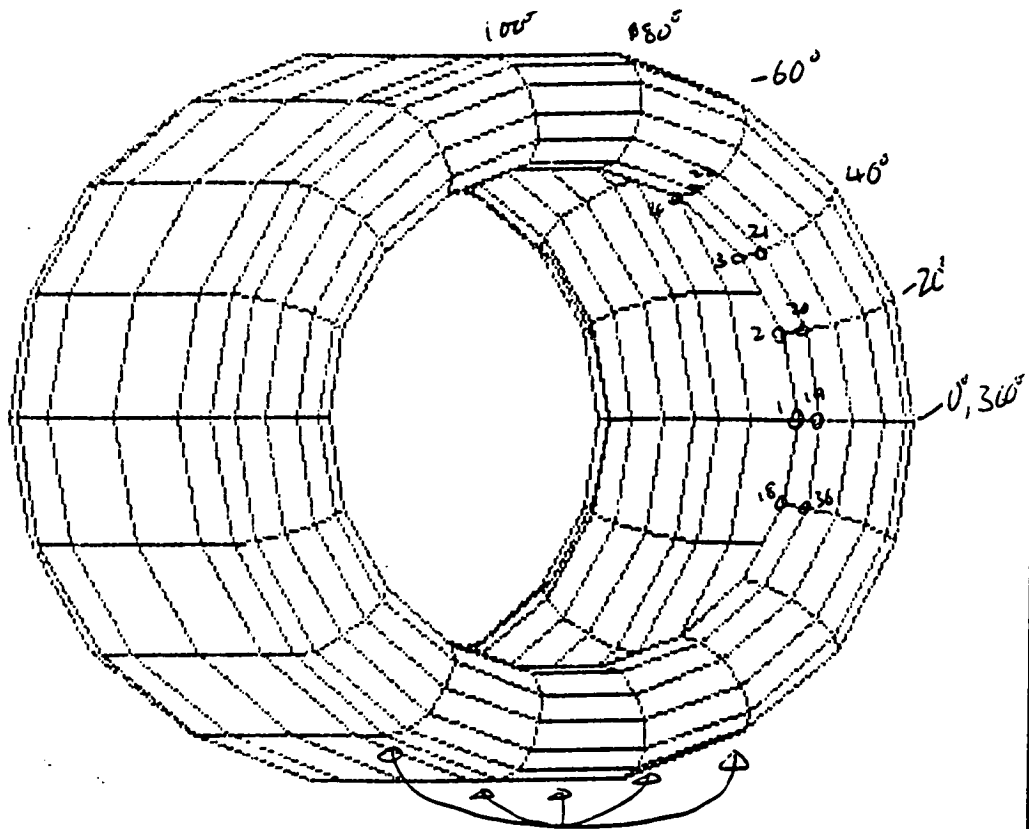
ZERO
TA 1,2,3,4,5,6,7,8,9,10,11,12,13,14,15,16,17,18
TA 289,290,291,292,293,294,295,296,297,298,299,300
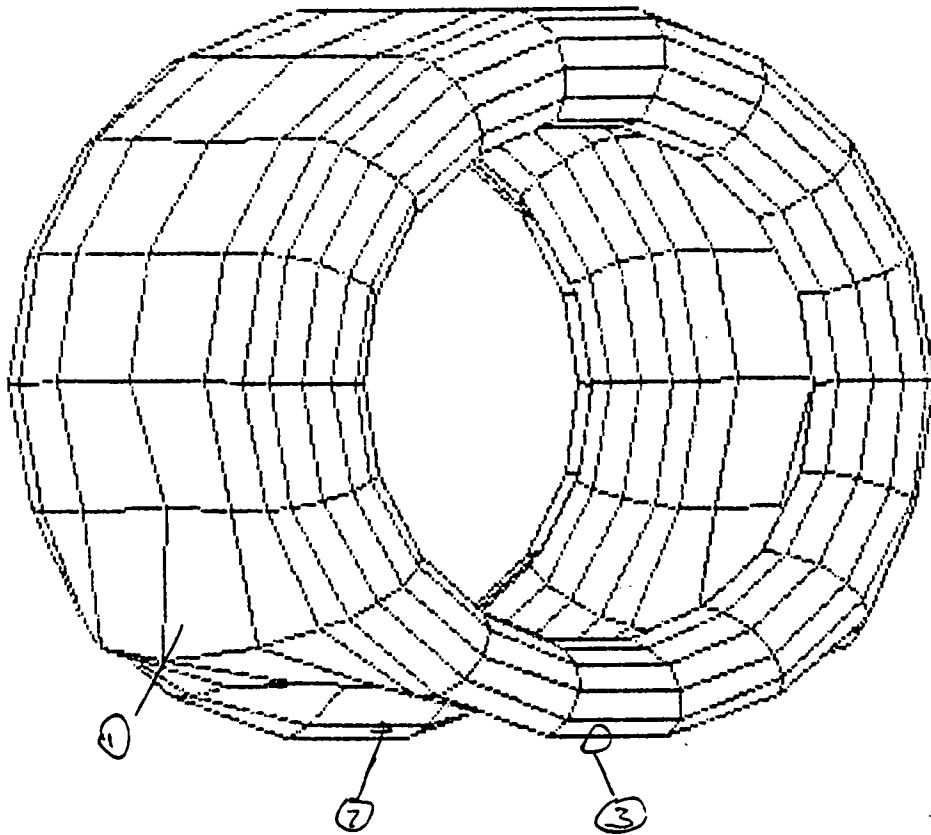TA 301,302,303,304,305,306

END DEFINITION

— these will fix
the points at
the edge of the hub

Pressure load
will be applied
to these

18

Results:

Note: ① A slight bulge was seen at the side of the wheel
② The deflection Profile was hard to see.
③ The side wall deflect very little.

```
C        LOAD FILE FOR TAB.TXT
C        SUBCASE 1
C        PRESSURE LOAD OF 3.104N OVER THE BASE OF 60 DEGREES
C        AREA IS 0.00399 m^2
PRESSURE LOAD APPLIED 21
777.979 121,124,196,1,18

SOLVE

QUIT
```
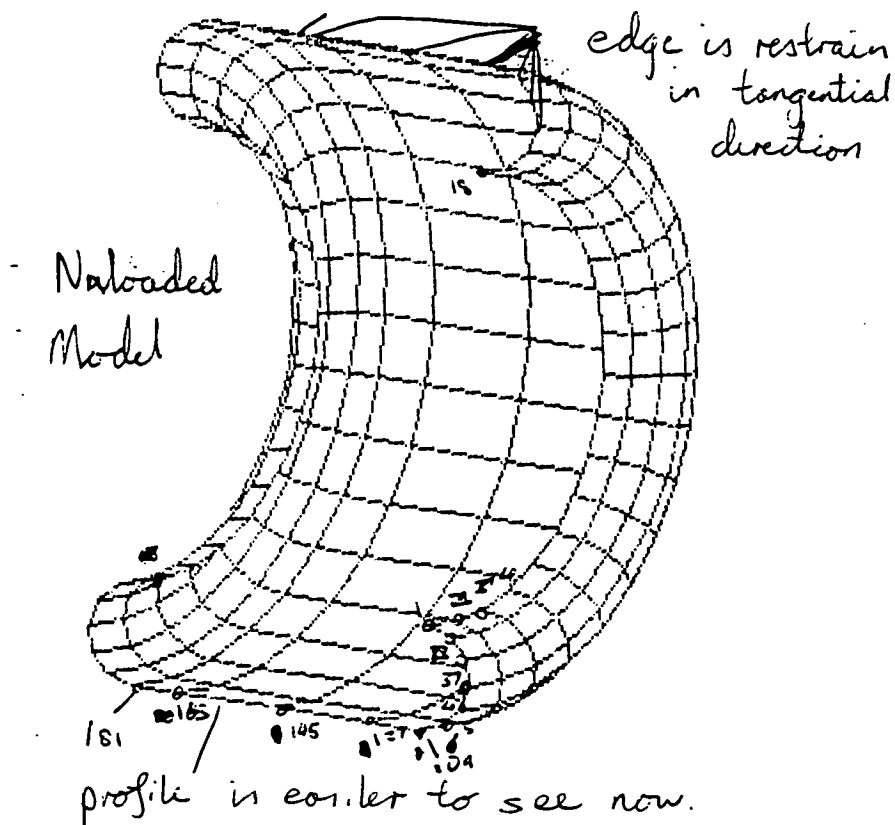
Changes made:
1) Only half the wheel will be model
   - to make the deflection profile easier to see.
   - Finer grid pattern using the same number of points
2) Side wall thickness will be made smaller to increase side wall deflection

Value used:

   Thread thickness = 0.04 cm
   Side wall thickness = 0.01 cm

edge is restrain in tangential direction

- Naloaded
- Model

profile is easier to see now.

110

```
TITLE TAB-WHEEL-1
C        SECOND MODEL OF WHEEL
C        CHANGE : ONLY HALF OF THE WHEEL IS MODELED
C             THICKNESS OF SIDE WALL      = 0.01 cm
C             THICKNESS OF WHEEL THREAD = 0.04 cm
C        LOAD FILE IS T2LOAD.TXT

NODAL POINT LOCATIONS 3
1,0.0435,-90,0.03 THROUGH 18,0.0435,90,0.03
19,0.0448,-90,0.035 THROUGH 36,0.0448,90,0.035
37,0.0485,-90,0.0387 THROUGH 54,0.0485,90,0.0387
55,0.0535,-90,0.04 THROUGH 72,0.0535,90,0.04
73,0.0585,-90,0.0387 THROUGH 90,0.0585,90,0.0387
91,0.0621,-90,0.035  THROUGH 108,0.0621,90,0.035
109,0.0635,-90,0.03 THROUGH 126,0.0635,90,0.03
127,0.0635,-90,0.02 THROUGH 144,0.0635,90,0.02
145,0.0635,-90,0 THROUGH 162,0.0635,90,0
163,0.0635,-90,-0.02 THROUGH 180,0.0635,90,-0.02
181,0.0635,-90,-0.03 THROUGH 198,0.0635,90,-0.03
199,0.0621,-90,-0.035 THROUGH 216,0.0621,90,-0.035
217,0.0585,-90,-0.0387 THROUGH 234,0.0585,90,-0.0387
235,0.0535,-90,-0.04 THROUGH 252,0.0535,90,-0.04
253,0.0485,-90,-0.0387 THROUGH 270,0.0485,90,-0.0387
271,0.0448,-90,-0.035 THROUGH 288,0.0448,90,-0.035
289,0.0435,-90,-0.03 THROUGH 306,0.0435,90,-0.03


MATERIAL PROPERTIES 207E9,79E9,7.7E6,.3,313.7E9
QUADRILATERAL PLATE TYPE 1.1,0.0001
GENERATE CONNECTS 1,109,126,18,1
QUADRILATERAL PLATE TYPE 1,1,0.0004
GENERATE CONNECTS 109,181,198,18,1
QUADRILATERAL PLATE TYPE 1.1,0.0001
GENERATE CONNECTS 181,289,306,18,1

ZERO
TA 1,2,3,4,5,6,7,8,9,10,11,12,13,14,15,16,17,18
TA 289,290,291,292,293,294,295,296,297,298,299,300
TA 301,302,303,304,305,306
TX 1,19,37,55,73,91,109,127,145,163,181,199,217,235,253,271,289
TX 18,36,54,72,90,108,126,144,162,180,198,216,234,252,270,288,306

END DEFINITION
```
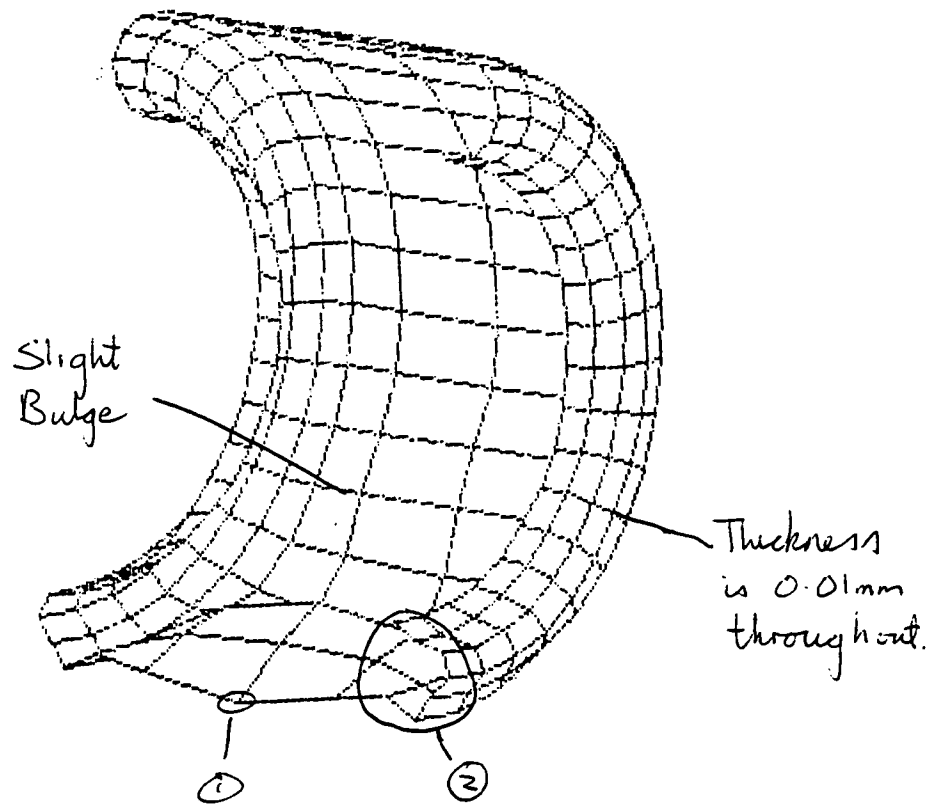
Handwritten annotations:

- Half of wheel only
- → define the nodal point for the half wheel model
- Side wall thickness
- wheel thread thickness
- By constrain them in the x transverse direction we can made half a wheel model react like a full wheel model. This is true only for symmetrical loading.

111

Results:

Slight Bulge
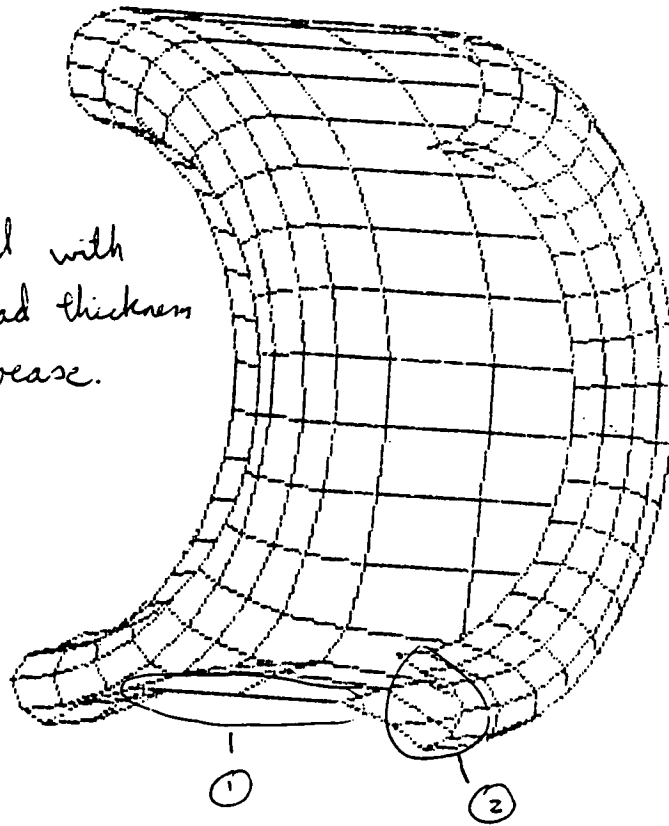
Thickness is 0.01mm throughout.

① ②

Note ① This point is confusing. It should deflect up.

② The side walls look like it is crumbling under the load.

Changes made: The new material thickness is applied

Result:

Model with
thread thickness
increase.

① ②

Note : ① Deflection at this point is much
better

② Sidewalls looks more like spring
deflection now.


```
C       LOAD FILE FOR TAB1.TXT
C       SUBCASE 1
C       PRESSURE LOAD OF 1.552N OVER THE BASE OF 30 DEGREES
C       AREA IS 0.001995 m^2
PRESSURE LOAD APPLIED 21
777.979 109,112,184,1,18

SOLVE

QUIT
```

TITLE TAB-WHEEL-2
```
C       THIRD MODEL OF WHEEL
C       CHANGE : MORE NODES ARE ADDED TO THE BASE OF THE WHEEL WHERE
C               MORE DEFLECTION IS EXPECT TO OCCURS
```

NODAL POINT LOCATIONS 3
```
1,0.0435,-90,0.03 THROUGH 9,0.0435,-50,0.03
10,0.0435,-40,0.03 THROUGH 14,0.0435,0,0.03
15,0.0435,15,0.03 THROUGH 20,0.0435,90,0.03
21,0.0448,-90,0.035 THROUGH 29,0.0448,-50,0.035
30,0.0448,-40,0.035 THROUGH 34,0.0448,0,0.035
35,0.0448,15,0.035 THROUGH 40,0.0448,90,0.035
41,0.0485,-90,0.0387 THROUGH 49,0.0485,-50,0.0387
50,0.0485,-40,0.0387 THROUGH 54,0.0485,0,0.0387
55,0.0485,15,0.0387 THROUGH 60,0.0485,90,0.0387
61,0.0535,-90,0.04 THROUGH 69,0.0535,-50,0.04
70,0.0535,-40,0.04 THROUGH 74,0.0535,0,0.04
75,0.0535,15,0.04 THROUGH 80,0.0535,90,0.04
81,0.0585,-90,0.0387 THROUGH 89,0.0585,-50,0.0387
90,0.0585,-40,0.0387 THROUGH 94,0.0585,0,0.0387
95,0.0585,15,0.0387 THROUGH 100,0.0585,90,0.0387
101,0.0621,-90,0.035  THROUGH 109,0.0621,-50,0.035
110,0.0621,-40,0.035  THROUGH 114,0.0621,0,0.035
115,0.0621,15,0.035  THROUGH 120,0.0621,90,0.035
121,0.0635,-90,0.03 THROUGH 129,0.0635,-50,0.03
130,0.0635,-40,0.03 THROUGH 134,0.0635,0,0.03
135,0.0635,15,0.03 THROUGH 140,0.0635,90,0.03
141,0.0635,-90,0.02 THROUGH 149,0.0635,-50,0.02
150,0.0635,-40,0.02 THROUGH 154,0.0635,0,0.02
155,0.0635,15,0.02 THROUGH 160,0.0635,90,0.02
161,0.0635,-90,0.01 THROUGH 169,0.0635,-50,0.01
170,0.0635,-40,0.01 THROUGH 174,0.0635,0,0.01
175,0.0635,15,0.01 THROUGH 180,0.0635,90,0.01
181,0.0635,-90,0 THROUGH 189,0.0635,-50,0
190,0.0635,-40,0 THROUGH 194,0.0635,0,0
195,0.0635,15,0 THROUGH 200,0.0635,90,0
201,0.0635,-90,-0.01 THROUGH 209,0.0635,-50,-0.01
210,0.0635,-40,-0.01 THROUGH 214,0.0635,0,-0.01
215,0.0635,15,-0.01 THROUGH 220,0.0635,90,-0.01
221,0.0635,-90,-0.02 THROUGH 229,0.0635,-50,-0.02
230,0.0635,-40,-0.02 THROUGH 234,0.0635,0,-0.02
235,0.0635,15,-0.02 THROUGH 240,0.0635,90,-0.02
241,0.0635,-90,-0.03 THROUGH 249,0.0635,-50,-0.03
250,0.0635,-40,-0.03 THROUGH 254,0.0635,0,-0.03
255,0.0635,15,-0.03 THROUGH 260,0.0635,90,-0.03
261,0.0621,-90,-0.035 THROUGH 269,0.0621,-50,-0.035
270,0.0621,-40,-0.035 THROUGH 274,0.0621,0,-0.035
275,0.0621,15,-0.035 THROUGH 280,0.0621,90,-0.035
281,0.0585,-90,-0.0387 THROUGH 289,0.0585,-50,-0.0387
290,0.0585,-40,-0.0387 THROUGH 294,0.0585,0,-0.0387
295,0.0585,15,-0.0387 THROUGH 300,0.0585,90,-0.0387
301,0.0535,-90,-0.04 THROUGH 309,0.0535,-50,-0.04
310,0.0535,-40,-0.04 THROUGH 314,0.0535,0,-0.04
315,0.0535,15,-0.04 THROUGH 320,0.0535,90,-0.04
```

This model gives a much finer grid at the base of the wheel.
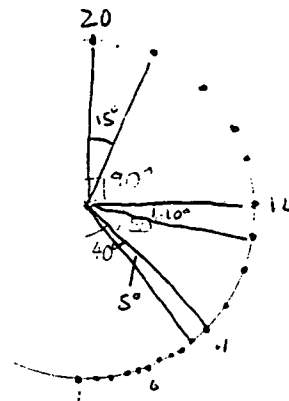
The model starts with 5°/plate then 10°/plate ending with 15°/plate

```
321,0.0485,-90,-0.0387 THROUGH 329,0.0485,-50,-0.0387
330,0.0485,-40,-0.0387 THROUGH 334,0.0485,0,-0.0387
335,0.0485,15,-0.0387 THROUGH 340,0.0485,90,-0.0387
341,0.0448,-90,-0.035 THROUGH 349,0.0448,-50,-0.035
350,0.0448,-40,-0.035 THROUGH 354,0.0448,0,-0.035
355,0.0448,15,-0.035 THROUGH 360,0.0448,90,-0.035
361,0.0435,-90,-0.03 THROUGH 369,0.0435,-50,-0.03
370,0.0435,-40,-0.03 THROUGH 374,0.0435,0,-0.03
375,0.0435,15,-0.03 THROUGH 380,0.0435,90,-0.03


MATERIAL PROPERTIES 207E9,79E9,7.7E6,.3,313.7E9
QUADRILATERAL PLATE TYPE 2,1,0.0004
GENERATE CONNECTS 1,121,140,20,1
QUADRILATERAL PLATE TYPE 2,1,0.00
GENERATE CONNECTS 121,241,260,20,1
QUADRILATERAL PLATE TYPE 2,1,0.000
GENERATE CONNECTS 241,361,380,20,1
```

change to the new thickness (handwritten annotation)

```
ZERO 11
TA 1 THROUGH 20 STEP 1
TA 361 THROUGH 380 STEP 1
TX 1 THROUGH 361 STEP 20
TX 20 THROUGH 380 STEP 20

END DEFINITION




C        LOAD FILE FOR TAB2.TXT
C        SUBCASE 1
C        PRESSURE LOAD IS 1.554N OVER 30 DEGREES OF THE BASE
C        AREA OF CONTACT IS 0.001995 m^2

PRESSURE LOAD APPLIED 21
777.979 121,127,247,1,20

SOLVE

QUIT
```
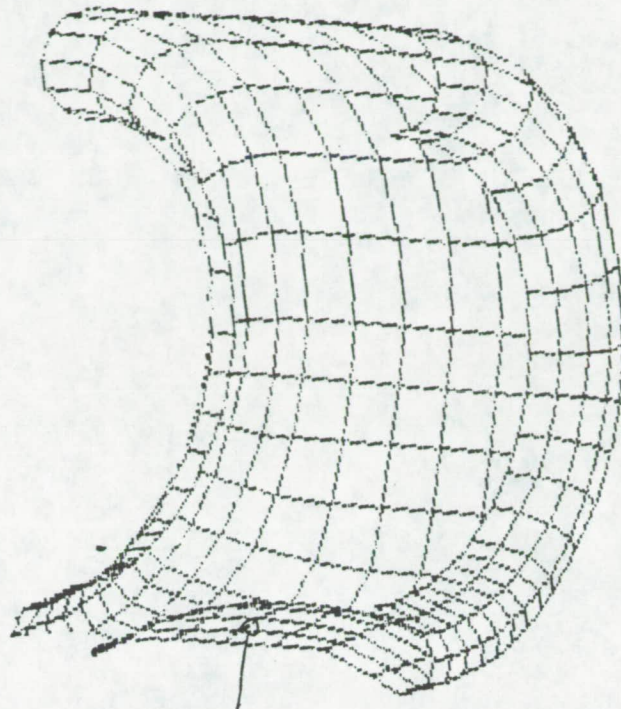
Result.

| 9.1037E-08 | maximum deflection |

The maximum deflection is 9.183×10^{-8} m

This is way too small.

Reasons for small deflection:
1) Model is wrong.

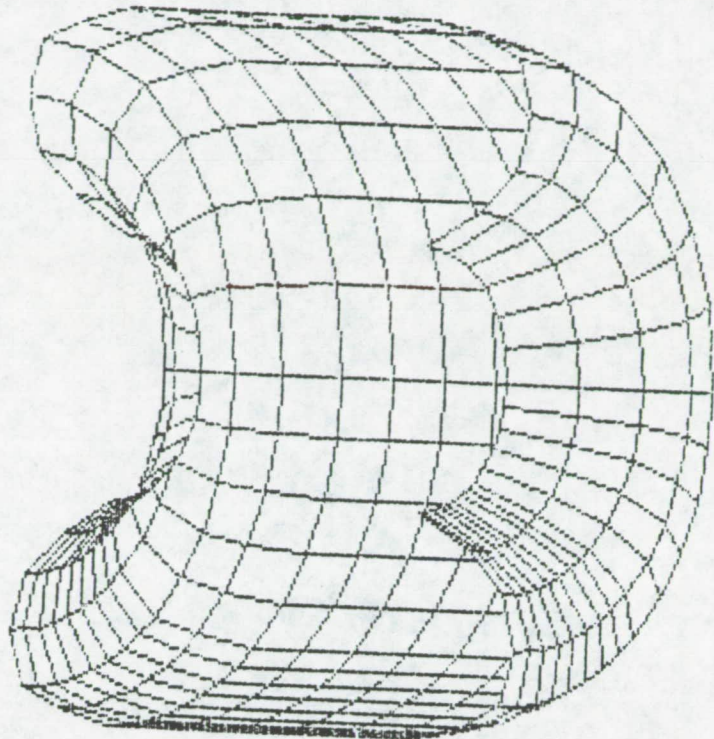2) Side wall is contributing too much interference to the stiffness.

Changes:
1) Reduce side wall area, or increase torus diameter

Result: Increase torus diameter

Unloaded model

| 1.2286E-07 | maximum deflection

By increasing the torus diameter from
2 cm to 4 cm, an increasing in deflection of
1.2286×10^{-7} m from 9.1037×10^{-8} m was seen.
However, this deflection is still too small.

117

TITLE TAB-WHEEL-5
C   SIXTH MODEL OF WHEEL
C   CHANGE : SIDE WALL AREA OF THE WHEEL HAVE BEEN REDUCE BY HALF
:T C   TORUS DIAMETER   = 2.000 cm
C   INNER DIAMETER   = 8.700 cm
C   ⌐ SIDE WALL THICKNESS = 0.010 cm
C   WHEEL TIRE THICKNESS = 0.050 cm
C   YOUNG MODULUS   = 70.0E9 Pa
C   LOAD FILE IS T51LOAD.TXT

NODAL POINT LOCATIONS 3
1 1,0.0435,-87.5,0.03 THROUGH 36,0.0435,87.5,0.03
2 37,0.0448,-87.5,0.035 THROUGH 72,0.0448,87.5,0.035
3 73,0.0485,-87.5,0.0387 THROUGH 108,0.0485,87.5,0.0387
4 109,0.0535,-87.5,0.04 THROUGH 144,0.0535,87.5,0.04
5 145,0.0585,-87.5,0.0387 THROUGH 180,0.0585,87.5,0.0387
6 181,0.0621,-87.5,0.035 THROUGH 216,0.0621,87.5,0.035
7 217,0.0635,-87.5,0.03 THROUGH 252,0.0635,87.5,0.03
8 253,0.0635,-87.5,0.02 THROUGH 288,0.0635,87.5,0.02
9 289,0.0635,-87.5,0.01 THROUGH 324,0.0635,87.5,0.01
10 325,0.0635,-87.5,0 THROUGH 360,0.0635,87.5,0
11 361,0.0635,-87.5,-0.01 THROUGH 396,0.0635,87.5,-0.01
12 397,0.0635,-87.5,-0.02 THROUGH 432,0.0635,87.5,-0.02
13 433,0.0635,-87.5,-0.03 THROUGH 468,0.0635,87.5,-0.03
14 469,0.0621,-87.5,-0.035 THROUGH 504,0.0621,87.5,-0.035
15 505,0.0585,-87.5,-0.0387 THROUGH 540,0.0585,87.5,-0.0387
16 541,0.0535,-87.5,-0.04 THROUGH 576,0.0535,87.5,-0.04
17 577,0.0485,-87.5,-0.0387 THROUGH 612,0.0485,87.5,-0.0387
18 613,0.0448,-87.5,-0.035 THROUGH 648,0.0448,87.5,-0.035
19 649,0.0435,-87.5,-0.03 THROUGH 684,0.0435,87.5,-0.03
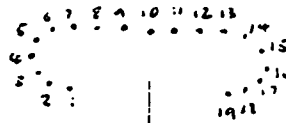
[handwritten: — nodal points from -87.5° to 87.5°]

NODAL POINT LOCATION 1
685,0,-0.0635,0.03 THROUGH 691,0,-0.0635,-0.03
692,0,0.0635,0.03 THROUGH 698,0,0.0635,-0.03

[handwritten: the other 2.5° is make by these nodal points]

MATERIAL PROPERTIES 70E9,0,0,.3
QUADRILATERAL PLATE TYPE 1,1,0.0001
DO CONNECT 1,2,38,37 THROUGH 181,182,218,217 STEP 36,36,36,36
DO CONNECT 3,4,40,39 THROUGH 183,184,220,219 STEP 36,36,36,36
DO CONNECT 5,6,42,41 THROUGH 185,186,222,221 STEP 36,36,36,36
DO CONNECT 7,8,44,43 THROUGH 187,188,224,223 STEP 36,36,36,36
DO CONNECT 9,10,46,45 THROUGH 189,190,226,225 STEP 36,36,36,36
DO CONNECT 11,12,48,47 THROUGH 191,192,228,227 STEP 36,36,36,36
DO CONNECT 13,14,50,49 THROUGH 193,194,230,229 STEP 36,36,36,36
DO CONNECT 15,16,52,51 THROUGH 195,196,232,231 STEP 36,36,36,36
DO CONNECT 17,18,54,53 THROUGH 197,198,234,233 STEP 36,36,36,36
DO CONNECT 19,20,56,55 THROUGH 199,200,236,235 STEP 36,36,36,36
DO CONNECT 21,22,58,57 THROUGH 201,202,238,237 STEP 36,36,36,36
DO CONNECT 23,24,60,59 THROUGH 203,204,240,239 STEP 36,36,36,36
DO CONNECT 25,26,62,61 THROUGH 205,206,242,241 STEP 36,36,36,36
DO CONNECT 27,28,64,63 THROUGH 207,208,244,243 STEP 36,36,36,36
DO CONNECT 29,30,66,65 THROUGH 209,210,246,245 STEP 36,36,36,36
DO CONNECT 31,32,68,67 THROUGH 211,212,248,247 STEP 36,36,36,36
DO CONNECT 33,34,70,69 THROUGH 213,214,250,249 STEP 36,36,36,36

[handwritten: connects the side walls — every single line make a U spring]

```
DO CONNECT 35,36,72,71 THROUGH 215,216,252,251 STEP 36,36,36,36
DO CONNECT 433,434,470,469 THROUGH 613,614,650,649 STEP 36,36,36,36
DO CONNECT 435,436,472,471 THROUGH 615,616,652,651 STEP 36,36,36,36
DO CONNECT 437,438,474,473 THROUGH 617,618,654,653 STEP 36,36,36,36
DO CONNECT 439,440,476,475 THROUGH 619,620,656,655 STEP 36,36,36,36
DO CONNECT 441,442,478,477 THROUGH 621,622,658,657 STEP 36,36,36,36
DO CONNECT 443,444,480,479 THROUGH 623,624,660,659 STEP 36,36,36,36
DO CONNECT 445,446,482,481 THROUGH 625,626,662,661 STEP 36,36,36,36
DO CONNECT 447,448,484,483 THROUGH 627,628,664,663 STEP 36,36,36,36
DO CONNECT 449,450,486,485 THROUGH 629,630,666,665 STEP 36,36,36,36
DO CONNECT 451,452,488,487 THROUGH 631,632,668,667 STEP 36,36,36,36
DO CONNECT 453,454,490,489 THROUGH 633,634,670,669 STEP 36,36,36,36
DO CONNECT 455,456,492,491 THROUGH 635,636,672,671 STEP 36,36,36,36
DO CONNECT 457,458,494,493 THROUGH 637,638,674,673 STEP 36,36,36,36
DO CONNECT 459,460,496,495 THROUGH 639,640,676,675 STEP 36,36,36,36
DO CONNECT 461,462,498,497 THROUGH 641,642,678,677 STEP 36,36,36,36
DO CONNECT 463,464,500,499 THROUGH 643,644,680,679 STEP 36,36,36,36
DO CONNECT 465,466,502,501 THROUGH 645,646,682,681 STEP 36,36,36,36
DO CONNECT 467,468,504,503 THROUGH 647,648,684,683 STEP 36,36,36,36
DO CONNECT 685,217,253,686 THROUGH 690,397,433,691 STEP 1,36,36,1
DO CONNECT 252,692,693,288 THROUGH 432,697,698,468 STEP 36,1,1,36
QUADRILATERAL PLATE TYPE 1,1,0.0005
GENERATE CONNECTS 217,252,468,1,36

ZERO 11
TA 1 THROUGH 36 STEP 1
TA 649 THROUGH 684 STEP 1
TX 685 THROUGH 694 STEP 1
TX 692 THROUGH 698 STEP 1

END DEFINITION
```

another command to use is Generate Connec (handwritten)

connects the wheel thread with the rest of the c spring (handwritten)

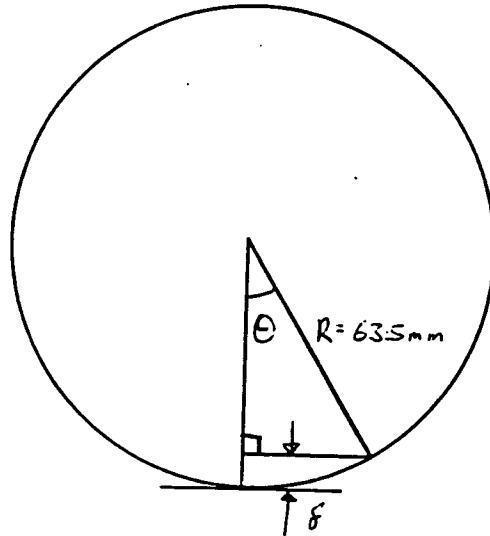*Undeflected model of wheel with 50% Sidewall area removed.* (handwritten caption)
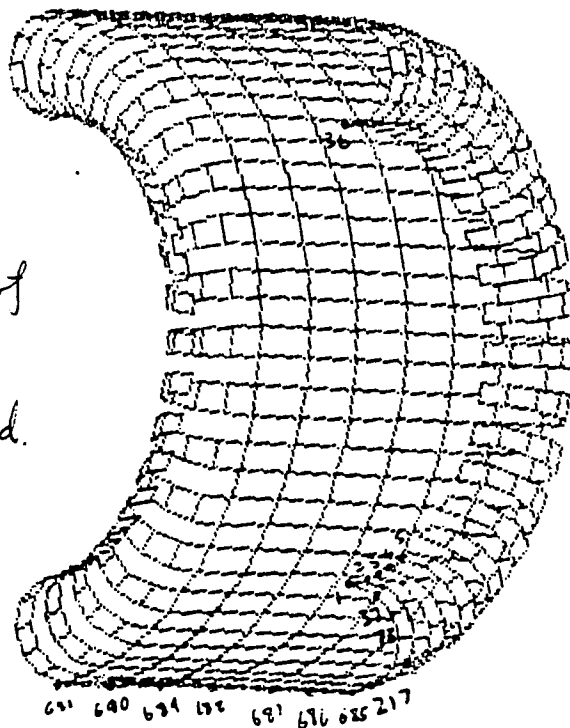
Load File Calculations

$\delta = 15\%$ of torus diameter

torus diameter $= 20_{mm}$

$\delta = 3_{mm}$

$\theta = \cos^{-1} \dfrac{63.5 - 3}{63.5}$

$\quad = 17.68°$

Nearest θ possible in
model is $17.5°$

Area in contact

Area is $\dfrac{\theta w \pi D}{180}$ where $\theta = 17.5°$

$\qquad\qquad\qquad\qquad\qquad\qquad W = 0.06\,m$

$\qquad\qquad\qquad\qquad\qquad\qquad D = 0.127m$

$\quad$ Area $= \dfrac{17.5 \times 0.06 \times \pi \times 0.127}{180}$

$\qquad\qquad = 0.002323 \ m^2$

Pressure applied is $\dfrac{\text{Force}}{\text{Area}}$

$\quad$ Force $= 3.104 N$ — weight per wheel

$\quad P_A = \dfrac{3.104}{0.002323} = 1333.68 \ N/m^2$

```
C       SUBCASE 1                              17.5
C       NORMAL FORCE LOAD ONLY OVER 25 DRGREES OF BASE
C       FORCES IS HALF OF 3.014N = 1.552N
C       AREA IS 0.001229 m^2   0.001163
PRESSURE LOAD APPLIED 21
1333.679 217,220,436,1,36
        pressure load
PRESSURE LOAD APPLIED 12
1333.679 685,217,253,686 THROUGH 690,397,433,691 STEP 1,36,36,1

SOLVE

C       SUBCASE 2
C       SIDE LOADING EQUILIVENT TO GOING ALONG A SLOPE OF 27 DEGREES
C       SIDE LOAD  = 1.409N/2
C       NORNAL LOAD = 2.765N/2
PRESSURE LOAD APPLIED 21
1188.3167 217,220,436,1,36
        pressure load
PRESSURE LOAD APPLIED 12
1188.3167 685,217,253,686 THROUGH 690,397,433,691 STEP 1,36,36,1

FORCES AND MOMENTS APPLIED 21
FZ 0.01118 217,220,436,1,36
        side forces
FORCES AND MOMENTS APPLIED 11
FZ 0.01118 685 THROUGH 691 STEP 1

SOLVE

QUIT
```
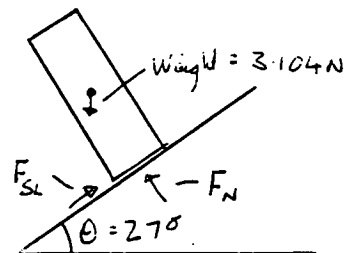
$\underline{Side\ load\ force}$

$\theta = 27° =$ the angle of repose in main soil

$F_N = \cos 27 \times 3.104$
$\quad = 2.765\ N$

$F_{SL} = \sin 27 \times 3.104$
$\quad = 1.409\ N$
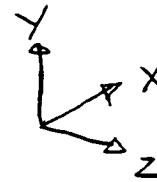
Weight = 3.104N F_{SL} F_N $\theta = 27°$

Radial Load only
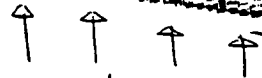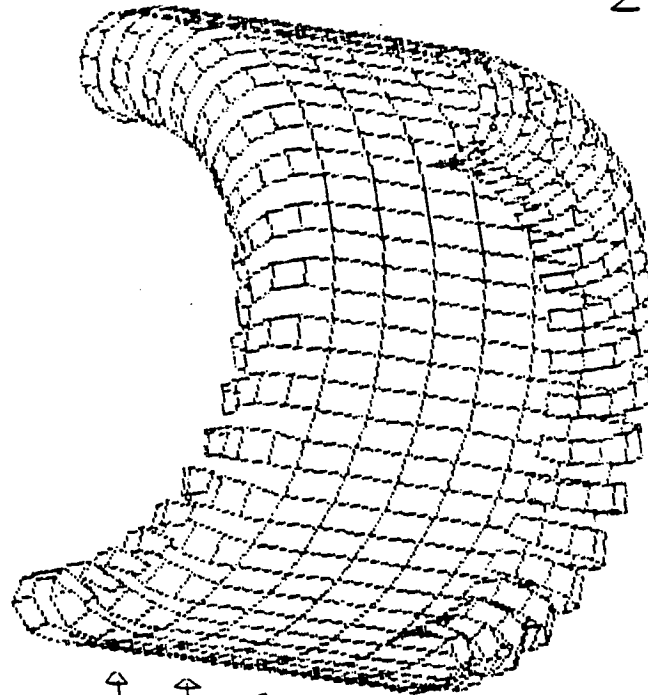
load applied = 1.552N

1.6880E-03 — maximum deflection

Results: Radial deflection have increase from
1.22×10⁻³m to 1.688×10⁻³m.

Target deflection is 3.0×10⁻³m

Wheel show promise, thus we will
pursue this model.

Axially and radially loaded wheel
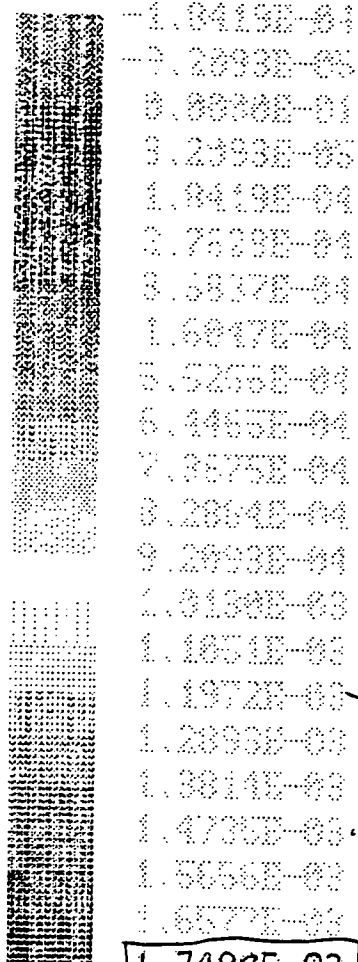
1.7498E-03 — maximum deflection

$F_2 = 1.409 N$

$F_N = 2.765 N$
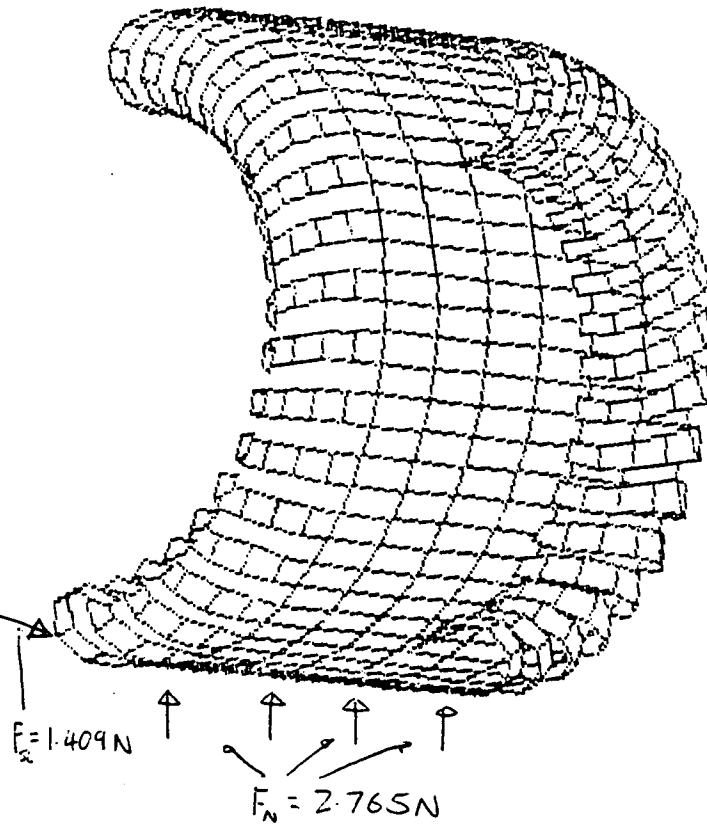
Results: The maximum deflection under axial and radial load is slightly larger than only radial loaded wheel deflection.

This would most prob. come from the side load force.
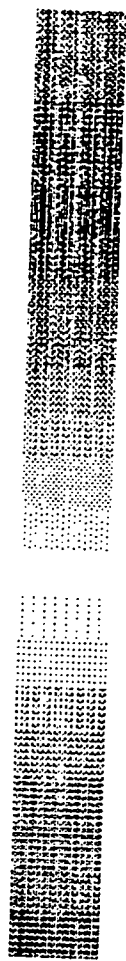
123

TRANS. DISPL. Z

side loaded model showing axial deflection
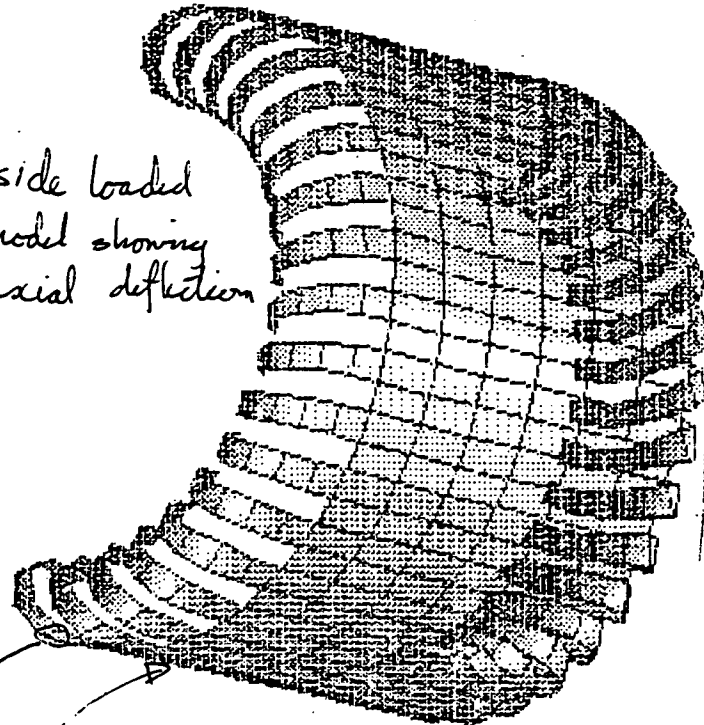
Maximum axial deflection is 1.35×10^{-3} m

Result: Axial deflection is around the same order of magnitude as radial deflection. This is bad news as one of the design requirement is to reduce axial to one tenth or less than the radial deflection

By trial and error, it was found that a thickness of 0.075mm gives the nearest radial deflection of 3.18mm when aluminum was used as the wheel material.

However, axial deflection was 2.91mm. Which was 91.5% of axial deflection. The Target deflection was 10%. Therefore, ways have to be found to reduce axial deflection.

One method that was considered, was to increase the thickness at the highest stress location due to axial load. However, when this was tried out on the wheel model, it was found that the highest stress due to radial and axial load is around the same location of the wheel.

When we realized that the axial deflection cannot be reduce through changing the thickness at the highest stress location, we decided to find a new wheel design that will have smaller axial deflection

After a group discussion, a new geometry, shown below was choosen to meet the small axial deflection requirement.
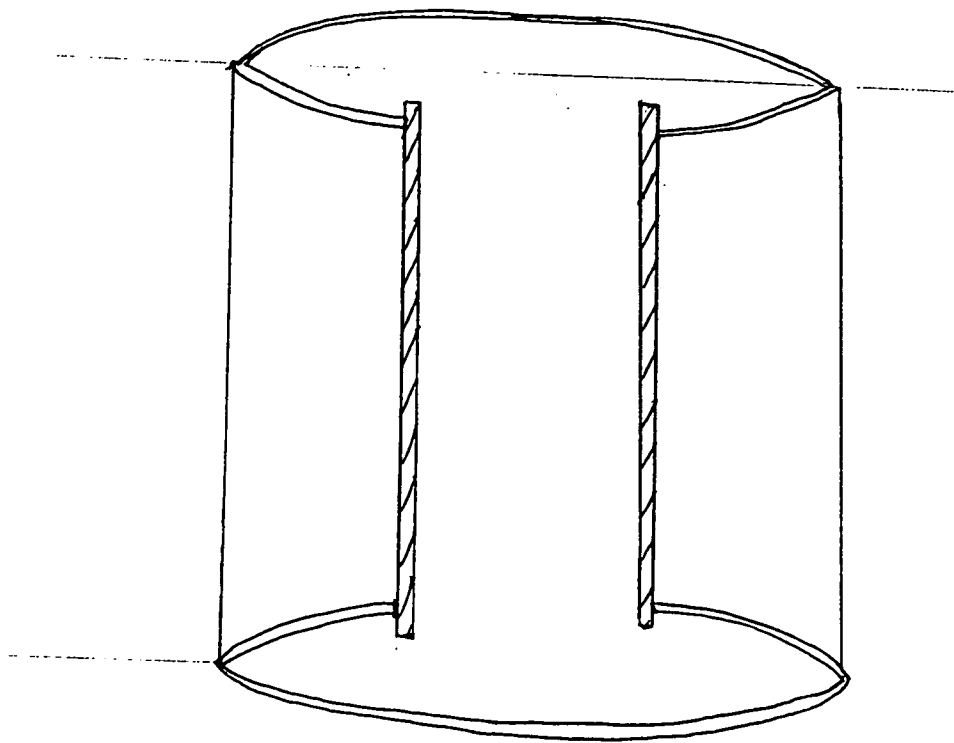
New Wheel Model

This wheel model went thought several modification to its geometry before arriving at the final design. Each modification aim was to achive the target of 1.5mm radial deflection and 0.15mm axial deflection.

All the PAL2 listing of the NEW model
are listed below. Together with the listing,
the equations used to calculate the
geometry are also shown (curved models only).

First Model
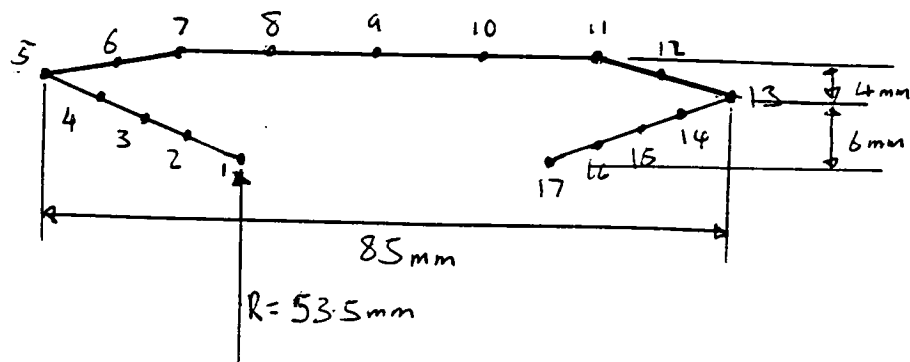
Note: Width for all model is 85mm

Second Model

Third Model

Curve 1

Curve 2

R: 53.5mm

42.3mm

2mm
2mm
4mm
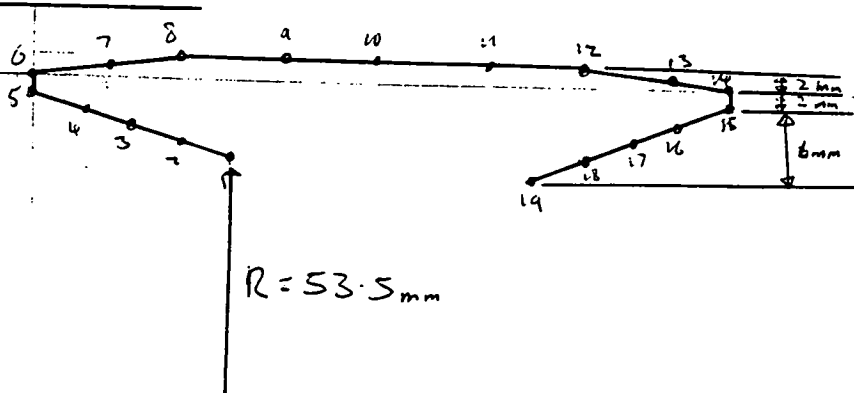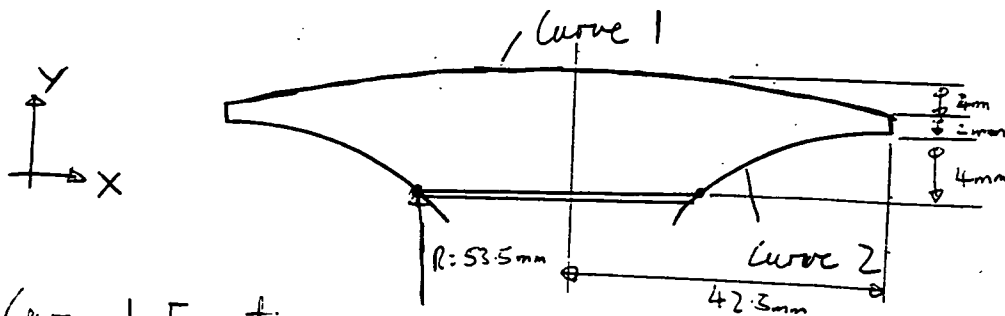
Curve 1 Equation

$$y = 63.5 - \left(R - \sqrt{R^2 - x^2} \right)$$

where $R = \dfrac{8^2 + x_{max}^2}{28}$

Example

8

x_{max}
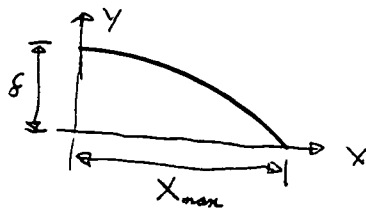
Curve 2 Equation

$$y = 57.5 - \left(R - \sqrt{R^2 - (42.5 - x)^2} \right)$$

Fourth Model

Curve 1

Curve 3

R: 53.5mm

12.5mm

4mm
2mm
4mm
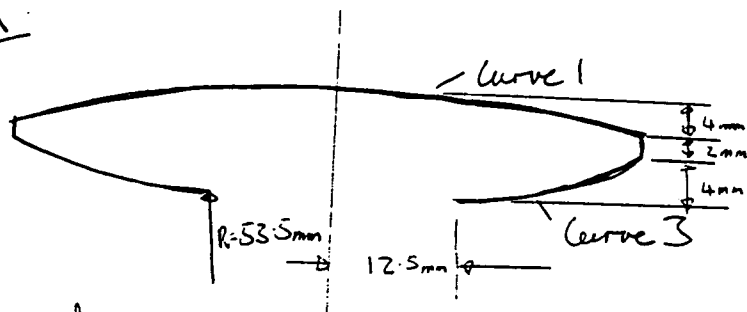
Curve 3 Equation

$$y = 53.5 + \left(R - \sqrt{R^2 - (x - 12.5)^2} \right)$$

Fifth Model

27.5 mm

Curve 4

4mm
2 mm
4mm
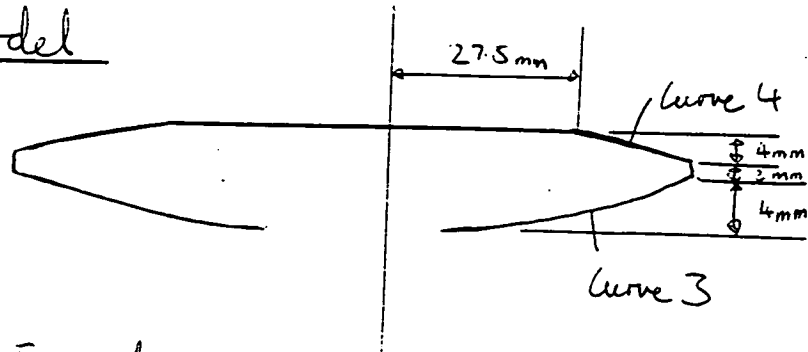
Curve 3

Curve 4 Equation

$$y = 63.5 - \left(R - \sqrt{R^2 - (x - 27.5)^2}\right)$$

Model of
the New Wheel.
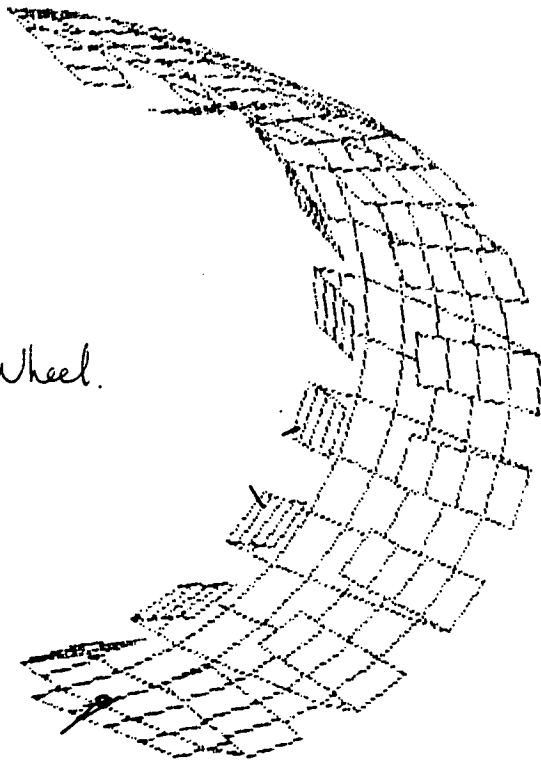
TITLE DIAMOND-WHEEL-1
C   FIRST MODEL OF WHEEL
C   DIAMETER OF WHEEL   = 12.7 cm
C   HUB DIAMETER   = 10.7 cm
C   WIDTH OF WHEEL   = 8.5 cm
C   SIDE WALL THICKNESS = 0.01 cm
C   WHEEL TIRE THICKNESS = 0.01 cm
C   YOUNG MODULUS   = 70E9 Pa
C   LOAD FILE IS D11LOAD.TXT

NODAL POINT LOCATIONS 3
1,0.0535,-85,0.0125 THROUGH 18,0.0535,85,0.0125
19,0.0555,-85,0.02 THROUGH 36,0.0555,85,0.02
37,0.0575,-85,0.0275 THROUGH 54,0.0575,85,0.0275
55,0.0595,-85,0.035 THROUGH 72,0.0595,85,0.035
73,0.0615,-85,0.0425 THROUGH 90,0.0615,85,0.0425
91,0.0625,-85,0.035 THROUGH 108,0.0625,85,0.035
109,0.0635,-85,0.0275 THROUGH 126,0.0635,85,0.0275
127,0.0635,-85,0.01375 THROUGH 144,0.0635,85,0.01375
145,0.0635,-85,0 THROUGH 162,0.0635,85,0
163,0.0635,-85,-0.01375 THROUGH 180,0.0635,85,-0.01375
181,0.0635,-85,-0.0275 THROUGH 198,0.0635,85,-0.0275
199,0.0625,-85,-0.035 THROUGH 216,0.0625,85,-0.035
217,0.0615,-85,-0.0425 THROUGH 234,0.0615,85,-0.0425
235,0.0595,-85,-0.035 THROUGH 252,0.0595,85,-0.035
253,0.0575,-85,-0.0275 THROUGH 270,0.0575,85,-0.0275
271,0.0555,-85,-0.02 THROUGH 288,0.0555,85,-0.02
289,0.0535,-85,-0.0125 THROUGH 306,0.0535,85,-0.0125

NODAL POINT LOCATION 1
307,0,-0.0635,0.0275 THROUGH 311,0,-0.0635,-0.0275
312,0,0.0635,0.0275 THROUGH 316,0,0.0635,-0.0275

MATERIAL PROPERTIES 70E9,0,0,0.3
C   LOWER PLATE
QUADRILATERAL PLATE TYPE 1,1,0.0001
GENERATE CONNECTS 1,2,74,1,18
GENERATE CONNECTS 3,4,76,1,18
GENERATE CONNECTS 5,6,78,1,18
GENERATE CONNECTS 7,8,80,1,18
GENERATE CONNECTS 9,10,82,1,18
GENERATE CONNECTS 11,12,84,1,18
GENERATE CONNECTS 13,14,86,1,18
GENERATE CONNECTS 15,16,88,1,18
GENERATE CONNECTS 17,18,90,1,18
GENERATE CONNECTS 217,218,290,1,18
GENERATE CONNECTS 219,220,292,1,18
GENERATE CONNECTS 221,222,294,1,18
GENERATE CONNECTS 223,224,296,1,18
GENERATE CONNECTS 225,226,298,1,18
GENERATE CONNECTS 227,228,300,1,18
GENERATE CONNECTS 229,230,302,1,18
GENERATE CONNECTS 231,232,304,1,18
GENERATE CONNECTS 233,234,306,1,18

130

```
C        UPPER PLATE
QUADRILATERAL PLATE TYPE 1,1,0.0001
GENERATE CONNECTS 73,74,110,1,18
GENERATE CONNECTS 75,76,112,1,18
GENERATE CONNECTS 77,78,114,1,18
GENERATE CONNECTS 79,80,116,1,18
GENERATE CONNECTS 81,82,118,1,18
GENERATE CONNECTS 83,84,120,1,18
GENERATE CONNECTS 85,86,122,1,18
GENERATE CONNECTS 87,88,124,1,18
GENERATE CONNECTS 89,90,126,1,18
GENERATE CONNECTS 181,182,218,1,18
GENERATE CONNECTS 183,184,220,1,18
GENERATE CONNECTS 185,186,222,1,18
GENERATE CONNECTS 187,188,224,1,18
GENERATE CONNECTS 189,190,226,1,18
GENERATE CONNECTS 191,192,228,1,18
GENERATE CONNECTS 193,194,230,1,18
GENERATE CONNECTS 195,196,232,1,18
GENERATE CONNECTS 197,198,234,1,18
C        WHEEL THREAD
QUADRILATERAL PLATE TYPE 1,1,0.0001
DO CONNECT 307,109,127,308 THROUGH 310,163,182,311 STEP 1,18,18,1
DO CONNECT 126,312,313,144 THROUGH 180,315,316,198 STEP 18,1,1,18
GENERATE CONNECTS 109,126,198,1,18

ZERO 11
TA 1 THROUGH 18 STEP 1
TA 289 THROUGH 306 STEP 1
TX 307 THROUGH 316 STEP 1
RZ 307 THROUGH 316 STEP 1
END DEFINITION
```

131

TITLE DIAMOND-WHEEL-2
C   FIRST MODEL OF WHEEL
C   DIAMETER OF WHEEL = 12.7 cm
C   HUB DIAMETER   = 10.7 cm
C   WIDTH OF WHEEL   = 8.5 cm
C   SIDE WALL THICKNESS = 0.01 cm
C   WHEEL TIRE THICKNESS = 0.01 cm
C   YOUNG MODULUS   = 70E9 Pa
C   LOAD FILE IS D21LOAD.TXT

NODAL POINT LOCATIONS 3
1,0.0535,-85,0.0125 THROUGH 18,0.0535,85,0.0125
19,0.055,-85,0.02 THROUGH 36,0.055,85,0.02
37,0.0565,-85,0.0275 THROUGH 54,0.0565,85,0.0275
55,0.0580,-85,0.035 THROUGH 72,0.0580,85,0.035
73,0.0595,-85,0.0425 THROUGH 90,0.0595,85,0.0425
91,0.0615,-85,0.0425 THROUGH 108,0.0615,85,0.0425
109,0.0625,-85,0.035 THROUGH 126,0.0625,85,0.035
127,0.0635,-85,0.0275 THROUGH 144,0.0635,85,0.0275
145,0.0635,-85,0.01375 THROUGH 162,0.0635,85,0.0137
163,0.0635,-85,0 THROUGH 180,0.0635,85,0
181,0.0635,-85,-0.01375 THROUGH 198,0.0635,85,-0.0137$
199,0.0635,-85,-0.0275 THROUGH 216,0.0635,85,-0.0275
217,0.0625,-85,-0.035 THROUGH 234,0.0625,85,-0.035
235,0.0615,-85,-0.0425 THROUGH 252,0.0615,85,-0.0425
253,0.0595,-85,-0.0425 THROUGH 270,0.0575,85,-0.0425
271,0.0580,-85,-0.035 THROUGH 288,0.0580,85,-0.035
289,0.0565,-85,-0.0275 THROUGH 306,0.0565,85,-0.0275
307,0.055,-85,-0.02 THROUGH 324,0.055,85,-0.02
325,0.0535,-85,-0.0125 THROUGH 342,0.0535,85,-0.0125

NODAL POINT LOCATIONS 1
343,0,-0.0635,0.0275 THROUGH 347,0,-0.0635,-0.0275
348,0,0.0635,0.0275 THROUGH 352,0,0.0635,-0.0275

MATERIAL PROPERTIES 70E9,0,0,0.3
C   LOWER PLATE
QUADRILATERAL PLATE TYPE 1,1,0.0001
GENERATE CONNECTS 1,2,74,1,18
GENERATE CONNECTS 3,4,76,1,18
GENERATE CONNECTS 5,6,78,1,18
GENERATE CONNECTS 7,8,80,1,18
GENERATE CONNECTS 9,10,82,1,18
GENERATE CONNECTS 11,12,84,1,18
GENERATE CONNECTS 13,14,86,1,18
GENERATE CONNECTS 15,16,88,1,18
GENERATE CONNECTS 17,18,90,1,18
GENERATE CONNECTS 253,254,326,1,18
GENERATE CONNECTS 255,256,328,1,18
GENERATE CONNECTS 257,258,330,1,18
GENERATE CONNECTS 259,260,332,1,18
GENERATE CONNECTS 261,262,334,1,18
GENERATE CONNECTS 263,264,336,1,18
GENERATE CONNECTS 265,266,338,1,18

132

```
GENERATE CONNECTS 267,268,340,1,18
GENERATE CONNECTS 269,270,342,1,18
C        CENTER PLATE
QUADRILATERAL PLATE TYPE 1,1,0.0001
CONNECT 73,74,92,91
CONNECT 75,76,94,93
CONNECT 77,78,96,95
CONNECT 79,80,98,97
CONNECT 81,82,100,99
CONNECT 83,84,102,101
CONNECT 85,86,104,103
CONNECT 87,88,106,105
CONNECT 89,90,108,107
CONNECT 235,236,254,253
CONNECT 237,238,256,255
CONNECT 239,240,258,257
CONNECT 241,242,260,259
CONNECT 243,244,262,261
CONNECT 245,246,264,263
CONNECT 247,248,266,265
CONNECT 249,250,268,267
CONNECT 251,252,270,269
C        UPPER PLATE
QUADRILATERAL PLATE TYPE 1,1,0.0001
GENERATE CONNECTS 91,92,128,1,18
GENERATE CONNECTS 93,94,130,1,18
GENERATE CONNECTS 95,96,132,1,18
GENERATE CONNECTS 97,98,134,1,18
GENERATE CONNECTS 99,100,136,1,18
GENERATE CONNECTS 101,102,138,1,18
GENERATE CONNECTS 103,104,140,1,18
GENERATE CONNECTS 105,106,142,1,18
GENERATE CONNECTS 107,108,144,1,18
GENERATE CONNECTS 199,200,236,1,18
GENERATE CONNECTS 201,202,238,1,18
GENERATE CONNECTS 203,204,240,1,18
GENERATE CONNECTS 205,206,242,1,18
GENERATE CONNECTS 207,208,244,1,18
GENERATE CONNECTS 209,210,246,1,18
GENERATE CONNECTS 211,212,248,1,18
GENERATE CONNECTS 213,214,250,1,18
GENERATE CONNECTS 215,216,252,1,18
C        WHEEL THREAD
QUADRILATERAL PLATE TYPE 1,1,0.0001
DO CONNECT 343,127,145,344 THROUGH 346,182,200,347 STEP 1,18,18,1
DO CONNECT 144,348,349,162 THROUGH 198,351,352,216 STEP 18,1,1,18
GENERATE CONNECTS 127,144,216,1,18

ZERO 11
TA 1 THROUGH 18 STEP 1
TA 325 THROUGH 342 STEP 1
TX 343 THROUGH 352 STEP 1
TZ 343 THROUGH 352 STEP 1
END DEFINITION
```

TITLE DIAMOND-WHEEL-3
C   *Third* ~~FIRST~~ MODEL OF WHEEL
C   DIAMETER OF WHEEL   = 12.7 cm
C   HUB DIAMETER   = 10.7 cm
C   WIDTH OF WHEEL   = 8.5 cm
C   SIDE WALL THICKNESS = 0.01 cm
C   WHEEL TIRE THICKNESS = 0.01 cm
C   YOUNG MODULUS   = 70E9 Pa
C   LOAD FILE IS D21LOAD.TXT
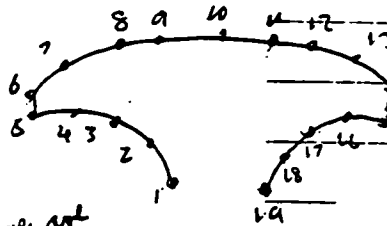
NODAL POINT LOCATIONS 3   *, Here value are change*
1 1,0.0535,-85,0.0125 THROUGH 18,0.0535,85,0.0125
2 19,0.05527,-85,0.02 THROUGH 36,0.05527,85,0.02
3 37,0.05651,-85,0.0275 THROUGH 54,0.05651,85,0.0275
4 55,0.05725,-85,0.035 THROUGH 72,0.05725,85,0.035
5 73,0.0575,-85,0.0425 THROUGH 90,0.0575,85,0.0425
6 91,0.0595,-85,0.0425 THROUGH 108,0.0595,85,0.0425
7 109,0.0608,-85,0.035 THROUGH 126,0.0608,85,0.035
8 127,0.0618,-85,0.0275 THROUGH 144,0.0618,85,0.0275
9 145,0.0631,-85,0.01375 THROUGH 162,0.0631,85,0.01375
10 163,0.0635,-85,0 THROUGH 180,0.0635,85,0
11 181,0.0631,-85,-0.01375 THROUGH 198,0.0631,85,-0.01375
12 199,0.0618,-85,-0.0275 THROUGH 216,0.0618,85,-0.0275
13 217,0.0608,-85,-0.035 THROUGH 234,0.0608,85,-0.035
14 235,0.0595,-85,-0.0425 THROUGH 252,0.0595,85,-0.0425
16 253,0.0575,-85,-0.0425 THROUGH 270,0.0575,85,-0.0425
17 271,0.05725,-85,-0.035 THROUGH 288,0.05725,85,-0.035
17 289,0.05651,-85,-0.0275 THROUGH 306,0.05651,85,-0.0275
18 307,0.05527,-85,-0.02 THROUGH 324,0.05527,85,-0.02
19 325,0.0535,-85,-0.0125 THROUGH 342,0.0535,85,-0.0125

NODAL POINT LOCATIONS 1
343,0,-0.0618,0.0275
344,0,-0.0631,0.01375
345,0,-0.0635,0
346,0,-0.0631,-0.01375
347,0,-0.0618,-0.0275
348,0,0.0618,0.0275
349,0,0.0631,0.01375
350,0,0.0635,0
351,0,0.0631,-0.01375
352,0,0.0618,-0.0275

Curve point on the thread.

MATERIAL PROPERTIES 70E9,0,0,0.3   *thickness*
C   LOWER PLATE
QUADRILATERAL PLATE TYPE 1,1,0.0001
GENERATE CONNECTS 1,2,74,1,18
GENERATE CONNECTS 3,4,76,1,18
GENERATE CONNECTS 5,6,78,1,18
GENERATE CONNECTS 7,8,80,1,18
GENERATE CONNECTS 9,10,82,1,18
GENERATE CONNECTS 11,12,84,1,18
GENERATE CONNECTS 13,14,86,1,18
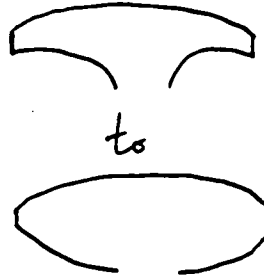GENERATE CONNECTS 15,16,88,1,18

the rest of the file is the same as the second model

TITLE DIAMOND-WHEEL 4

C   FIRST MODEL OF WHEEL
C   DIAMETER OF WHEEL   = 12.7 cm
C   HUB DIAMETER   = 10.7 cm
C   WIDTH OF WHEEL   = 8.5 cm
C   SIDE WALL THICKNESS = 0.01 cm
C   WHEEL TIRE THICKNESS = 0.01 cm
C   YOUNG MODULUS   = 70E9 Pa
C   LOAD FILE IS D21LOAD.TXT

NODAL POINT LOCATIONS 3
1,0.0535,-85,0.0125 THROUGH 18,0.0535,85,0.0125
19,0.05375,-85,0.02 THROUGH 36,0.05375,85,0.02
37,0.05449,-85,0.0275 THROUGH 54,0.05449,85,0.0275
55,0.05573,-85,0.035 THROUGH 72,0.05573,85,0.035
73,0.0575,-85,0.0425 THROUGH 90,0.0575,85,0.0425
91,0.0595,-85,0.0425 THROUGH 108,0.0595,85,0.0425
109,0.0608,-85,0.035 THROUGH 126,0.0608,85,0.035
127,0.0618,-85,0.0275 THROUGH 144,0.0618,85,0.0275
145,0.0631,-85,0.01375 THROUGH 162,0.0631,85,0.01375
163,0.0635,-85,0 THROUGH 180,0.0635,85,0
181,0.0631,-85,-0.01375 THROUGH 198,0.0631,85,-0.01375
199,0.0618,-85,-0.0275 THROUGH 216,0.0618,85,-0.0275
217,0.0608,-85,-0.035 THROUGH 234,0.0608,85,-0.035
235,0.0595,-85,-0.0425 THROUGH 252,0.0595,85,-0.0425
253,0.0575,-85,-0.0425 THROUGH 270,0.0575,85,-0.0425
271,0.05573,-85,-0.035 THROUGH 288,0.05573,85,-0.035
289,0.05449,-85,-0.0275 THROUGH 306,0.05449,85,-0.0275
307,0.05375,-85,-0.02 THROUGH 324,0.05375,85,-0.02
325,0.0535,-85,-0.0125 THROUGH 342,0.0535,85,-0.0125

NODAL POINT LOCATIONS 1
343,0,-0.0618,0.0275
344,0,-0.0631,0.01375
345,0,-0.0635,0
346,0,-0.0631,-0.01375
347,0,-0.0618,-0.0275
348,0,0.0618,0.0275
349,0,0.0631,0.01375
350,0,0.0635,0
351,0,0.0631,-0.01375
352,0,0.0618,-0.0275

From

to

the rest of the file is the same as the second model.

135

TITLE DIAMOND-WHEEL-7
C   FIRST MODEL OF WHEEL
C   DIAMETER OF WHEEL   = 12.7 cm
C   HUB DIAMETER   = 10.7 cm
C   WIDTH OF WHEEL   = 8.5 cm
C   SIDE WALL THICKNESS = 0.0125 cm
C   WHEEL TIRE THICKNESS = 0.0125 cm
C   YOUNG MODULUS   = 70E9 Pa
C   LOAD FILE IS DZ1LOAD.TXT

NODAL POINT LOCATIONS 3
1,0.0535, 85,0.0125 THROUGH 18,0.0535,85,0.0125
19,0.0538,-85,0.02 THROUGH 36,0.0538,85,0.02
37,0.05472, 85,0.0275 THROUGH 54,0.05472,85,0.0275
55,0.05628,-85,0.035 THROUGH 72,0.05628,85,0.035
73,0.0585,-85,0.0425 THROUGH 90,0.0585,85,0.0425
91,0.0605,-85,0.0425 THROUGH 108,0.0605,85,0.0425
109,0.06277,-85,0.035 THROUGH 126,0.06277,85,0.035
127,0.0635,-85,0.0275 THROUGH 144,0.0635,85,0.0275
145,0.0635,-85,0.01375 THROUGH 162,0.0635,85,0.01375
163,0.0635,-85,0 THROUGH 180,0.0635,85,0
181,0.0635, 85, 0.01375 THROUGH 198,0.0635,85,-0.01375
199,0.0635,-85,-0.0275 THROUGH 216,0.0635,85,-0.0275
217,0.06277, 85, 0.035 THROUGH 234,0.06277,85,-0.035
235,0.0605,-85,-0.0425 THROUGH 252,0.0605,85,-0.0425
253,0.0585, 85, 0.0425 THROUGH 270,0.0585,85,-0.0425
271,0.05628,-85,-0.035 THROUGH 288,0.05628,85,-0.035
289,0.05472, 85, 0.0275 THROUGH 306,0.05472,85,-0.0275
307,0.0538,-85,-0.02 THROUGH 324,0.0538,85,-0.02
325,0.0535,-85,-0.0125 THROUGH 342,0.0535,85,-0.0125

NODAL POINT LOCATIONS 1
343,0,-0.0635,0.0275
344,0, 0.0635,0.01375
345,0,-0.0635,0
346,0, 0.0635, 0.01375
347,0,-0.0635,-0.0275
348,0,0.0635,0.0275
349,0,0.0635,0.01375
350,0,0.0635,0
351,0,0.0635,-0.01375
352,0,0.0635,-0.0275

MATERIAL PROPERTIES 70E9,0,0,0.3
C   LOWER PLATE
QUADRILATERAL PLATE TYPE 1,1,0.00015
GENERATE CONNECTS 1,2,74,1,18
GENERATE CONNECTS 3,4,76,1,18
GENERATE CONNECTS 5,6,78,1,18
GENERATE CONNECTS 7,8,80,1,18
GENERATE CONNECTS 9,10,82,1,18
GENERATE CONNECTS 11,12,84,1,18
GENERATE CONNECTS 13,14,86,1,18

The rest of the file is the same as the second model

I36

TITLE DIAMOND-WHEEL-8
C   LAST MODEL OF WHEEL (FULL MODEL)
C   DIAMETER OF WHEEL   = 12.7 cm
C   HUB DIAMETER   = 10.7 cm
C   WIDTH OF WHEEL   = 8.5   cm
C   SIDE WALL THICKNESS = 0.015 cm
C   WHEEL TIRE THICKNESS = 0.015 cm
C   YOUNG MODULUS   = 70E9 Pa
C   LOAD FILE IS D31LOAD.TXT

NODAL POINT LOCATIONS 3
1,0.0535,-85,0.0125 THROUGH 36,0.0535,265,0.0125
37,0.0538,-85,0.02 THROUGH 72,0.0538,265,0.02
73,0.05472,-85,0.0275 THROUGH 108,0.05472,265,0.0275
109,0.05628,-85,0.035 THROUGH 144,0.05628,265,0.035
145,0.0585, 85,0.0425 THROUGH 180,0.0585,265,0.0425
181,0.0605,-85,0.0425 THROUGH 216,0.0605,265,0.0425
217,0.06277, 85,0.035 THROUGH 252,0.06277,265,0.035
253,0.0635,-85,0.0275 THROUGH 288,0.0635,265,0.0275
289,0.0635, 85,0.01375 THROUGH 324,0.0635,265,0.01375
325,0.0635,-85,0 THROUGH 360,0.0635,265,0
361,0.0635,-85,-0.01375 THROUGH 396,0.0635,265,-0.01375
397,0.0635,-85,-0.0275 THROUGH 432,0.0635,265,-0.0275
433,0.06277,-85,-0.035 THROUGH 468,0.06277,265,-0.035
469,0.0605,-85,-0.0425 THROUGH 504,0.0605,265,-0.0425
505,0.0585,-85,-0.0425 THROUGH 540,0.0585,265,-0.0425
541,0.05628,-85,-0.035 THROUGH 576,0.05628,265,-0.035
577,0.05472, 85, 0.0275 THROUGH 612,0.05472,265,-0.0275
613,0.0538,-85,-0.02 THROUGH 648,0.0538,265,-0.02
649,0.0535,-85,-0.0125 THROUGH 684,0.0535,265,-0.0125

MATERIAL PROPERTIES 70E9,0,0,0.3
QUADRILATERAL PLATE TYPE 1,1,0.000125
C   SPRING ELEMENTS
GENERATE CONNECTS 1,2,254,1,36
GENERATE CONNECTS 3,4,256,1,36
GENERATE CONNECTS 5,6,258,1,36
GENERATE CONNECTS 7,8,260,1,36
GENERATE CONNECTS 9,10,262,1,36
GENERATE CONNECTS 11,12,264,1,36
GENERATE CONNECTS 13,14,266,1,36
GENERATE CONNECTS 15,16,268,1,36
GENERATE CONNECTS 17,18,270,1,36
GENERATE CONNECTS 19,20,272,1,36
GENERATE CONNECTS 21,22,274,1,36
GENERATE CONNECTS 23,24,276,1,36
GENERATE CONNECTS 25,26,278,1,36
GENERATE CONNECTS 27,28,280,1,36
GENERATE CONNECTS 29,30,282,1,36
GENERATE CONNECTS 31,32,284,1,36
GENERATE CONNECTS 33,34,286,1,36
GENERATE CONNECTS 35,36,288,1,36
GENERATE CONNECTS 397,398,650,1,36
GENERATE CONNECTS 399,400,652,1,36

137

```
GENERATE CONNECTS 401,402,654,1,36
GENERATE CONNECTS 403,404,656,1,36
GENERATE CONNECTS 405,406,658,1,36
GENERATE CONNECTS 407,408,660,1,36
GENERATE CONNECTS 409,410,662,1,36
GENERATE CONNECTS 411,412,664,1,36
GENERATE CONNECTS 413,414,666,1,36
GENERATE CONNECTS 415,416,668,1,36
GENERATE CONNECTS 417,418,670,1,36
GENERATE CONNECTS 419,420,672,1,36
GENERATE CONNECTS 421,422,674,1,36
GENERATE CONNECTS 423,424,676,1,36
GENERATE CONNECTS 425,426,678,1,36
GENERATE CONNECTS 427,428,680,1,36
GENERATE CONNECTS 429,430,682,1,36
GENERATE CONNECTS 431,432,684,1,36
C       WHEEL THREAD
GENERATE CONNECTS 253,288,432,1,36
DO CONNECTS 288,253,289,324 THROUGH 396,361,397,432 STEP 36,36,36,36

ZERO 11
TA 1 THROUGH 36 STEP 1
TA 649 THROUGH 684 STEP 1

END DEFINITION
```

This last model is a full wheel model.
The purposes of this file is to measure
the tangential deflection, which the
half wheel model cannot measure.

```
C        LOAD FILE FOR DIA1.TXT
C        SUBCASE 1
C        NORMAL FORCE LOAD ONLY AND OVER 15 DRGREES OF THE BASE
C        FORCES IS HALF OF 3.014N = 1.552N
C        AREA IS 0.0005642 m^2
PRESSURE LOAD APPLIED 21
1697.41 109,110,182,1,18

PRESSURE LOAD APPLIED 12
1697.41 307,109,127,308 THROUGH 310,163,181,311 STEP 1,18,18,1

SOLVE


C        SUBCASE 2
C        SIDE LOADING EQUILIVENT TO GOING ALONG A SLOPE OF 27 DEGREES
C        SIDE LOAD  = 1.409N
C        NORMAL LOAD = 2.765N
PRESSURE LOAD APPLIED 21
1512.4 109,110,182,1,18

PRESSURE LOAD APPLIED 12
1512.4 307,109,127,308 THROUGH 310,163,181,311 STEP 1,18,18,1

FORCES AND MOMENTS APPLIED 21
FZ 0.07045 109,110,182,1,18

SOLVE

QUIT
C        LOAD FILE FOR DIA2.TXT
C        SUBCASE 1
C        NORMAL FORCE LOAD ONLY AND OVER 15 DRGREES OF THE BASE
C        FORCES IS HALF OF 3.014N = 1.552N
C        AREA IS 0.0005642 m^2
PRESSURE LOAD APPLIED 21
1697.41 127,128,200,1,18

PRESSURE LOAD APPLIED 12
1697.41 343,127,145,344 THROUGH 346,181,199,347 STEP 1,18,18,1

SOLVE


C        SUBCASE 2
C        SIDE LOADING EQUILIVENT TO GOING ALONG A SLOPE OF 27 DEGREES
C        SIDE LOAD  = 1.409N
C        NORMAL LOAD = 2.765N
PRESSURE LOAD APPLIED 21
1512.4 127,128,200,1,18

PRESSURE LOAD APPLIED 12
1512.4 343,127,145,344 THROUGH 346,181,199,347 STEP 1,18,18,1

FORCES AND MOMENTS APPLIED 21
FZ 0.07045 127,128,200,1,18

SOLVE

QUIT
```

```
C       LOAD FILE FOR DIA8.TXT(FULL WHEEL MODEL)
C       SUBCASE 1
C       NORMAL FORCE LOAD ONLY AND OVER 15 DEGREES OF THE BASE
C       FORCES IS 3.014N
C       AREA IS 0.0005642 m^2
PRESSURE LOAD APPLIED 21
1697.41 253,254,398,1,36


PRESSURE LOAD APPLIED 21
1697.41 287,288,432,1,36


PRESSURE LOAD APPLIED 12
1697.41 288,253,289,324 THROUGH 396,361,397,432 STEP 36,36,36,36


SOLVE


C       SUBCASE 2
C       SIDE LOADING EQUILIVENT TO GOING UP A SLOPE OF 27 DEGREES
C       TANGENT LOAD  = 1.409N
C       NORMAL LOAD   = 2.765N
PRESSURE LOAD APPLIED 21
1512.41 253,254,398,1,36


PRESSURE LOAD APPLIED 21
1512.41 287,288,432,1,36


PRESSURE LOAD APPLIED 12
1512.41 288,253,289,324 THROUGH 396,361,397,432 STEP 36,36,36,36


FORCES AND MOMENTS APPLIED 21
FX 0.07045 253,254,398,1,36


FORCES AND MOMENTS APPLIED 21
FX 0.07045 287,288,432,1,36


SOLVE


C       SUBCASE 3
C       SIDE LOADING EQUILIVENT TO GOING ALONG A SLOPE OF 27 DEGREES
C       RADIAL LOAD  = 1.409N
C       NORMAL LOAD  = 2.765N
PRESSURE LOAD APPLIED 21
1512.41 253,254,398,1,36


PRESSURE LOAD APPLIED 21
1512.41 287,288,432,1,36


PRESSURE LOAD APPLIED 12
1512.41 288,253,289,324 THROUGH 396,361,397,432 STEP 36,36,36,36


FORCES AND MOMENTS APPLIED 21
FZ 0.07045 253,254,398,1,36
FZ 0.07045 287,288,432,1,36


SOLVE

QUIT
```

Results

Model 1

Radial Load : Radial Deflection $= 3.98 \times 10^{-4}$ m

Radial and : Radial Deflection $= 4.5 \times 10^{-4}$ m
Axial load : Axial Deflection $= 1.365 \times 10^{-4}$ m

$$\frac{A}{R} = \frac{\text{Axial Deflection}}{\text{Radial Deflection}} = \frac{1.365 \times 10^{-4}}{4.5 \times 10^{-4}} = 30.3\%$$

Model 2

Radial Load : Radial Deflection $= 1.22 \times 10^{-3}$ m

Radial and : Radial Deflection $= 1.37 \times 10^{-3}$ m
Axial load : Axial Deflection $= 2.94 \times 10^{-4}$ m

$$\frac{A}{R} = \frac{2.94 \times 10^{-4}}{1.37 \times 10^{-3}} = 21.47\%$$

Model 3

Radial load : Radial Deflection $= 1.65 \times 10^{-3}$ m

Radial and : Radial Deflection $= 1.56 \times 10^{-3}$ m
Axial Load : Axial Deflection $= 3.01 \times 10^{-4}$ m

$$\frac{A}{R} = \frac{3.01 \times 10^{-4}}{1.56 \times 10^{-3}} = 19.3\%$$

Results

Model 4

Radial Load : Radial Deflection = 2.91×10^{-3} m

Radial and : Radial Deflection = 3.064×10^{-3} m
Axial Load : Axial Deflection = 5.515×10^{-4} m

$$\frac{A}{R} = \frac{5.515 \times 10^{-4}}{3.064 \times 10^{-3}} = 17.99\%$$

Model 5

Radial Load : Radial Deflection = 4.21×10^{-3} m

Radial and : Radial Deflection = 4.19×10^{-3} m
Axial load : Axial Deflection = 7.24×10^{-4} m

$$\frac{A}{R} = \frac{7.24 \times 10^{-4}}{4.19 \times 10^{-3}} = 17.28\%$$

Using trial and error, the thickness of the wheel at 0.15 mm gives the nearest target deflection of 1.5 mm.

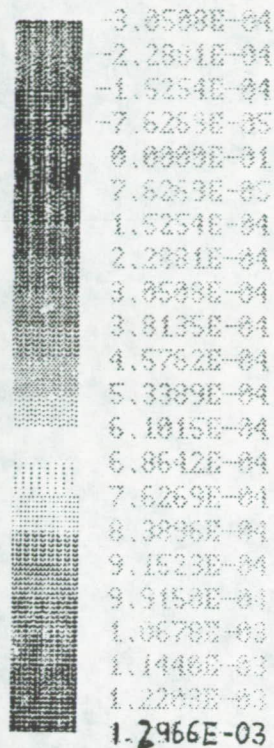Using this thickness, the deflection is:

Radial Deflection = 1.29×10^{-3} m and 1.31×10^{-3} m
Axial Deflection = 2.22×10^{-4} m

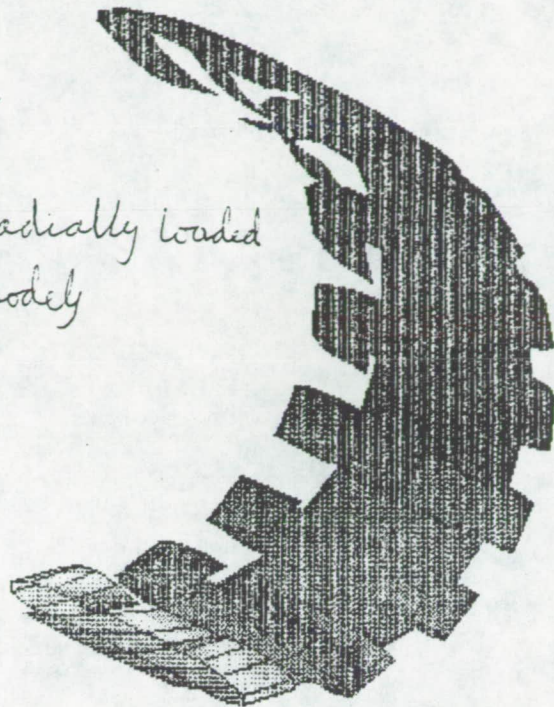$$\frac{A}{R} = \frac{2.22 \times 10^{-4}}{1.29 \times 10^{-3}} = 16.94\%$$

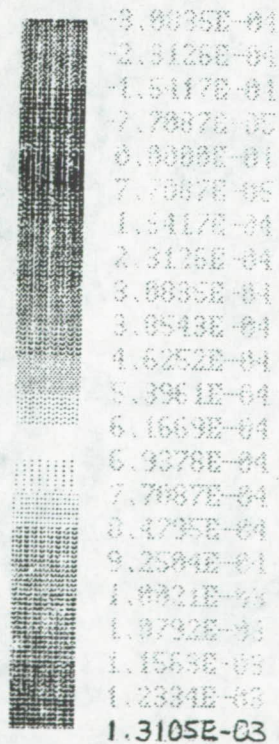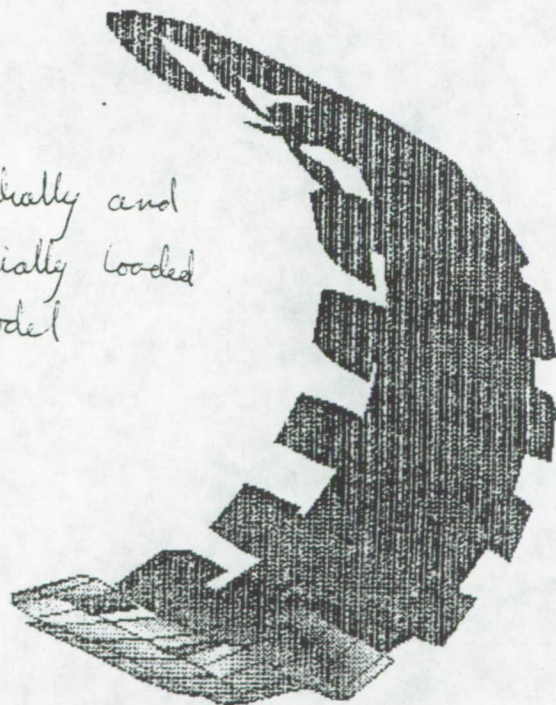<u>Results:</u> TRANS. DEFL. Y (Radial Deflection)

```
-3.0588E-04
-2.2801E-04
-1.5254E-04
-7.6269E-05
0.0003E-01
7.6269E-05
1.5254E-04
2.2881E-04
3.0508E-04
3.8135E-04
4.5762E-04
5.3389E-04
6.1015E-04
6.8642E-04
7.6269E-04
8.3896E-04
9.1523E-04
9.9150E-04
1.0678E-03
1.1440E-03
1.2203E-03
1.2966E-03
```

Radially loaded
Model

TRANS. DEFL. Y (Radial Deflection)

```
-3.0035E-04
-2.3126E-04
-1.5117E-04
-7.7087E-05
0.0008E-01
7.7087E-05
1.5417E-04
2.3126E-04
3.0035E-04
3.8543E-04
4.6252E-04
5.3961E-04
6.1669E-04
6.9378E-04
7.7087E-04
8.4795E-04
9.2504E-04
1.0021E-03
1.0792E-03
1.1563E-03
1.2334E-03
1.3105E-03
```

Radially and
axially loaded
Model

143

<u>Results</u>

TRANS. DEFL. Z (Axial Deflection)

-3.7138E-05
-2.4733E-05
-1.2367E-05
-9.7919E-13
1.2367E-05
2.4733E-05
3.7100E-05
4.9467E-05
6.1834E-05
7.4200E-05
8.6567E-05
9.8934E-05
1.1130E-04
1.2367E-04
1.3603E-04
1.4840E-04
1.6077E-04
1.7313E-04
1.8550E-04
1.9787E-04
2.1023E-04
2.2260E-04
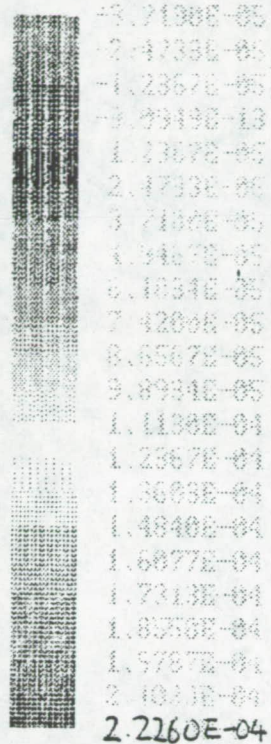
Radially and
Axially loaded
Model

<u>Final Wheel Dimension</u>

|15mm| 55mm |15mm|

R1   R2   4mm
                    2mm
                    4mm
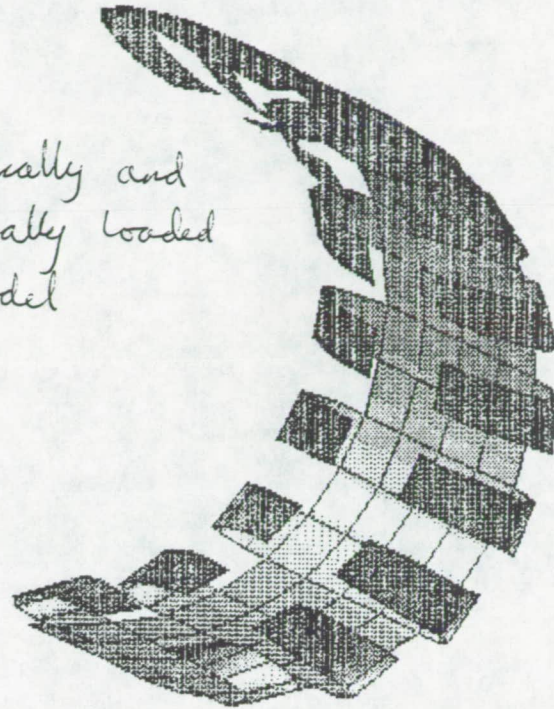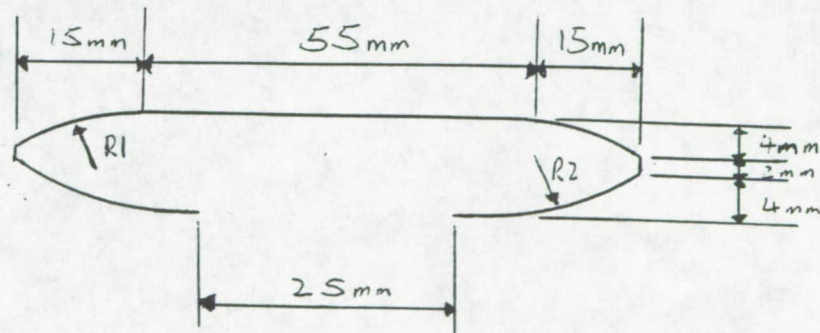
25mm

R1 = 30.125 mm   R2 = 114.5 mm

Wheel diameter = 0.127 m

144
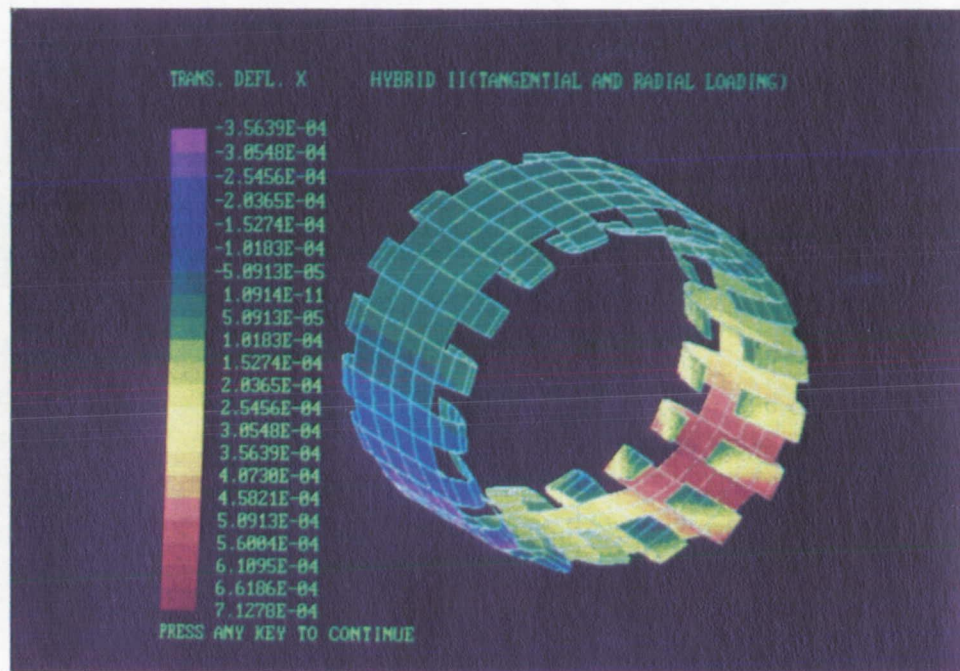
Above shows the tangential deflection of the final design.
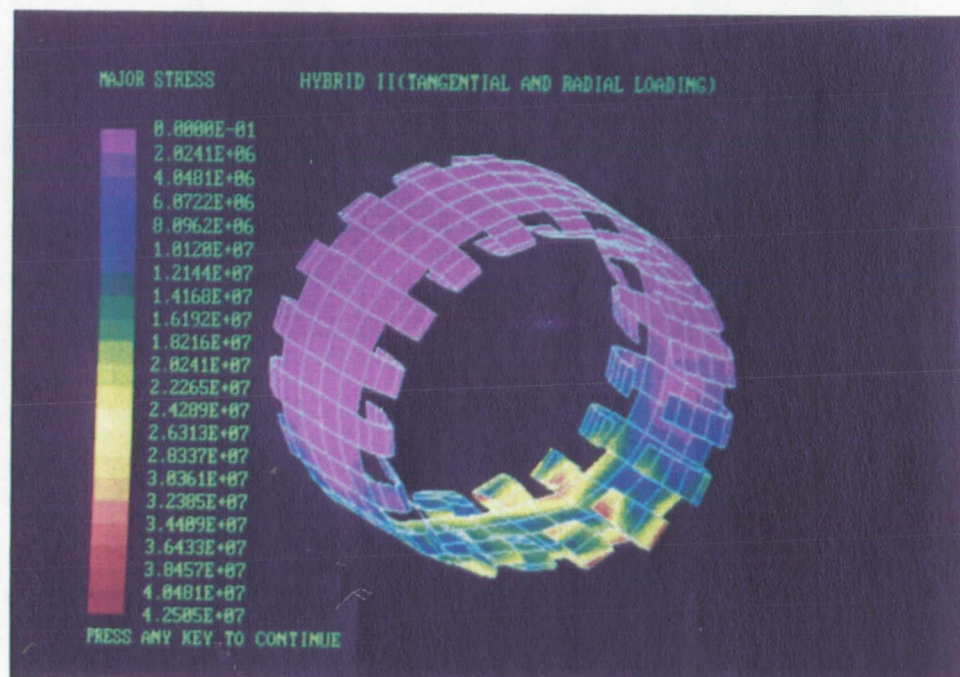
Above shows the major stress of the final design.

145

Appendix J

Breakdown of Costs

This appendix contains a breakdown of costs. It is essentially a rough estimate since the cost will depend upon the results of wheel, soil, and material testing. A conservative cost multiplying factor of 1.5 has been added to cover unknown factors that may result from these tests.

Item	Cost
Soil Simulant Synthesis	$30,000
Wheel Testing	$250,000
Material Testing	$20,000
Injection Mold for Wheel	$100,000
Sub-Total	$400,000
Production Cost Multiplying Factor	1.5
Total Cost	**$600,000**